Title
Transcriptional and translational regulation of HAC1 mRNA in the unfolded protein response

Author
Leber, Jess Herter

Publication Date
2004

Peer reviewed|Thesis/dissertation

Transcriptional and Translational Regulation of *HAC1* mRNA

in the Unfolded Protein Response

by

Jess Herter Leber

DISSERTATION

Submitted in partial satisfaction of the requirements for the degree of

DOCTOR OF PHILOSOPHY

in

GENETICS

in the

GRADUATE DIVISION

of the

UNIVERSITY OF CALIFORNIA, SAN FRANCISCO

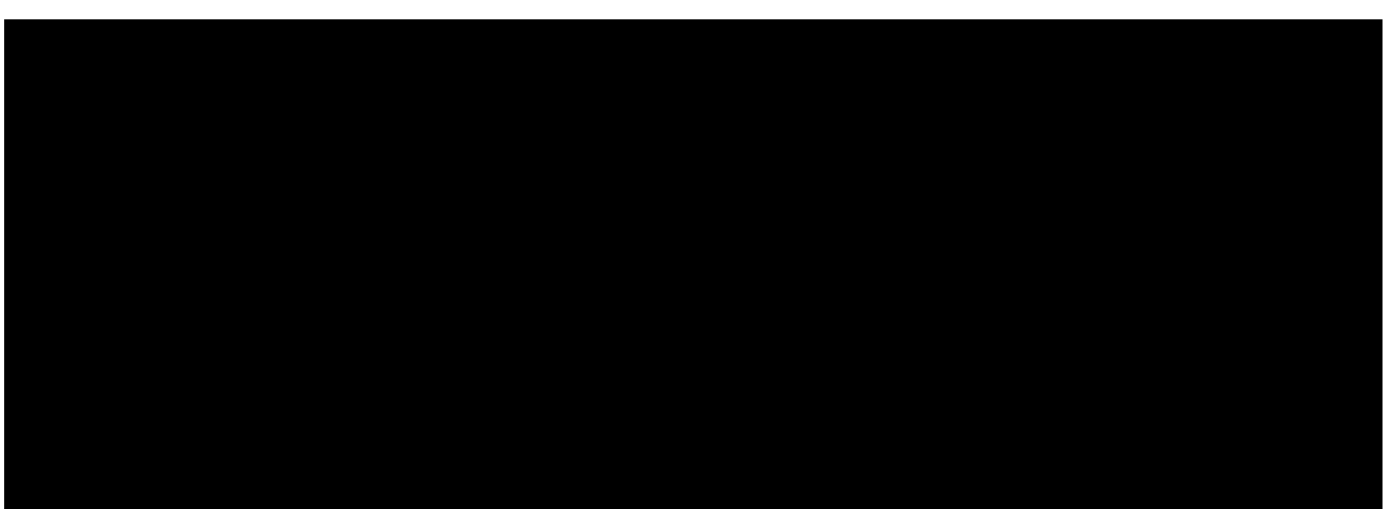

University Librarian

Date Degree Conferred: .....

This dissertation is dedicated both to my wife,

whose patience and understanding provide a respite from the rigors of science,

and to the Walter Lab family,

whose camaraderie made coming into lab a pleasure

Acknowledgements

First and foremost, I thank Peter Walter for both his clarity of vision and his boundless, infectious mirth. Both in analyzing data and writing papers, Peter brings a laser-like focus to his mission of stamping out "fuzziness" wherever it may hide. If I can carry with me a fraction of his insight I will count myself fortunate. Equally important, Peter maintains a research atmosphere that promotes creativity and fun, and tolerated my flammable proclivities.

I have been lucky during my time in the Walter lab to be surrounded by talented and benevolent post-docs, from whom I have learned much. In particular, from Ted Powers: almost zen-like unflappability; from Maho Niwa: fierce determination and a passion for Jolly Rancher candies; and from Jason Bricker, my partner in crime: boundless patience and curiosity, and a knack for denying responsibility for any practical joke.

Of course, students are the heart of any lab, and the many exceptional past and present students in the Walter Lab have made my tenure both personally and scientifically rewarding. I will especially remember my interactions with friend and colleague Chris Patil, whose caustic wit made me think twice before speaking, but whose sharp mind was always an invaluable resource. I feel confident that Sebastián Bernales will continue to do "perfecto" work on the Super UPR, and that the newest additions to the Walter Lab will maintain and nourish all that makes it unique and good.

I am grateful to those who make the UCSF community so special, and whose contributions are often unheralded. I am particularly thankful to Teresa Donovan and Sue Adams, who seemed to keep me out of trouble before I even knew I was in it, and

whose tireless behind-the-scenes efforts were always more than one could ever expect. There are many who made my time here so enjoyable, and I will continue to value the friendship of Adam Carroll, Jessica Blumstein, Marc Meneghini, and Zemer Gitai. We have many more bottles of wine left to drink together.

Finally, I wish to thank the members of my thesis committee, Ira Herskowitz, Jonathan Weissman, and Christine Guthrie, for their excellent advice, discussions, and occasional use of ozone-free bench space (JSW). To Ira I owe special gratitude for hopefully helping me convince Peter that genetics is hard work, and not just "something that happens on your bench when you go home at night".

ELSEVIER

2 March 2004

Our Ref: HWjj/Mar04/J027
Your Ref:

Jess Leber
Via email jleber@mac.com

Dear Jess Leber

CELL, Vol 107, 2001, pp 103-114, Rüegsegger et al: "Block of HAC1 mRNA translation...

As per your letter dated 1 March 2004, we hereby grant you permission to reprint the aforementioned material at no charge **in your thesis** subject to the following conditions:

1. If any part of the material to be used (for example, figures) has appeared in our publication with credit or acknowledgement to another source, permission must also be sought from that source. If such permission is not obtained then that material may not be included in your publication/copies.

2. Suitable acknowledgment to the source must be made, either as a footnote or in a reference list at the end of your publication, as follows:

   "Reprinted from Publication title, Vol number, Author(s), Title of article, Pages No., Copyright (Year), with permission from Elsevier".

3. Reproduction of this material is confined to the purpose for which permission is hereby given.

4. This permission is granted for non-exclusive world **English** rights only. For other languages please reapply separately for each one required. Permission excludes use in an electronic form. Should you have a specific electronic project in mind please reapply for permission.

5. This includes permission for UMI to supply single copies, on demand, of the complete thesis. Should your thesis be published commercially, please reapply for permission.

Yours sincerely

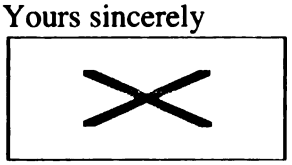

Helen Wilson

Transcriptional and Translational Regulation of *HAC1* mRNA

in the Unfolded Protein Response

by

Jess Herter Leber

Abstract

In eukaryotic cells, an accumulation of misfolded proteins in the endoplasmic reticulum (ER) triggers a change in gene expression without which cells could not survive. Information is transmitted from the ER to the nucleus by an intracellular signaling pathway, termed the unfolded protein response (UPR). The bifunctional transmembrane endoribonuclease Ire1p both senses adverse folding conditions in the ER lumen and subsequently initiates non-canonical splicing of *HAC1* mRNA in the cytoplasm. Spliced *HAC1* is translated to produce the bZip transcription factor Hac1p, which then enters the nucleus and activates the transcription of UPR target genes. Targets include ER lumenal chaperones, components of the ER-associated degradation pathway, and phospholipids important for ER and other membranes. Thus, regulation of Hac1p is of paramount importance for cellular survival of misfolded proteins. This thesis describes my work toward understanding two mechanisms regulating Hac1p abundance.

The regulated splicing of *HAC1* mRNA by Ire1p provides a "switch" governing Hac1p abundance, causing the removal of an intron that otherwise attenuates translation. In the unspliced message, the *HAC1* intron directly base-pairs with the 5' untranslated region (5'UTR), trapping ribosomes and preventing their further elongation. This *HAC1*-polyribosome complex waits poised in the cytoplasm; upon UPR activation, removal of the intron by Ire1p allows the ribosomes to resume translation, and Hac1p is quickly and

robustly made. This unique "intramolecular anti-sense" regulation both efficiently represses Hac1p production in uninduced cells and allows for extremely rapid translation of Hac1p upon UPR activation.

In addition to having an on/off switch, the UPR also possesses "gain control". When cells are subjected to a specific combination of stresses, an *IRE1*-independent ER surveillance pathway upregulates the *HAC1* promoter to allow for greater Hac1p production. With increased levels of Hac1p, the induction of specific target genes is amplified; if cells cannot correctly boost Hac1p levels, they die. Gene expression patterns suggest that a second transcription factor collaborates with Hac1p to produce the "Super-UPR", but the identity of this "UPR Modulatory Factor" remains unknown. By thus linking a gain control element to the basic UPR circuit, a simple switch is converted into a complex response.

Table of Contents

List of Figures and Tables

Chapter 1

Chapter 2

Chapter 3

Chapter 4

Chapter 1

Introduction:

The Unfolded Protein Response in *S. cerevisiae*

Protein folding in the endoplasmic reticulum

The proper folding and maturation of proteins is an essential task required of all cells. This mission is compounded for secreted proteins, which must be prepared for an extracellular, oxidizing environment very different from the intracellular space, and for membrane proteins, whose hydrophobic nature imposes additional thermodynamic limitations. The earliest eukaryotic efforts addressing this task likely began with a simple membrane involution, which conferred the benefit of a defined space in which protein-folding factors could be concentrated, yet still maintained the oxidizing environment most suitable for the folding proteins. These early efforts led to the evolution of the endoplasmic reticulum (ER), an organelle dedicated to the tasks of protein folding and trafficking. The ER is the gateway through which all secreted and membrane proteins much first pass.

Nascent proteins are delivered to the ER either post-translationally, having been fully synthesized in the cytoplasm and subsequently translocated into the ER, or co-translationally, in a coupled reaction whereby a translating ribosome directly feeds its cargo through a translocation complex into the ER as it is being made (reviewed in (Schnell and Hebert, 2003)). In the ER, proteins are subject to a multitude of modifications that help them assume the proper structure necessary for their designed function (reviewed in (Patil and Walter, 2001) and references therein). ER-lumenal chaperones guide proteins into their correct three-dimensional form. Disulfide bond isomerases promote the correct linking of cysteine residues necessary for the protein structure. Carbohydrate modifications aid in folding and also likely influence the function of the protein. Proteins are often then assembled into multi-subunit complexes

before entering the secretory pathway to be trafficked to their appropriate final destination.

The ER is a dynamic organelle, capable of adjusting its folding capacity in response to increased demand. For example, as resting B cells differentiate into antibody-secreting plasma cells, the ER undergoes massive expansion such that it occupies a significant volume of the cell (Figure 1-1; (Wiest et al., 1990) and references therein). By gauging the secretory load of the ER, and adjusting the folding capacity of the ER accordingly, cells maintain homeostatic control of organelle function.

The Unfolded Protein Response

Eukaryotic cells monitor and adjust the folding capacity of the ER with an unusual signal transduction pathway, termed the unfolded protein response (UPR) (reviewed in (Kaufman, 2002; Ma and Hendershot, 2001; Patil and Walter, 2001; Ron, 2002)). In response to an accumulation of unfolded proteins in the ER lumen, the UPR directs the coordinated transcriptional activation of a number of genes that aid in the correct processing of membrane and secreted proteins. Having been initially characterized in the yeast *Saccharomyces cerevisiae*, the UPR is conserved amongst all eukaryotes studied. In yeast, three components of the pathway have been described to date: *IRE1*, encoding a transmembrane endoribonuclease/kinase (Cox et al., 1993); *RLG1*, encoding tRNA ligase (Sidrauski et al., 1996); and *HAC1*, encoding a bZip transcription factor (Cox and Walter, 1996). When unfolded proteins accumulate, the UPR regulates the increased abundance of Hac1p, which in turn activates the expression of genes that enable the cell to survive

this otherwise lethal stress (Cox et al., 1997; Kozutsumi et al., 1988; Lee, 1987; Travers et al., 2000; Urano et al., 2000).

Hac1p abundance is controlled primarily by post-transcriptional modification of the *HAC1* mRNA, and it is the unique mechanism of this regulation that distinguishes the UPR from other signal transduction pathways (Figure 1-2). Ire1p, spanning the ER membrane, contains an N-terminal domain that resides in the ER lumen and senses unfolded proteins. This domain has been shown to interact with ER lumenal chaperones, and it is believed that this interaction keeps Ire1p in an inactive conformation (Bertolotti et al., 2000). When unfolded proteins accumulate, these chaperones are titrated off Ire1p, which then dimerizes and trans-autophosphorylates (Shamu and Walter, 1996) (Papa et al., 2003). This, in turns, activates a site-specific endoribonuclease activity in the carboxy-terminus of Ire1p, residing in the cytoplasm, that directly cleaves the *HAC1* mRNA (Sidrauski and Walter, 1997). The *HAC1*^{u} ("*u*" for UPR-*u*ninduced) mRNA contains a 252 base intron at the 3' end of the message that separates the DNA binding and dimerization domains from a 3' exon encoding residues important for full Hac1p activity (Mori et al., 2000). Additionally, the *HAC1* intron represses the translation of unspliced *HAC1* mRNA (Chapman and Walter, 1997). Ire1p cleaves at precise bases flanking this intron, and the two *HAC1* exons are then joined by tRNA ligase. This spliced *HAC1*^{i} mRNA ("*i*" for UPR-*i*nduced), freed from the translation-inhibiting intron, is then translated to produce the Hac1p^{i} transcription factor. Hac1p^{i} enters the nucleus, where it binds to the promoters of UPR-responsive genes, many of which contain at least one of a number of defined unfolded protein response elements (UPREs) (Mori et al., 1992; Patil et al., 2004). From early work in mammalian cells, UPR targets were known

to include ER lumenal protein folding chaperones such as *KAR2*, a member of the Hsp70-family of chaperones, and *PDI1*, encoding protein disulfide bond isomerase (Dorner et al., 1990; Kozutsumi et al., 1988; Lee, 1987). A comprehensive genomic expression analysis of the UPR in yeast by Travers *et al.*, however, revealed the full breadth of the transcriptional response (Travers et al., 2000)(Figure 1-3). In addition to upregulating protein folding chaperones, the UPR activates the transcription of genes affecting virtually every step of the secretory process. These targets include components of the ER-associated degradation pathway (ERAD) for the disposal of terminally misfolded proteins, and COPII vesicle components to help clear the ER of correctly folded proteins that no longer require chaperone assistance.

This work describes the regulation of Hac1p abundance. Commensurate with its central role in the UPR, the expression of Hac1p appears to be regulated by multiple mechanisms. In Chapters 2 and 3 of this thesis, I describe our efforts toward understanding the regulation of *HAC1* translation and transcription, respectively. Anecdotal and circumstantial evidence, however, suggests that additional regulation of Hac1p expression is likely; ectopic expression of Hac1p yields less-than-expected amounts of Hac1p, suggesting that either or both mRNA or protein stability can be down-regulated (J. Leber, C. Patil, and others, personal observations). Furthermore, the ramifications of the schizophrenic nature of *HAC1* mRNA remain largely unexplored; *HAC1* is presumably exported by PolII transcript-specific pathways and components, yet the chemistry of the *HAC1* splicing reaction is clearly akin to that of tRNAs (Gonzalez et al., 1999). For instance, Inada and Guthrie (Inada and Guthrie, 2004) find that *HAC1* mRNA associates with Lhp1p, a chaperone normally associated with tRNAs and other

non-coding transcripts. Finally, in Chapter 4, I present data suggesting that Hac1p can be differentially phosphorylated, and discuss the potential implications for modulation of Hac1p activity.

While this thesis has hopefully furthered our understanding of Hac1p regulation and the Unfolded Protein Response, I have no doubt that future researchers will find many astounding and satisfying stories still hidden in this beautiful signal transduction pathway.

HAC1 translational regulation

In Chapter 2 of this thesis, I describe the mechanisms controlling the fate of the unspliced, *HAC1*^{u} mRNA. In the absence of UPR induction, why is Hac1p^{u} not made? While splicing by Ire1p and tRNA ligase places a new 3' exon at the end of the *HAC1* message, the unspliced mRNA contains sequence that should allow for the production of a transcription factor, different only in the 18 amino acids at the carboxy tail (Figure 1-4). At the time of the initial identification and characterization of *HAC1* and the Unfolded Protein Response, it was hypothesized that Hac1p^{u} is produced, but is degraded so quickly as be undetectable (Cox and Walter, 1996). However, Chapman et al. (Chapman and Walter, 1997) found that Hac1p^{u} and Hac1p^{i} have similar half-lives, thus making the protein degradation hypothesis unlikely to be correct. Furthermore, they found that *HAC1*^{u} mRNA is just as stable as *HAC1*^{i} mRNA, and is exported from the nucleus to the cytoplasm where it stably associates with polyribosomes. Intriguingly, a HA-epitope inserted into the N-terminal region of Hac1p was translated, but the full-length protein was not, suggesting that translation initiates on the *HAC1* message but does not elongate

fully. This translational attenuation was mediated by the *HAC1* 3' intron, and was transferable to heterologous messages, but the mechanism of the repression was not clear.

With this knowledge I set out to investigate the mechanism of translational attenuation of Hac1p^u. Initial attempts at repeating the experiments described in Chapman *et al.* proved frustrating, as I found the *HAC1* intron insufficient to attenuate the translation of a heterologous message. Upon comparing the reporter I was using to those used in Chapman *et al.*, I found that earlier experiments had used a reporter containing additional *cis* elements from the *HAC1* message (Figure 1-5). I was able to further define the *HAC1* sequences required for translation attenuation, and discovered that, in addition to the 3' intron, the 5' untranslated region (5' UTR) was absolutely required. Examination of this region, with the aid of a predicted structure of the *HAC1* mRNA created by Chris Patil using the mfold program (Zuker, 2003), revealed am unpaired stretch of nucleotides within the 5'UTR, surrounded by paired sequence (Figure 1-6). Further examination revealed complementary nucleotides within the intron. Subsequent mutation of these sequences established that these regions directly base-pair, and that this pairing is essential for translational attenuation of the message (Figure 1-7).

In a fruitful and enjoyable collaboration with Ursula Rüegsegger, at that time a post-doc in the Walter lab, we combined our biochemical and genetic expertise to further examine this unique mechanism of translational repression (Rüegsegger et al., 2001). In our paper, we not only resolved previous inconsistencies regarding the minimal *HAC1* *cis*-elements required for translational attenuation of a heterologous reporter, but also established long-range base-pairing within an mRNA as a unique, "intramolecular" anti-sense mechanism of translational regulation. Of particular personal interest is whether

this mechanism of regulation is conserved in metazoans, in which the *HAC1* ortholog *XBP-1* contains a much shorter intron that does appear capable of base-pairing with the 5' UTR (Calfon et al., 2002; Yoshida et al., 2001). Finally, an auxiliary consequence of our studies was to establish that *HAC1* mRNA can be spliced while ribosome-bound in the cytoplasm, thereby establishing the topology of Ire1p as spanning the ER membrane between the ER lumen and the cytoplasm.

HAC1 transcriptional regulation

The unfolded protein response finds a way to humble us at every turn, so it came as no surprise that translational attenuation turned out to be only one of several mechanisms regulating Hac1p abundance. While Hac1p regulates the transcription of a large number of target genes, scant attention had been paid to the possibility of transcriptional regulation of *HAC1* itself. In fact, hints that *HAC1* transcription might be regulated existed for some time, before their implications became clear. Vlad Denic, while a rotation student working with Rowan Chapman on potential *trans*-acting factors involved in *HAC1* translational attenuation, isolated a number of mutants increasing the fluorescence of a green fluorescent protein (*GFP*) reporter replacing the *HAC1* ORF, flanked by *HAC1* sequence. One of these mutants, generated by insertional mutagenesis using the Snyder library (Ross-Macdonald et al., 1997), was a partial loss-of-function allele of *PIK1* (*pik1-100*), a phosphatidylinositol-4 kinase involved in both cytoskeletal architecture and secretion (Flanagan et al., 1993; Garcia-Bustos et al., 1994; Hama et al., 1999). Further examination revealed that this mutant activated the *GFP* reporter not by disrupting attenuation, but instead by upregulating the *HAC1* promoter with which the

reporter was expressed; even with *HAC1 cis*-elements repressing translation of the reporter, a small amount of "leakiness" was amplified by increased promoter activity (Figure 1-8A).

At this point my involvement with this project began. Rather than attempting to fully characterize what appeared to be a very unusual mutant allele of *PIK1*, I instead chose to focus on what compromised function of *PIK1* led to the upregulation of *HAC1*. After establishing that the *pik1-100* mutant had a defect in secretion (Figure 1-8B), I quickly moved to better-characterized *sec* mutants to study *HAC1* transcriptional regulation.

In Chapter 3, I present the result of those efforts. We find that the *HAC1* promoter is upregulated in response to a bipartite signal, comprised of ER protein folding stress and either inositol starvation or elevated temperature. This upregulation is *IRE1*-independent, revealing that a novel ER surveillance pathway operates in yeast to regulate the transcription of *HAC1*. The resulting increase in Hac1p production is necessary for the cells to survive the conditions that trigger this response. This parallel ER-to-nucleus signaling pathway serves as "gain control" by modifying the UPR-driven transcriptional program. Based on these data, we now envision a model of the UPR whereby modular signal transduction elements are combined to allow for a more complex transcriptional response function. Furthermore, the results suggest a surprising conservation among all eukaryotes of the ways by which the elements of the UPR signaling circuit are connected.

Unfinished business, loose ends, and perspectives on *HAC1* and the UPR

In Chapter 4, I conclude this thesis with thoughts on the future directions of the work I began in the Walter lab. Hopefully, I will have raised more questions that I have answered. In particular, I discuss the on-going hunt for the factor(s) involved in *HAC1* mRNA upregulation, utilizing a screen developed as a consequence of the plate phenotype described in Figure 4C. This work is being carried out by Sebastián Bernales, a talented new student with whom I have greatly enjoyed working. Additionally, I share data from unfinished projects that will hopefully be useful and appetizing to future researchers. Specifically, I describe an extension of observations by Ursula Rüegsegger regarding a peculiar high magnesium requirement for *HAC1* mRNA association with stalled ribosomes. I outline how this empirical biochemical quirk might be used in a microarray-based approach to discover other mRNAs whose translation is regulated at the elongation step. Also, I present data regarding the differential phosphorylation of Hac1p during extended secretory stress, and potential interactions between the UPR and the cell wall integrity pathway that were suggested by Noah Dephore in a rotation project.

REFERENCES

Bertolotti, A., Zhang, Y., Hendershot, L. M., Harding, H. P., and Ron, D. (2000). Dynamic interaction of BiP and ER stress transducers in the unfolded-protein response. Nature Cell Biology *2*, 326-332.

Calfon, M., Zeng, H., Urano, F., Till, J. H., Hubbard, S. R., Harding, H. P., Clark, S. G., and Ron, D. (2002). IRE1 couples endoplasmic reticulum load to secretory capacity by processing the XBP-1 mRNA. Nature *415*, 92-96.

Chapman, R. E., and Walter, P. (1997). Translational attenuation mediated by an mRNA intron. Current Biology *7*, 850-859.

Cox, J. S., Chapman, R. E., and Walter, P. (1997). The unfolded protein response coordinates the production of endoplasmic reticulum protein and endoplasmic reticulum membrane. Mol Biol Cell *8*, 1805-1814.

Cox, J. S., Shamu, C. E., and Walter, P. (1993). Transcriptional induction of genes encoding endoplasmic reticulum resident proteins requires a transmembrane protein kinase. Cell *73*, 1197-1206.

Cox, J. S., and Walter, P. (1996). A novel mechanism for regulating activity of a transcription factor that controls the unfolded protein response. Cell *87*, 391-404.

Dorner, A. J., Wasley, L. C., Raney, P., Haugejorden, S., Green, M., and Kaufman, R. J. (1990). The Stress Response in Chinese Hamster Ovary Cells. The Journal of Biological Chemistry *265*, 22029-22034.

Flanagan, C. A., Schnieders, E. A., Emerick, A. W., Kunisawa, R., Admon, A., and Thorner, J. (1993). Phosphatidylinositol 4-kinase: gene structure and requirement for yeast cell viability. Science *262*, 1444-1448.

Garcia-Bustos, J. F., Marini, F., Stevenson, I., Frei, C., and Hall, M. N. (1994). PIK1, an essential phosphatidylinositol 4-kinase associated with the yeast nucleus. Embo J *13*, 2352-2361.

Gonzalez, T. N., Sidrauski, C., Dörfler, S., and Walter, P. (1999). Mechanism of non-spliceosomal mRNA splicing in the unfolded protein response pathway. EMBO Journal *18*, 3119-3132.

Hama, H., Schnieders, E. A., Thorner, J., Takemoto, J. Y., and DeWald, D. B. (1999). Direct involvement of phosphatidylinositol 4-phosphate in secretion in the yeast Saccharomyces cerevisiae. J Biol Chem *274*, 34294-34300.

Inada, M., and Guthrie, C. (2004). Identification of Lhp1p-associated RNAs by microarray analysis in Saccharomyces cerevisiae reveals association with coding and noncoding RNAs. Proc Natl Acad Sci U S A *101*, 434-439.

Kaufman, R. J. (2002). Orchestrating the unfolded protein response in health and disease. J Clin Invest *110*, 1389-1398.

Kozutsumi, Y., Segal, M., Normington, K., Gething, M. J., and Sambrook, J. (1988). The presence of malfolded proteins in the endoplasmic reticulum signals the induction of glucose-regulated proteins. Nature *332*, 462-464.

Lee, A. S. (1987). Coordinated regulation of a set of genes by glucose and calcium ionophores in mammalian cells. Trends Biochem Sci *12*, 20-23.

Ma, Y., and Hendershot, L. M. (2001). The unfolding tale of the unfolded protein response. Cell *107*, 827-830.

Mori, K., Ogawa, N., Kawahara, T., Yanagi, H., and Yura, T. (2000). mRNA splicing-mediated C-terminal replacement of transcription factor Hac1p is required for efficient activation of the unfolded protein response. Proceedings of the National Academy of Sciences of the United States of America *97*, 4660-4665.

Mori, K., Sant, A., Kohno, K., Normington, K., Gething, M. J., and Sambrook, J. F. (1992). A 22 bp cis-acting element is necessary and sufficient for the induction of the yeast KAR2 (BiP) gene by unfolded proteins. Embo Journal *11*, 2583-2593.

Papa, F. R., Zhang, C., Shokat, K., and Walter, P. (2003). Bypassing a kinase activity with an ATP-competitive drug. Science *302*, 1533-1537.

Patil, C., Li, H., and Walter, P. (2004). A Role for Gcn4 and Novel Upstream Activating Sequences in the Unfolded Protein Response. PLoS Biology, *submitted.*

Patil, C., and Walter, P. (2001). Intracellular signaling from the endoplasmic reticulum to the nucleus: the unfolded protein response in yeast and mammals. Curr Opin Cell Biol *13*, 349-355.

Ron, D. (2002). Translational control in the endoplasmic reticulum stress response. J Clin Invest *110*, 1383-1388.

Ross-Macdonald, P., Sheehan, A., Roeder, G. S., and Snyder, M. (1997). A multipurpose transposon system for analyzing protein production, localization, and function in Saccharomyces cerevisiae. Proc Natl Acad Sci U S A *94*, 190-195.

Rüegsegger, U., Leber, J. H., and Walter, P. (2001). Block of HAC1 mRNA translation by long-range base pairing is released by cytoplasmic splicing upon induction of the unfolded protein response. Cell *107*, 103-114.

Schnell, D. J., and Hebert, D. N. (2003). Protein translocons: multifunctional mediators of protein translocation across membranes. Cell *112*, 491-505.

Shamu, C. E., and Walter, P. (1996). Oligomerization and phosphorylation of the Ire1p kinase during intracellular signaling from the endoplasmic reticulum to the nucleus. EMBO Journal *15*, 3028-3039.

Sidrauski, C., Cox, J. S., and Walter, P. (1996). tRNA ligase is required for regulated mRNA splicing in the unfolded protein response [see comments]. Cell *87*, 405-413.

Sidrauski, C., and Walter, P. (1997). The transmembrane kinase Ire1p is a site-specific endonuclease that initiates mRNA splicing in the unfolded protein response. Cell *90*, 1031-1039.

Travers, K. J., Patil, C. K., Wodicka, L., Lockhart, D. J., Weissman, J. S., and Walter, P. (2000). Functional and genomic analyses reveal an essential coordination between the unfolded protein response and ER-associated degradation. Cell *101*, 249-258.

Urano, F., Wang, X., Bertolotti, A., Zhang, Y., Chung, P., Harding, H. P., and Ron, D. (2000). Coupling of stress in the ER to activation of JNK protein kinases by transmembrane protein kinase IRE1. Science *287*, 664-666.

Wiest, D. L., Burkhardt, J. K., Hester, S., Hortsch, M., Meyer, D. I., and Argon, Y. (1990). Membrane Biogenesis during B Cell Differentiation: Most Endoplasmic Reticulum Proteins Are Expressed Coordinately. J Cell Biol *110*, 1501-1511.

Yoshida, H., Matsui, T., Yamamoto, A., Okada, T., and Mori, K. (2001). XBP1 mRNA is induced by ATF6 and spliced by IRE1 in response to ER stress to produce a highly active transcription factor. Cell *107*, 881-891.

Zuker, M. (2003). Mfold web server for nucleic acid folding and hybridization prediction. Nucleic Acids Res *31*, 3406-3415.

Figure 1-1: The ER is a dynamic organelle

Shown are a resting B cell (left) and an activated, antibody secreting plasma cell (right). Note that in the plasma cell the endoplasmic reticulum occupies a significant portion of the cell volume.

Figure 1-1

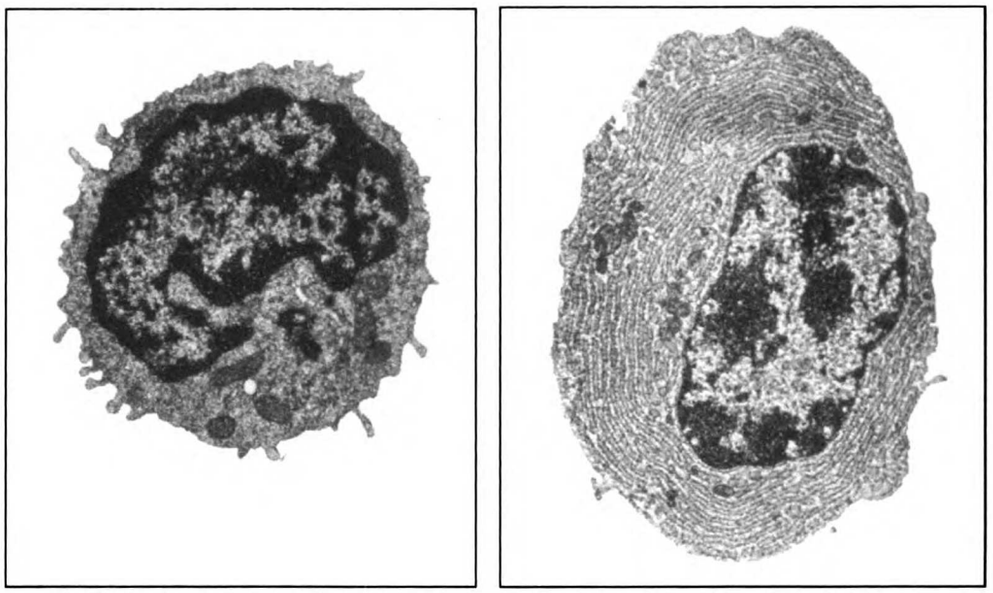

Resting B or T cell

Activated B cell
(plasma cell)

Figure 1-2: The Unfolded Protein Response in *S. cerevisiae*

In the absence of ER stress, *HAC1*^{u} mRNA is exported to the cytoplasm, where it stably associates with ribosomes. Translation of Hac1p^u is attenuated by direct base-pairing between the 5'UTR and an intron at the 3' end of the message, trapping elongating ribosomes. When unfolded proteins accumulate in the ER, activated Ire1p endonuclease splices ribosome-bound *HAC1*^{u}, excising the inhibitory intron. The two *HAC1* exons are then joined by tRNA ligase. Translation resumes on the message, producing the Hac1p transcription factor, which enters the nucleus and activates the transcription of target genes.

Figure 1-2

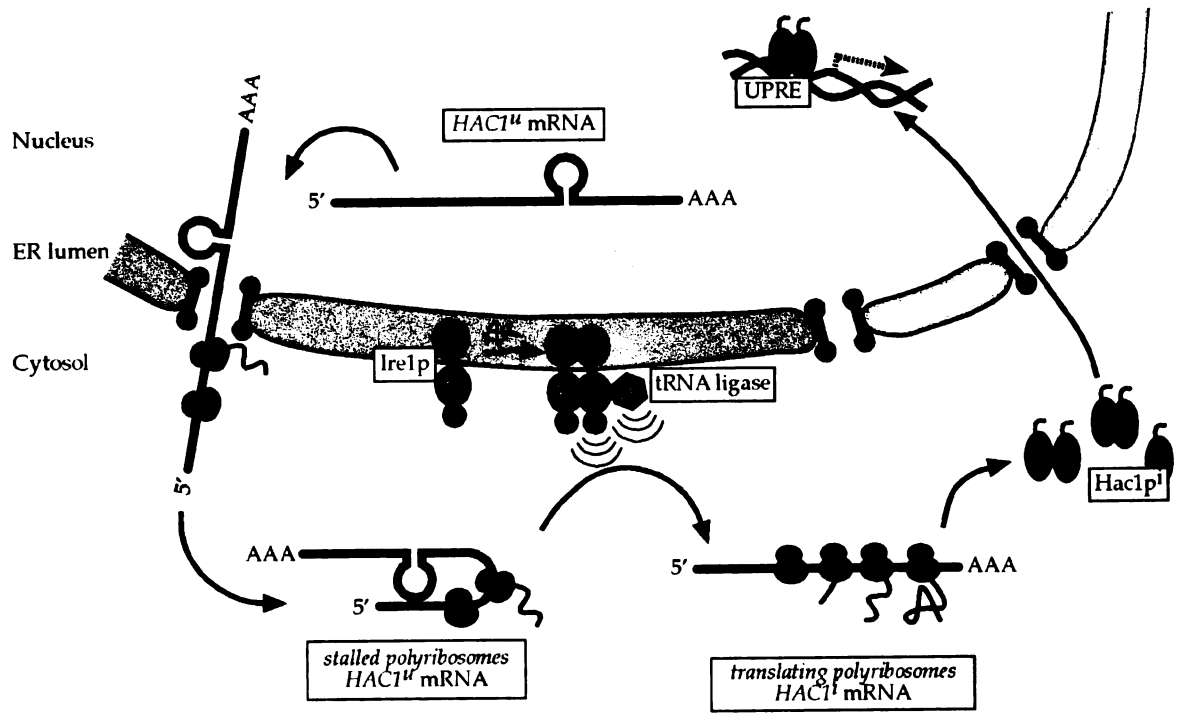
Nucleus
ER lumen
Cytosol
AAA
HAC1u mRNA
5′
AAA
UPRE
Ire1p
tRNA ligase
5′
Hac1p^i
AAA
5′
AAA
5′
stalled polyribosomes
HAC1u mRNA
translating polyribosomes
HAC1i mRNA

Figure 1-3: Many aspects of secretory pathway function are regulated by the UPR

A schematic diagram of the secretory pathway, with a classification of the genes identified as targets of the UPR (adapted from Travers *et al.* (2000)).

Figure 1-3

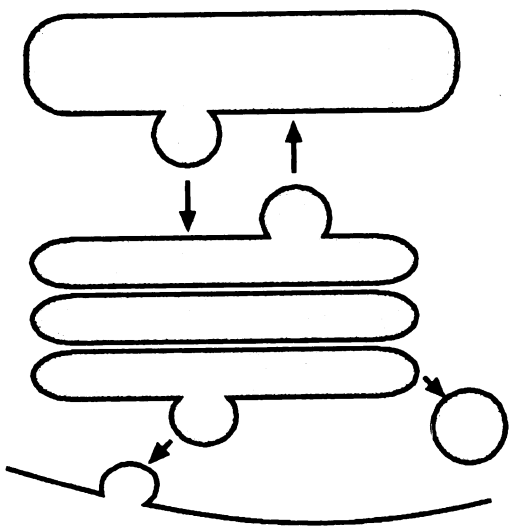

	(UPR targets)
Translocation	(7)
Lipid / Inositol	(19)
Protein Folding	(10)
Glycosylation ER	(17)
Protein Degradation	(6)
ER - Golgi Transport	(11)
Golgi - ER Retrieval	(5)
Glycosylation Golgi	(6)
Vaculolar Targeting	(7)
Distal Secretion	(9)
Cell Wall	(16)

Figure 1-4: *HAC1* encodes two different transcription factors

Upon UPR activation, the *HAC1*^{u} mRNA is spliced by Ire1p and tRNA ligase, removing a 252 base intron, to produce the *HAC1*^{i} mRNA. This message is robustly translated to produce the Hac1p^{i} transcription factor, which activates the expression of target genes. In the absence of UPR activation, the hypothetical Hac1p^{u} is not produced from *HAC1*^{u}, even though it differs from Hac1p^{i} only in the few amino acids at the carboxy terminus.

Figure 1-4

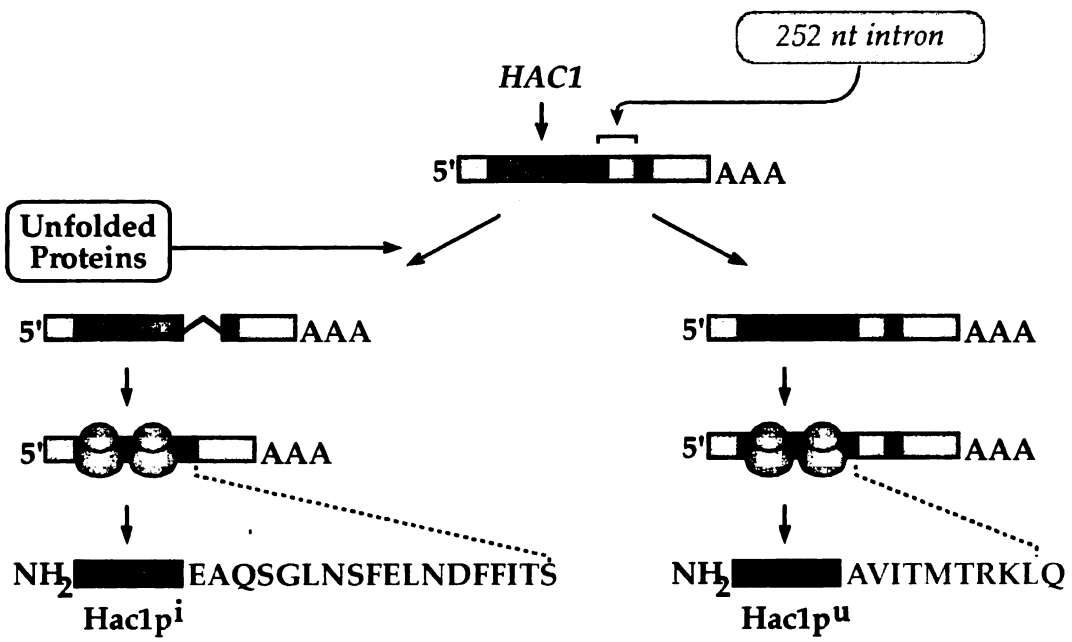
252 nt intron
HAC1
5'
AAA
Unfolded Proteins
5'
AAA
5'
AAA
5'
AAA
5'
AAA
NH2
EAQSGLNSFELNDFFITS
Hac1pi
NH2
AVITMTRKLQ
Hac1pu

Figure 1-5: A comparison of reporters used to study *HAC1* translation attenuation

The reporters used by Rowan Chapman (above the dashed red line), and those used in my attenuation studies (below the dashed line). Note that in the Chapman reporters, which meant to focus only on the action of the *HAC1* intron, the *HAC1* 5'UTR is also present.

Figure 1-5

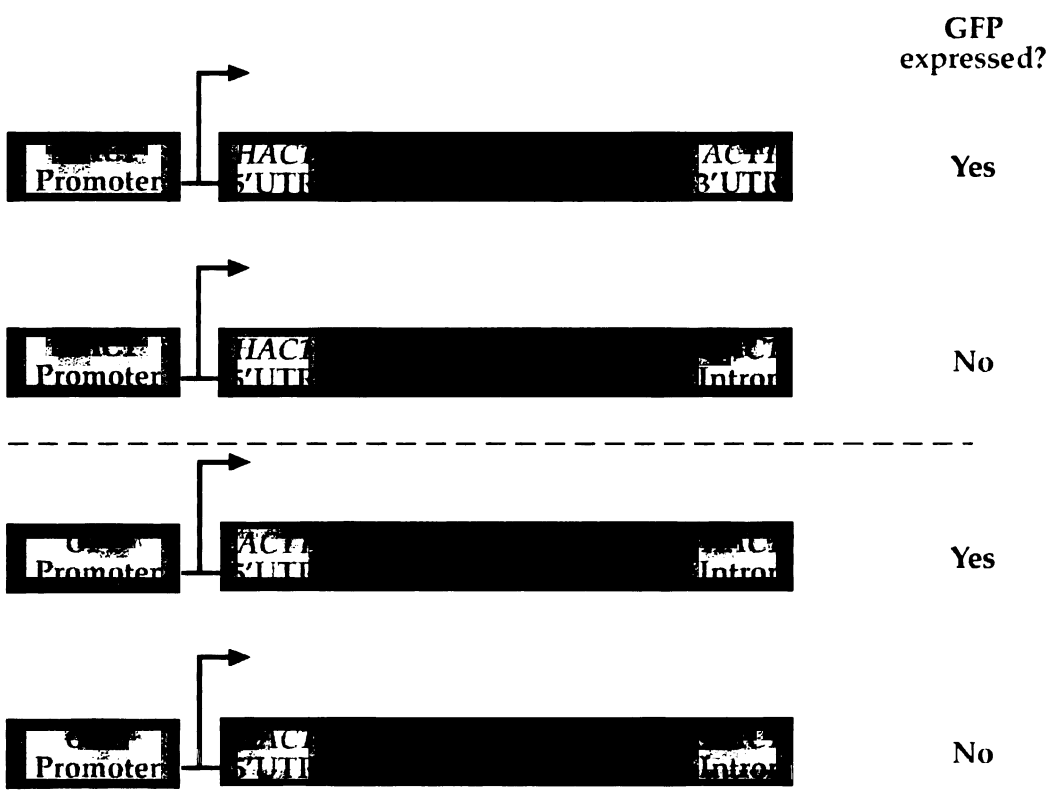

Figure 1-6: A predicted structure of the *HAC1*^{u} mRNA reveals potential base-pairing between the 5'UTR and the intron

A hypothetical structure of the *HAC1*^{u} mRNA was created, using the mfold program with help from Chris Patil. In many of the possible structures, unpaired regions were present at both the 5'UTR and the intron. Visual examination of these regions revealed extensive stretches of complementarity.

Figure 1-6

Predicted *HAC1* mRNA structure

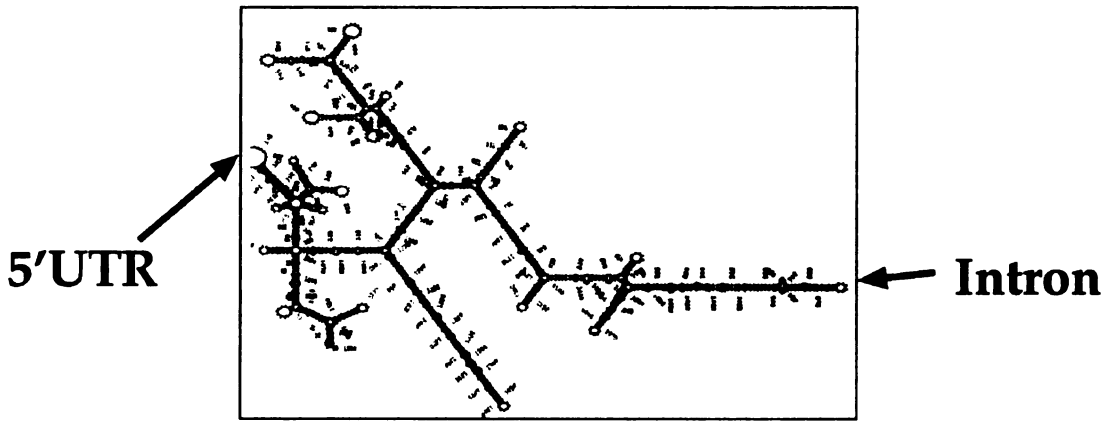

Intron

3′ **AAAUUGGCCGAGGAGGGGGUAGU**

5′ **AACAACCUCCUCCUCCCCCACCU**

5′ UTR

Figure 1-7: Direct base-pairing between the *HAC1* 5'UTR and intron is required for translation attenuation

The stretches of complementarity in the *HAC1* 5'UTR (blue icon) and intron (green icon) were mutated, and the resulting effect on translation attenuation was assayed by Western blot. Replacing the 5'UTR sequence with the complementary sequence form the intron (structure with two green icons, lanes 3 and 4), or replacing the intron sequence with the 5'UTR sequence (structure with two blue icons, lanes 5 and 6), resulted in derepression and subsequent expression of Hac1p^{u}. Replacing both regions with their counterpart, such that complementarity was restored, results in re-establishment of full translational attenuation (lanes 7 and 8).

Figure 1-7

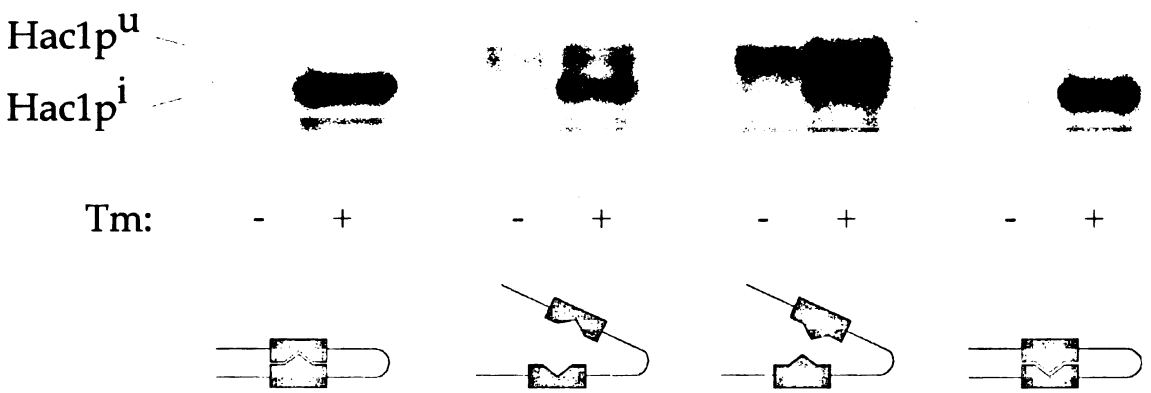

Figure 1-8: *pik1-100* upregulates *HAC1* abundance and is defective for secretion

(A) Northern analysis of *HAC1* mRNA in *pik1-100* and WT cells. The *pik1-100* mutant produces roughly 5-fold more *HAC1* mRNA than WT cells. (B) Invertase secretion assay. The *pik1-100* mutant secretes less efficiently than WT cells (compare 30% secretion of secreted invertase for *pik1-100*, vs. 60% for WT cells).

Figure 1-8

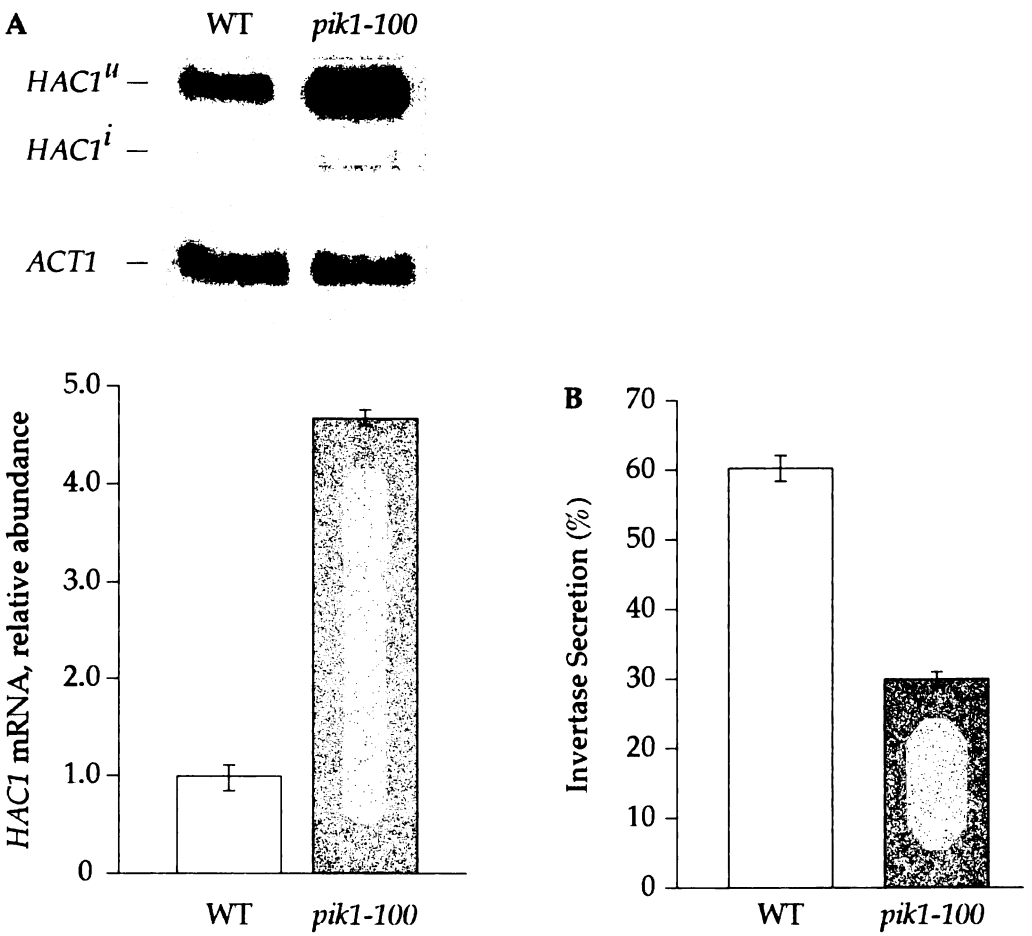
A
WT
pik1-100
HAC1u
HAC1i
ACT1
HAC1 mRNA, relative abundance
5.0
4.0
3.0
2.0
1.0
0
WT
pik1-100
B
Invertase Secretion (%)
70
60
50
40
30
20
10
0
WT
pik1-100

Chapter 2

Block of *HAC1* mRNA translation by long-range base pairing is released by cytoplasmic splicing upon induction of the unfolded protein response

Block of *HAC1* mRNA translation by long-range base pairing is released by cytoplasmic splicing upon induction of the unfolded protein response

Ursula Rüegsegger*, Jess H. Leber*, and Peter Walter#

Howard Hughes Medical Institute and
Department of Biochemistry and Biophysics
University of California at San Francisco
San Francisco, CA 94143-0448
USA

* Both authors contributed equally to this work

Corresponding author: phone: ++1-415-476-5017
fax: ++1-415-476-5233
e-mail: walter@cgl.ucsf.edu

Reprinted from Cell *107*, 103-114 (2001).

SUMMARY

Expression of the yeast transcription factor Hac1p, which controls the unfolded protein response, is regulated posttranscriptionally. Hac1p is only produced when an intron at the 3' end of its mRNA is removed by a non-conventional, regulated splicing reaction. We show that a previously unrecognized base-pairing interaction between the intron and the 5' untranslated region is required and sufficient to block mRNA translation. Unspliced *HAC1* mRNA is stable, located in the cytosol, and is associated with polyribosomes, yet does not produce protein, indicating that the ribosomes engaged on the mRNA are stalled. We show that the polysomal, cytoplasmic pool of *HAC1* mRNA is a substrate for splicing, suggesting that the stalled ribosomes may resume translation after the intron is removed.

INTRODUCTION

In eukaryotic cells, secreted and membrane-bound proteins are folded and assembled in the endoplasmic reticulum (ER). The protein-folding capacity of the ER is adaptable: when the capacity of the ER is exceeded and, as a result, unfolded proteins accumulate in the ER, an intracellular signaling pathway, the unfolded protein response (UPR), is induced. The UPR leads to the increased synthesis of ER-resident proteins required for protein folding as well as many other components of the secretory pathway (Travers et al., 2000), thus enabling the cell to cope with the increased load of unfolded proteins in the ER (reviewed in Kaufman, 1999; Mori, 2000; Urano et al., 2000; Patil and Walter, 2001).

In yeast, the expression of UPR-target genes is controlled by the UPR-specific transcription factor Hac1p (Cox and Walter, 1996; Kawahara et al., 1997). Hac1 protein is only detectable in cells when the UPR is induced, although its mRNA is present in uninduced and induced cells at comparable levels (Cox and Walter, 1996; Kawahara et al., 1997). The expression of Hac1p is therefore regulated posttranscriptionally. The key regulatory step to allow Hac1p synthesis upon UPR induction is the removal of an intron from *HAC1* mRNA by a non-conventional splicing mechanism. In this reaction, *HAC1* mRNA is cleaved at two splice sites by the transmembrane kinase/endonuclease Ire1p, and the thus liberated exons are then joined by tRNA ligase (Sidrauski and Walter, 1997). This splicing event is induced by the activation of Ire1p, which responds to the accumulation of unfolded proteins in the ER lumen (Cox et al., 1993; Mori et al., 1993; Welihinda and Kaufman, 1996; Shamu and Walter, 1996; Bertolotti et al., 2000).

Both the spliced (*HAC1*^{i}; "i" for *i*nduced) and the unspliced (*HAC1*^{u}; "u" for *u*ninduced) form of *HAC1* mRNA encode proteins, called Hac1p^{i} and Hac1p^{u}, respectively, which are identical except for their C-terminal tails. Splicing replaces a tail of 10 amino acids encoded in the intron of *HAC1*^{u} mRNA with a tail of 18 amino acids encoded in the second exon of *HAC1*^{i} mRNA. Only Hac1p^{i}, however, accumulates at detectable levels, while Hac1p^{u} is apparently not expressed.

Several lines of evidence from previous studies suggest that the expression of Hac1p^{u} is blocked at the translation level. *In situ* hybridization experiments localized *HAC1*^{u} mRNA primarily in the cytoplasm (Chapman and Walter, 1997), thus ruling out that *HAC1*^{u} mRNA is retained in the nucleus and can therefore not be translated. Also, a large portion of *HAC1*^{u} mRNA co-migrates with polyribosomes in sucrose gradients and can be immunoprecipitated with an antibody directed against an N-terminal epitope, demonstrating that the N-terminus of the protein is made and exposed outside the ribosome (Cox and Walter, 1996; Chapman and Walter, 1997). These results suggest that translation of Hac1p^{u} is initiated but that ribosomes then stall on the mRNA before translation is completed. The alternative explanation that Hac1p^{u} is synthesized but immediately degraded seems unlikely given that Hac1p^{u} can be produced in yeast cells from intron-less constructs and has a half-life similar to that of Hac1p^{i} ($t_{1/2}\cong 2$ min; Kawahara et al., 1997; Chapman and Walter, 1997).

Here we show that the *HAC1* mRNA intron represses translation of *HAC1*^{u} mRNA *in vivo* and *in vitro* by base pairing with the *HAC1* 5' UTR. We find that the cytoplasmic pool of *HAC1*^{u} mRNA is not a dead-end product but a substrate for the splicing reaction, indicating that splicing occurs in the cytoplasm on polyribosomes. The

finding that *HAC1*^{u} mRNA is polyribosome-associated, yet no protein is synthesized, parallels findings for the developmentally regulated *lin-14* and *nanos* mRNAs from *Caenorhabditis elegans* and *Drosophila melanogaster*, respectively (Olsen and Ambros, 1999; Clark et al., 2000). Understanding the mechanism by which the translation of *HAC1* mRNA is controlled may therefore have implications for regulatory events beyond the unfolded protein response.

RESULTS

Both the 5' UTR and intron of unspliced *HAC1*^{u} mRNA are required for translation attenuation

Previous studies showed that the *HAC1*^{u} mRNA intron represses expression of the green fluorescent protein (GFP) when placed in the 3' untranslated region (UTR) of a GFP-encoding mRNA (Chapman and Walter, 1997). The constructs used in those studies contained not only the *HAC1* intron but also the *HAC1* promoter and the *HAC1* 5' UTR followed by a small portion of the Hac1p N-terminus fused to GFP. To determine whether any elements in addition to the intron are necessary for translation attenuation, we expressed GFP (carrying no extra sequences) from a heterologous promoter with 5' UTR sequences derived either from *HAC1* or from Xenopus β-globin mRNA. For each 5' UTR, we made constructs that contained or lacked the *HAC1* intron. Our convention for naming constructs is as follows: the first three letters stand for the origin of the 5' UTR [i.e., "hac" for the *HAC1* 5' UTR and "glo" for the globin 5' UTR], the next three letters stand for the open reading frame (ORF) [i.e., "GFP" and "HAC" for Hac1p^u], and the last three letters for the sequences 3' of the ORF [i.e., "hac" for the *HAC1*^{u} 3' UTR, "int" for the *HAC1* intron followed by the *ACT1* 3' UTR, and "act" for the *ACT1* 3' UTR].

In agreement with previous results, cells showed only little fluorescence above background if they expressed GFP flanked by the *HAC1* 5' UTR and intron (Fig. 1, compare hac·GFP·int with the empty-vector control). Surprisingly, replacement of the *HAC1* 5' UTR by the globin 5' UTR (glo·GFP·int) relieved translation attenuation of

GFP to a similar degree as removal of the intron (hac·GFP·act), suggesting that both the *HAC1* 5' UTR and intron are required for translation attenuation. In both cases, cells were similarly fluorescent as cells expressing GFP flanked by the globin 5' UTR and the *ACT1* 3' UTR (glo·GFP·act).

To quantitate the effects of the *HAC1* 5' UTR and intron on GFP expression, we determined the mean fluorescence of the strains shown in Figure 1 by flow cytometry and measured the GFP mRNA levels by Northern blot (Table 1). From these data we calculated the fluorescence of each strain relative to the amount of GFP mRNA and found that the intron repressed GFP expression eight-fold if the 5' UTR was from *HAC1* (compare the normalized fluorescence of hac·GFP·int with that of hac·GFP·act) but had only a minor effect if the 5' UTR was from the heterologous globin mRNA (compare the normalized fluorescence of glo·GFP·int with that of glo·GFP·act). We therefore conclude that both the *HAC1* 5' UTR and intron are required for translation attenuation and that they act synergistically.

We next asked whether translation attenuation can be reconstituted *in vitro* in yeast translation extracts. We made four constructs similar to the GFP constructs described above but encoding HA-tagged Hac1p^{u} (HA-Hac1p^{u}). After *in vitro* transcription, we incubated equal amounts of capped mRNAs in nuclease-treated yeast *in vitro* translation extracts in the presence of [^{35}S]methionine and analyzed the products by SDS-polyacrylamide gel electrophoresis (SDS-PAGE) followed by autoradiography (Fig. 2A). As equal amounts of mRNA were added to each reaction, the amount of HA-Hac1p^{u} synthesized is a measure of the translation efficiency of each construct.

HA-Hac1p^u has a predicted molecular mass of 27 kDa but migrates abnormally slowly on SDS-polyacrylamide gels (Kawahara et al., 1997). In addition to the primary translation product (Fig. 2A, asterisk), multiple forms with higher molecular masses are expressed *in vivo* (Chapman and Walter, 1997) and *in vitro* (Fig. 2A, lanes 2 to 5). The multiple bands are different forms of HA-Hac1p^u, since they are recognized by an antibody directed against the HA epitope (data not shown) and likely correspond to differently phosphorylated species of the primary translation product (Chapman and Walter, 1997).

We observed that hac·HAC·hac was translated only inefficiently in yeast *in vitro* translation extracts (Fig. 2A, lane 2). Replacing the *HAC1*^{u} 3' UTR by the *ACT1* 3' UTR stimulated Hac1p^u synthesis five-fold (Fig. 2A, compare hac·HAC·hac with hac·HAC·act). This effect was robust: a five- to six-fold stimulation was observed over a wide range of mRNA concentrations and over the whole linear period of a time-course experiment, and it was unaffected by heat denaturation followed by snap cooling of the mRNAs prior to addition to the extracts (data not shown). *In vitro*, translation from the globin 5' UTR was two-fold less efficient than translation from the *HAC1* 5' UTR (Fig. 2A, compare glo·HAC·act with hac·HAC·act), but translation from this heterologous 5' UTR was unaffected by the *HAC1*^{u} 3' UTR (Fig. 2A, compare glo·HAC·act with glo-HAC·hac). While *in vitro* small amounts of Hac1p^u are still expressed from the hac-HAC·hac constructs, no Hac1p^u is detected *in vivo* in the absence of UPR induction. The reason for this apparently reduced efficiency of translation attenuation *in vitro* is unknown, but perhaps could be due to limiting amounts of a factor necessary to promote inhibition.

Taken together, these results show that *HAC1*^{u} mRNA is translationally attenuated *in vitro* and that attenuation requires sequences both 5' and 3' of the Hac1p^u ORF. The *cis*-acting elements at the 3' end are likely to be located in the *HAC1* intron, since the intron repressed GFP expression in the context of a heterologous 3' UTR (Fig. 1, Table 1).

A direct interaction of the *HAC1* 5' UTR and intron attenuates *HAC1*^{u} mRNA translation *in vitro*

The observation that the *HAC1* 5' UTR and intron act synergistically to attenuate translation suggested that they interact, either directly or indirectly. Such an interaction of regions at distant sites of the mRNA may be mediated by base pairing, by RNA-binding proteins, or both. Indeed, inspection of the intron for sequences complementary to the *HAC1* 5' UTR revealed a G-rich stretch of 19 nucleotides (nt), 16 of which could potentially base pair with the 5' UTR (Fig. 2B).

We therefore asked next whether translation attenuation by the *HAC1* 5' UTR and intron is mediated by the base pairing proposed in Figure 2B. If this base pairing is required for translation attenuation, disrupting the 5' UTR-intron interaction by annealing an oligonucleotide to the sequences predicted to be involved should relieve translation attenuation of *HAC1*^{u} mRNA. To test this prediction, 10- and 100-fold molar excesses of 2'-O-methyl oligoribonucleotides were preannealed to hac·HAC·hac or hac·HAC·act mRNAs, which were then added to translation extracts (Fig. 2C). Since it was shown previously that oligonucleotide-mRNA hybrids located within the 5' UTR, but not the 3' UTR, inhibit translation *in vitro* (Johansson et al., 1994), we first looked at the effect

of an oligonucleotide complementary to the intron sequences shown in Figure 2B (anti-intron). This oligonucleotide stimulated translation of hac·HAC·hac such that it was now as efficiently translated as hac·HAC·act (Fig. 2C, compare lane 6 with lane 9 or 13) but had no effect on the translation of hac·HAC·act (Fig. 2C, compare lanes 12 and 13 with lane 9). As expected, a non-specific oligonucleotide, which carried sequences from the *HAC1* ORF (sense-ORF), had no effect on translation of hac·HAC·hac (Fig. 2C, compare lanes 3 and 4 with lane 2) or hac·HAC·act (Fig. 2C, compare lanes 10 and 11 with lane 9). These results show that the intron sequences targeted by the anti-intron oligonucleotide are necessary for the attenuation of *HAC1*" mRNA translation.

As predicted from previous experiments (Johansson et al., 1994), an oligonucleotide complementary to the *HAC1* 5' UTR and targeted to the same site as the intron (anti-5' UTR) inhibited translation of both constructs (Fig. 2C, lanes 7, 8, 14, 15). The inhibition caused by the anti-5' UTR oligonucleotide was virtually complete, whereas the *HAC1* intron when present in *cis* in the mRNA attenuated translation only five- to six-fold (Fig. 2C, compare lane 2 with lane 9). The stronger inhibitory effect of the oligonucleotide is perhaps due to the fact that an oligonucleotide is more flexible than the corresponding stretch of nucleotides as part of a long RNA, in which structural and topological constraints may hinder complete base pairing over an extended region. For *HAC1* mRNA incomplete base pairing may be essential to allow the dissociation of the intron and 5' UTR after excision of the intron from the RNA upon splicing.

Disruption of the interaction between the *HAC1* 5' UTR and intron leads to the accumulation of Hac1p" *in vivo*

If the intron sequences targeted by the anti-intron oligonucleotide are required for translation attenuation of *HAC1*^{u} mRNA *in vivo*, then mutating those nucleotides should relieve translation attenuation and lead to the accumulation of Hac1p^{u}. Furthermore, if the intron sequences inhibit translation by interacting with the 5' UTR, then introducing mutations in the 5' UTR compensatory to the mutations in the intron should restore repression. To test these predictions, we generated three mutant forms of HA-*HAC1* mRNA (Fig. 3A). To mutate the intron, we replaced the intron sequences with sequences from the 5' UTR (pJL179). To restore base pairing in the intron mutant, we introduced compensatory mutations in the 5' UTR by replacing the 5' UTR sequences with sequences from the intron (pJL177). We also constructed a mutant in which only the 5' UTR was mutated (pJL178). This mutant is predicted to behave as the intron mutant except that the two mutants differ in the sequences of their 5' UTRs and may therefore differ in the efficiency with which they are translated.

We introduced the three mutants or, as a control, wild-type HA-*HAC1* [pJC316 (Cox and Walter, 1996)] on plasmids into a Δ*hac1* strain and asked first whether the mutant and wild-type mRNAs were expressed at comparable levels and whether the mutations affected splicing upon UPR induction. Northern blot analysis revealed that the amounts of HA-*HAC1* mRNA in uninduced cells were two- to four-fold lower in the strains with disrupted base pairing than in the strains with intact base pairing (Fig. 3B, compare lanes 1 and 7 with lanes 3 and 5). Upon UPR induction, HA-*HAC1* mRNA levels increased in all strains between 1.4- and 3.5-fold (for example, compare lanes 3 and 4). Whether these effects were due to transcriptional regulation, to differences in mRNA stability, or to a combination of the two remains to be investigated.

Splicing efficiency of the forms of HA-*HAC1* mRNA with intact 5' UTR-intron base pairing was above 80% (Fig. 3B, lanes 2 and 8). In contrast, splicing efficiency in the mutants with disrupted base pairing was reduced to ~40% and ~60%, respectively (Fig. 3B, lanes 4 and 6). Thus, the 5' UTR-intron interaction is necessary for efficient *HAC1* mRNA splicing.

We next monitored the expression of HA-Hac1p in uninduced and UPR-induced cells by Western blot with an antibody directed against the HA tag (Fig. 3C). As expected, no protein was synthesized at detectable levels from the wild-type plasmid in uninduced cells (pJC316; Fig. 3C, top and middle panel, lane 1; the band indicated with an open arrowhead is unrelated to HA-Hac1p). Removal of the intron by splicing after induction of the UPR with dithiothreitol (DTT) led to the synthesis of HA-Hac1p^{i} (Fig. 3C, lane 6, marked with a diamond in the bottom panel).

Intriguingly, when the base pairing was disrupted by mutations in either the intron (pJL179) or the 5' UTR (pJL178), HA-Hac1p^{u} accumulated in uninduced cells (Fig. 3C, middle panel, lanes 2 and 3). The multiple forms of HA-Hac1p^{u} (indicated by brackets and shown enlarged in the bottom panel of Fig. 3C) co-migrated by SDS-PAGE with HA-Hac1p^{u} expressed constitutively from an intron-less construct described previously [pJC834 (Chapman and Walter, 1997); Fig. 3C, bottom panel, lane 5]. Less protein was synthesized from the 5' UTR mutant, indicating that translation from this 5' UTR is less efficient than from the wild-type 5' UTR. Importantly, no Hac1p was synthesized in uninduced cells if the base pairing was restored by compensatory mutations in both the intron and the 5' UTR (pJL177; Fig. 3C, top and middle panel, lane 4). For this construct, induction of the UPR resulted in synthesis of HA-Hac1p^{i} (Fig. 3C, lane 9), thus

recapitulating the wild-type situation. Both mutants in which the base pairing between the 5' UTR and intron was disrupted expressed a mixture of HA-Hac1p^u and HA-Hac1p^i upon UPR induction (Fig. 3C, lanes 7 and 8; compare lane 7 with lanes 5 and 6 in the enlargement), which is not surprising given that these cells contained comparable amounts of HA-*HAC1*^{u} and HA-*HAC1*^{i} mRNA and that the mutant forms of HA-*HAC1*^{u} mRNA were efficiently translated in uninduced cells.

For all strains, the differences in protein levels correlated with the differences in mRNA levels as confirmed by quantitation of Western blots (data not shown), if mRNAs with identical 5' UTR sequences were compared. Most importantly, our data show that if the base-pairing interaction was disrupted by mutating the intron, the mutant *HAC1*^{u} mRNA was translated in uninduced cells with an efficiency comparable to that of wild-type *HAC1*^{i} mRNA produced by splicing: the level of Hac1p^u in mutant uninduced cells was five-fold lower than that of Hac1p^i in wild-type UPR-induced cells as determined by quantitative Western blot analysis with a radio-iodinated secondary antibody (data not shown), and the mRNA level in mutant cells was six-fold lower than that in wild-type cells (Fig. 3B, compare lane 3 with lane 2). Qualitatively, these conclusions are confirmed by the Western blot analysis shown in Figure 3D: to give an approximately equal ECL signal intensity, we needed to load 4- to 8-fold more total protein per gel lane from the mutant than from the wild-type strain (compare lane 1 with lanes 2 and 3).

Thus taken together, the data presented so far argue that the *HAC1* 5' UTR interacts with the *HAC1* intron by base pairing and that this interaction is the primary, if not only, determinant of *HAC1*^{u} mRNA translation attenuation.

Base pairing of the *HAC1* 5' UTR and intron diminishes the loading of ribosomes onto *HAC1*^{u} mRNA

To a first approximation, the efficiency of translation of an mRNA correlates with the number of ribosomes that are engaged with it. To determine the degree to which ribosome association of *HAC1*^{u} mRNA changes when the *HAC1* 5' UTR-intron interaction is disrupted, we fractionated polyribosomes from the wild-type and mutant strains described in Figure 3 by sedimentation in sucrose gradients. We isolated total RNA from all fractions across the gradients and analyzed it by Northern blot (Fig. 4A). Wild-type *HAC1*^{u} mRNA fractionated into two pools: about half (42%) of *HAC1*^{u} mRNA was recovered from the top of the gradient and therefore was not ribosome-associated (pJC316; fractions 1 to 4 in Fig. 4A; quantitation in Fig. 4B). The remainder (58%) was recovered from heavier fractions indicating occupancies ranging from one to ten or more ribosomes per mRNA (pJC316; fractions 5 to 14 in Fig. 4A; Fig. 4B). In contrast, if the intron was mutated so that it could no longer base pair with the 5' UTR, only a small amount (9%) of *HAC1*^{u} mRNA was recovered from the top of the gradient, whereas the majority of the mRNA (91%) was ribosome-associated (pJL179; fractions 5 to 14 in Fig. 4A; Fig. 4B). A similar distribution over the gradient was found for the 5' UTR mutant (pJL178; Fig. 4B). Restoring the base pairing by mutating both the *HAC1* 5' UTR and intron reestablished the degree of ribosome association found for the wild-type construct (compare pJL177 with pJC316 in Fig. 4B). These data suggest that the base pairing of the *HAC1* 5' UTR and intron diminishes ribosome loading onto *HAC1*^{u} mRNA.

Moreover, the data also underscore a previously raised paradox: if 58% of wild-type *HAC1*^{u} mRNA was indeed translated as the polyribosome profile in Figure 4A suggests and if translation occurred at the same rate as translation of the mutants with disrupted base pairing, then Hac1p^u should accumulate in wild-type cells at detectable levels, which is not what we observe. We estimate that, if *HAC1*^{u} mRNA was translated at even 10% of the rate of the base-pair-disrupted mutant mRNA, Hac1p^u would have been readily detectable by Western blot analysis.

To provide independent evidence that the portion of *HAC1*^{u} mRNA sedimenting as high-molecular-mass complexes is indeed ribosome-associated, we determined whether *HAC1*^{u} mRNA co-profiles with the UV absorbance reflective of the position of mRNAs associated with one ribosome, two ribosomes, etc. To this end, we collected many small fractions from the middle of a gradient and determined the presence of *HAC1*^{u} mRNA by Northern blot analysis. As shown in Figure 4C, the distribution of *HAC1*^{u} mRNA is discontinuous, with peaks and valleys precisely following the position of ribosomes.

Taken together, the data show that *HAC1*^{u} mRNA is associated with ribosomes that are not actively translating.

The cytoplasmic pool of *HAC1*^{u} mRNA is a substrate for splicing

The peculiar disposition of the unspliced *HAC1*^{u} mRNA on stalled, cytoplasmic polyribosomes raises the question of whether these polyribosomes have a physiological role in the cell. On one hand, *HAC1*^{u} polyribosomes could be dead-end products that are permanently arrested and eventually decay; all spliced *HAC1*^{i} mRNA would thus result

from newly transcribed *HAC1*^{u} mRNA. On the other hand, we can envision positive functions for the cytoplasmic polysomal pool of *HAC1*^{u} mRNA. For example, *HAC1*^{u} mRNA might be translated to produce Hac1p^u in response to some unknown physiological stimulus that leads to disruption of the base pairing of the 5' UTR and intron, thus allowing translation. An alternative and not mutually exclusive possible function for the cytoplasmic pool of *HAC1*^{u} mRNA is that it is the precursor of spliced *HAC1*^{i} mRNA.

To address this latter scenario experimentally, we determined whether *HAC1*^{u} mRNA could be spliced after transcription was inhibited. To this end, we took advantage of a temperature-sensitive allele of the largest subunit of RNA polymerase II (*rpb1-1*), which allowed us to shut off transcription by shifting the cells to the non-permissive temperature of 37°C (Nonet et al., 1987). In the experiment shown in Figure 5A, we induced the UPR by the addition of DTT 10, 20, and 40 min after a shift to 37°C and followed the effect of the DTT treatment on *HAC1* mRNA by Northern blot in a time-course experiment. *HAC1*^{u} mRNA decayed with a $t_{1/2}$ of ~25 min while, as expected, the levels of the RNA polymerase III transcript *SCR1* RNA remained unchanged (data not shown). Upon addition of DTT, *HAC1*^{u} mRNA was efficiently spliced (50-65% splicing within 5 min). Most importantly, splicing efficiency did not diminish appreciably when the UPR was induced as much as 40 min after the transcriptional block. Thus, splicing was still efficient even after almost two half-lives of the mRNA had passed and any transient nuclear pool of freshly transcribed mRNA should have been depleted by export to the cytoplasm. Given that *in situ* hybridization experiments showed that *HAC1*^{u} mRNA is primarily localized in the cytoplasm (Chapman and Walter, 1997), the efficient splicing

of *HAC1* mRNA in the absence of *de novo* transcription suggests that *HAC1*^{i} mRNA is produced by splicing of the cytoplasmic pool of *HAC1*^{u} mRNA.

To test whether polyribosome-assocated *HAC1* mRNA can be a substrate for cleavage and ligation *in vivo*, we froze translating ribosomes on their respective mRNAs with the elongation inhibitor cycloheximide, thus preventing the running-off as well as the loading of ribosomes onto the mRNA, and then added DTT to induce the UPR. After UPR induction in the presence of cycloheximide, any spliced *HAC1* mRNA that is associated with polyribosomes must have been polyribosome-associated prior to and during the splicing reaction. We found, however, that after cycloheximide pre-treatment, cells were completely refractory to UPR induction by DTT (data not shown). We reasoned that, as a consequence of inhibition of protein synthesis by cycloheximide, the ER may be depleted of proteins since no proteins are imported into the ER but export into the secretory pathway continues. Addition of the reducing agent DTT would therefore fail to induce the UPR after cycloheximide pre-treatment. To alleviate this problem, we took advantage of a temperature-sensitive allele of *SEC12*, which is required for vesicle transport from the ER to the Golgi (Oka et al., 1991; Novick et al., 1980). When the *sec12-1* cells were first shifted to the non-permissive temperature, at which protein export from the ER into the secretory pathway is blocked, and then treated with cycloheximide to freeze ribosomes on mRNAs, subsequent addition of DTT was now able to induce the UPR.

We therefore used this extended experimental protocol to assess whether polyribosome-associated *HAC1* mRNA is a substrate for the splicing reaction. To this end, we induced the UPR with DTT *sec12-1* cells that were first shifted to 37°C for 2

minutes and then cycloheximide-treated to freeze polyribosomes (Fig. 5B). We then fractionated on sucrose gradients cell extracts prepared at different times after DTT addition and analyzed fractions by Northern blot. As expected, in the absence of DTT, polyribosome-associated *HAC1* is unspliced ("*HAC1*^{u}", Fig. 5B top). In contrast, as a function of time after DTT addition, increasing amounts of spliced *HAC1*^{i} mRNA were produced (Fig. 5B, lower panels). Importantly, virtually all spliced *HAC1*^{i} mRNA produced in the presence of cycloheximide was polyribosome-associated, thus supporting the notion that cytoplasmic, polyribosome assciated *HAC1*^{u} mRNA can be spliced.

DISCUSSION

We have demonstrated both *in vitro* and *in vivo* that a long-range base-pairing interaction between the *HAC1* mRNA intron and 5' UTR is required for attenuation of translation of unspliced *HAC1*^{u} mRNA. In particular, we have shown that upon disruption of the interaction by mutation, Hac1p^u is synthesized from the unspliced mRNA with approximately the same efficiency as Hac1p^i from the spliced mRNA. Thus, base pairing between the *HAC1* mRNA intron and 5' UTR is key to preventing Hac1p from being synthesized unless the intron is removed by splicing upon accumulation of unfolded proteins in the ER. In agreement with previous studies, we found a large portion of the cellular *HAC1*^{u} mRNA engaged in polyribosomes, which, we propose, must be translationally arrested as no Hac1p^u can be detected in these cells. Moreover, we show that splicing does not require *de novo* transcription and that polyribosome associated *HAC1*^{u} mRNA is a substrate for splicing *in vivo*. Taken together with the observation that the cellular pool of *HAC1*^{u} mRNA has been localized to the cytoplasm by *in situ* hybridization experiments (Chapman and Walter, 1997), these results suggest that *HAC1*^{u} mRNA splicing is a cytoplasmic event.

Inhibition of translation by the interaction of the 5' and 3' UTRs of an mRNA may be a generally applicable principle. Several natural and artificial cases have been described for yeast, plant, and animal cells (Spena et al., 1985; Kozak, 1989; van den Heuvel et al., 1990; Vega Laso et al., 1993). Moreover, considering the 5' UTR as an anti-sense RNA targeted against the intron to repress translation points to a striking parallel between translation attenuation of *HAC1*^{u} mRNA and the developmental regulation of *lin-14* expression in *Caenorhabditis elegans*: the small, non-coding *lin-4*

RNA represses the expression of *lin-14* posttranscriptionally by base-pairing with its 3' UTR (Lee et al., 1993; Wightman et al., 1993). As is the case for *HAC1*^{u} mRNA, the repressed *lin-14* mRNA is polyribosome-associated, and part of *lin-4* RNA co-sediments with polyribosomes (Olsen and Ambros, 1999). Stalling ribosomes by an anti-sense mechanism involving the 3' UTR may therefore be a more general way to inhibit translation.

The accumulation of *HAC1*^{u} mRNA on polyribosomes is puzzling, however, in light of the fact that the proposed translational regulation through the long-range base-pairing interaction involves the 5' UTR: as small ribosomal subunits have to traverse the 5' UTR to reach the start codon, one would expect a base-pairing interaction involving the 5' UTR to inhibit ribosome loading. Strong secondary structure elements or proteins bound to the 5' UTR are known to inhibit initiation of other mRNAs (reviewed in Gray and Wickens, 1998). Indeed, when we compared intron-containing and intron-less versions of *HAC1*^{u} mRNA in *in vitro* translation reactions, translation was impaired at the initiation step (data not shown). How then could one explain that a large portion of *HAC1*^{u} mRNA becomes engaged in polyribosomes *in vivo*?

One possible scenario is that those ribosomes are loaded onto *HAC1*^{u} mRNA before the base pairing is established (Fig. 6). In higher eukaryotes, mRNAs are exported from the nucleus 5' end first, and ribosomes engage with the leading ends of the mRNAs as soon as they reach the cytoplasm (Mehlin et al., 1992). Ribosomes may thus start immediately translating *HAC1*^{u} mRNA during the export of the mRNA from the nucleus to the cytoplasm, while the 3' end of the message is still in the nucleoplasm. Only after the 3' UTR of *HAC1*^{u} mRNA is exported to the cytosol can the intron interact with the

5' UTR. As the long-range base-pairing interaction is formed, it might not only inhibit the loading of new ribosomes but also stall and trap those ribosomes that are already engaged on the mRNA, possibly through inducing the formation of tight secondary and tertiary structural elements that the ribosomes cannot traverse.

The notion that the high-molecular-mass complexes with which *HAC1*^{u} mRNA is associated are indeed polyribosomes is strongly supported by the co-profiling experiment shown in Figure 4C. Moreover, as has been shown previously, a large portion of HA-*HAC1*^{u} mRNA can be immunoprecipitated with antibodies directed against the HA epitope, indicating that each of these mRNAs contains at least one functionally engaged ribosome displaying the N-terminus of HA-Hac1p^{u} (Chapman and Walter, 1997). However, in addition to the polyribosome-associated pool, we also isolated *HAC1*^{u} mRNA in a ribosome-free form (Fig. 4A). What is the origin of the two *HAC1*^{u} mRNA pools?

Since no significant nuclear pool of *HAC1*^{u} mRNA was detected by *in situ* hybridization (Chapman and Walter, 1997), both the ribosome-free and the polyribosome-associated pool of *HAC1*^{u} mRNA are likely to reside in the cytoplasm. With this premise, two scenarios could account for the heterogeneous distribution of *HAC1*^{u} mRNA in sucrose gradients. First, upon nuclear export, some *HAC1*^{u} mRNA molecules may escape ribosome loading. The distribution between the ribosome-free and the polyribosome-associated pool would then depend on the ratio of the nuclear export and the translation initiation rates. Alternatively, upon nuclear export all *HAC1*^{u} mRNAs may become polyribosome-associated at first, but the stalled ribosomes eventually fall off, either *in vivo* or upon cell fractionation, thus generating the two pools.

Mutant *HAC1"* mRNAs from which the translation block was removed by disrupting the 5' UTR-intron interaction also showed a splicing defect (Fig. 3B). The 5' UTR-intron interaction is therefore not only essential to repress Hac1p expression in uninduced cells but also to allow efficient splicing and Hac1p synthesis upon UPR induction. Base pairing may thus provide an additional - and until now unrecognized - *cis*-acting element for *HAC1* mRNA splicing, which is not essential but stimulatory. According to this view, the 5' UTR-intron interaction might be required to correctly position the splice sites in the stem-loop structures which have been shown to be essential for splicing *in vitro* (Gonzalez et al., 1999). Alternatively, the inhibition of splicing by disrupting the intron-5' UTR base pairing may be a consequence of the relief of the translational stall: since the 5' splice site is contained within the 3' end of the *HAC1"* ORF, the passage of translating ribosomes might prevent the 5' splice site from assuming a suitable secondary structure and thus prevent cleavage. Indeed, in the mutants with disrupted base pairing, significant amounts of a smaller form of *HAC1* mRNA accumulated upon UPR induction (marked with one asterisk in Fig. 3B). Based on its size and hybridization with a 5' exon-specific probe, this band is likely to correspond to the 5' exon-intron splicing intermediate (Cox and Walter, 1996; Sidrauski et al., 1996), indicating that cleavage at the 5' splice site is impaired in the base pair-disrupted *HAC1"* mRNA mutants. In agreement with this interpretation, splicing was more severely impaired in the mutant that was more efficiently translated (Fig. 3B and C, compare pJL179 and pJL178). Attenuation of translation may therefore be essential to keep *HAC1"* mRNA in a fully splicing-competent state.

Intriguingly, splicing can occur on *HAC1*^{u} mRNA associated with stalled ribosomes. The notion that polyribosome-associated *HAC1*^{u} mRNA is a splicing substrate further underscores the view that splicing is a cytoplasmic event. The disposition of Ire1p as an integral ER-membrane protein with its nuclease domain facing the cytoplasm is consistent with a cytoplasmic mechanism. tRNA ligase has been localized to the nucleus but, upon overexpression, was also detectable in the cytoplasm (Clark and Abelson, 1987). It is therefore likely that a sufficient amount of tRNA ligase is constitutively located in the cytoplasm or that tRNA ligase shuttles between the two compartments. Cytoplasmic splicing of polyribosome-associated *HAC1*^{u} mRNA thus is a plausible mechanism, although we cannot rule out that nuclear splicing of newly transcribed mRNA can also occur. Ribosomes that are pre-initiated and stalled on *HAC1*^{u} mRNA could finish translation after the intron is removed, thus leading to a rapid initial burst of Hac1p^{i} synthesis, perhaps to provide cells with an exceedingly rapid response to changing needs in the ER.

EXPERIMENTAL PROCEDURES

Plasmids

GFP constructs. All parts of the following constructs were generated by PCR amplification, sequenced and assembled between the PstI and ApaI sites of pRS315. Expression is driven by the GPD promoter (nt –676 to –37 of *TDH3* flanked by a PstI site at the 5' and a SmaI site at the 3' end; +1 refers in all constructs to the first nucleotide of the start codon of the corresponding gene). The 5' UTR is either from *HAC1* (nt –67 to —1; nt –67 corresponds to the 5' end of both *HAC1*^{u} and *HAC1*^{i} mRNA as mapped by primer extension and S1 analysis) or from the Xenopus β-globin gene (as present in pSPUTK) and flanked by SmaI and XbaI sites at the 5' and 3' end, respectively. The ORF of GFP is cloned downstream of the XbaI site and is followed by the *ACT1* 3' UTR (the *ACT1* stop codon plus 381 nt). In some constructs the *HAC1* intron (flanked by 37 nt of the 5' and 29 nt of the 3' exon) is inserted between the stop codon of GFP and the *ACT1* 3' UTR.

HAC1 constructs for in vitro transcription/translation. All inserts were cloned 3' of the SP6 promoter and 5' of the KpnI site of pSPUTK and carry a poly(A) tail at the 3' end. The poly(A) tail is flanked by a NotI site at the 5' end and a XbaI site at the 3' end, which allows the production of transcripts without or with poly(A) tail. The *HAC1* sequences are based on pJC316 (Cox and Walter, 1996). The anticipated sequences of the inserts were confirmed by sequencing. pUR10 (hac·HAC·hac; used for the experiment in Fig. 2) contains the first 5 nt of the pSPUTK 5' leader sequence followed by nt –75 to +1273 of HA-*HAC1*. pUR6 (hac·HAC·hac; used for the experiment

in Fig. 2C) is as pUR10 but contains nt –75 to +1397 of HA-*HAC1*. pUR11 (glo·HAC·hac) contains the entire 5' leader sequence of pSPUTK followed by nt +1 to +1273 of HA-*HAC1*. pUR9 (hac·HAC·act) is as pUR10 up to the Hac1p^{u} stop codon, which is followed by a linker of 32 nt and the *ACT1* 3' UTR as described for the GFP constructs. pUR8 (glo·HAC·act) is as pUR11 up to the Hac1p^{u} stop codon, which is followed by a linker of 32 nt and the *ACT1* 3' UTR as described for the GFP constructs.

HAC1 5' UTR-intron interaction mutants. Mutations were introduced into pJC316 with the QuikChange site-directed mutagenesis kit (Stratagene) and confirmed by sequencing. The following three plasmids are identical with pJC316 except for the regions indicated: pJL178: nt –38 to –22 of HA-*HAC1* were replaced with 5' TTGGCCGAGGAGGGGGT 3'; pJL179: nt +796 to +815 of HA-*HAC1* were replaced with 5' ACCCCCTCCTCCTCCAAAA 3'; pJL177 carries the mutations of both pJL178 and pJL179.

2'-O-Methyl oligoribonucleotides

2'-O-methyl oligoribonucleotides with the following sequences were used in *in vitro* translation experiments: 5' UCUCUUGACGAGUACAGGGAU 3' (sense-ORF), 5' GGUGGGGGAGGAGGAGGUU 3' (anti-5' UTR), 5' AACCGGCUCCUCCCCCAUC 3' (anti-intron).

Isolation of total RNA and Northern blot analysis

Total RNA for Northern blot analysis was isolated from yeast cells with a scaled-down and simplified version of the hot-phenol extraction procedure described by Köhrer and Domdey (1991). Northern blot analysis was carried out as described (Cox and Walter, 1996) but blots were washed in 2x SSC with 0.1% w/v SDS and quantitated on a Storm 840 imaging system with the ImageQuant software v1.2 (Molecular Dynamics). The amount of splicing was defined as the ratio of *HAC1*^{i} and the sum of *HAC1*^{u} and *HAC1*^{i} multiplied by 100 (% splicing).

All probes were generated by PCR amplification and were labeled with [α-^{32}P]dCTP and Ready-To-Go DNA labelling beads (Pharmacia Biotech). The GFP probe was directed against the coding region of GFP, the *SCR1* probe against the full-length *SCR1* RNA, the *HAC1*-5' exon/intron probe against nt –45 to +986 of *HAC1*, the *HAC1*-5' exon probe against nt –45 to +626 or nt +375 to +653 of *HAC1*.

Isolation of proteins from yeast cells

Cells were collected from cultures by filtration, frozen in liquid nitrogen and disrupted in ~500 μl 8 M urea by vortexing for 5 min at 4°C in the presence of 500 μl 0.5 mm Zir/Silica beads. After adding 75 μl 20% w/v SDS, the samples were boiled for 5 min and the lysates cleared by centrifugation at 20800 x g for 5 min at room temperature. The protein concentrations of the lysates were determined with the BCA protein assay from Pierce.

Analysis of GFP-expressing strains

Analysis on plates. The yeast strain W303 (*MAT A, ade2-1, trp1-1, can1-100, leu2-3, -112, his3-11, -15, ura3)* was transformed with pRS315 carrying no insert or one of the four GFP constructs, plated on selective minimal medium without leucine and the plate scanned with the fluorescent scanner FluorImager SI (emission filter 530 DF 30; Molecular Dynamics).

Analysis in liquid. The same strains as analyzed on a plate were grown in selective minimal medium without leucine to optical densities at 600 nm (OD_{600}) of 0.3 to 0.7. The cultures were sonicated immediately prior to analysis and the fluorescence of the cells measured with a Becton Dickinson FACScan flow cytometer. The mean fluorescence of uniform cell populations was determined with the software CellQuest v3.3. The amount of mRNA encoding GFP relative to the amount of *SCR1* RNA was determined from aliquots of the same cultures by Northern blot analysis.

In vitro transcription

Plasmids pUR6, pUR8, pUR9, pUR10 and pUR11 were linearized with NotI and used as templates in *in vitro* transcription reactions. Capped RNA transcripts were prepared with SP6 RNA polymerase in the presence of $m^7G(5')ppp(5')G$ according to standard procedures. Note that transcription from NotI-linearized pUR6 terminates prematurely leading to a uniform population of transcripts of ~1400 nt. The transcripts were purified by extracting with phenol/chloroform and subsequent ethanol precipitation and resuspended in water. The RNA concentrations were calculated based on the absorbance at 260 nm and the relative amounts and the integrity of the transcripts were verified by Northern blot analysis.

In vitro translation

Yeast extracts for *in vitro* translation experiments were prepared from strain yAS1874 (*MATa, ade2, his3, leu2, trp1, ura3, mak10::URA3, pep4::HIS3, Δprb1, Δprc1*; a kind gift from Dr. Alan Sachs) according to Tarun Jr. and Sachs (1995) with the following modifications: cells from 1 l of an OD_{600}=1.5 yeast culture in YPD were harvested by centrifugation at 4°C and washed four times. Buffer A contained 30 mM HEPES-KOH (pH 7.4), 100 mM KOAc, 2 mM $Mg(OAc)_2$, 0.5 mM DTT, 0.5 mM phenylmethylsulfonyl fluoride (PMSF), 0.4 μg/ml leupeptin hemisulfate and no mannitol throughout the whole procedure.

15 μl *in vitro* translation reactions were set up as described by Tarun Jr. and Sachs (1995) with nuclease-treated extract, 200 fmol capped RNA and 3.6 to 5 μCi L-[^{35}S]methionine instead of unlabeled methionine. The samples were incubated at room temperature (26°C) and the reactions stopped at the time indicated by mixing with equal volumes of 2x SDS-protein gel sample buffer. 5 to 15 μl aliquots of the stopped reactions were separated by electrophoresis through 10-15% SDS-polyacrylamide gels. Gels were stained with Coomassie blue, destained, dried, and the amount of full-length HA-Hac1p^u (all forms) determined by quantitation on a Storm 840 imaging system with the ImageQuant software v1.2 (Molecular Dynamics).

Where indicated, 2 or 20 pmol 2'-O-methyl oligoribonucleotide were annealed to 200 fmol hac·HAC·hac or hac·HAC·act in 20 mM HEPES-KOH (pH 7.4)/100 mM KOAc by heating to 95°C for 90 s and then cooling down to room temperature over 40 min.

Analysis of *HAC1* polyribosomes

pJC316, pJL177, pJL178 and pJL179 were transformed into yJL118 (W303 except *hac1::URA3*) and the resulting strains grown in 400 ml synthetic medium without histidine but supplemented with 100 μg/ml myo-inositol. At OD_{600}≅0.7, 600 μl 1 M DTT were added to 75 ml aliquots of the cultures to induce *HAC1* splicing. After 50 min at 30°C aliquots from the treated and untreated cultures were taken for RNA and protein analysis.

To isolate polyribosomes, 1 ml 15 mg/ml cycloheximide was added to 250 ml of the same cultures as used for the RNA and protein preparations, but at OD_{600}≅1.3. After 10 min at 30°C, cells were harvested by centrifugation at room temperature. All subsequent steps were carried out at 0-4°C with ice-cold buffer. Cells were washed twice with 50 ml LBC (30 mM HEPES-KOH (pH 7.4), 100 mM KOAc, 30 mM $Mg(OAc)_2$, 0.5 mM DTT, 0.5 mM PMSF, 0.4 μg/ml leupeptin hemisulfate), resuspended in LBC (1 ml final volume) and sodium heparin was added to 0.2 mg/ml. Cells were disrupted by vortexing in the presence of 500 μl 0.5 mm Zir/Silica beads. The lysates were cleared by centrifugation at 5200 x g, then at 10600 x g and finally at 20800 x g for 5 min each. Aliquots (10 OD_{260}) of each extract were layered on top of 13 ml 10-50% w/v sucrose gradients in GBL (30 mM HEPES-KOH (pH 7.4), 50 mM KOAc, 12 mM $Mg(OAc)_2$, 0.1 mg/ml sodium heparin and spun in a SW 40 Ti rotor (Beckman) at 40000 rpm (285,000 x g_{max}) for 100 min at 4°C. Fractions of the gradients (750 μl for Figs. 4A and 4B, 180 μl for Fig. 4C, or 500 µl for Fig. 5B) were collected with a density gradient fractionator from ISCO (model 185) while recording the absorbance profile at 254 nm. RNA was isolated by phenol/chloroform extraction followed by precipitation with

isopropanol or ethanol. 5% of the loads and 50% of each fraction were analyzed by Northern blot.

Preparation of extracts and fractionation of from KRY80 cells (*sec12-1*, *MATα*, *trp1-289*, *leu2*, *his4*, *ura3-52*) was identical but sucrose gradients contained 100 mM KOAc and 30 mM $Mg(OAc)_2$,.

Transcription shut-off

The yeast strain JC218 (Sidrauski et al., 1996; *rpb1-1*) was grown in 260 ml YPD at room temperature to OD_{600}≅0.5 and the cells were pelleted by centrifugation. The cells were resuspended in 260 ml YPD (pH 5.4), which was prewarmed to 37°C, and the culture split into three 60 ml aliquots. The UPR was induced by adding 480 μl 1 M DTT to each 60 ml aliquot after 10, 20, and 40 min, respectively at 37°C. 10 ml aliquots were taken of each culture immediately before and 5, 10, 20, and 40 min after the addition of DTT. Cells were harvested by centrifugation and frozen in liquid nitrogen.

ACKNOWLEDGMENTS

We thank Jon Lorsch and Daniel Herschlag for advice on yeast *in vitro* translation assays, Randy Schekman for the *sec12-1* strain, and Alan Sachs for the yAS1874 strain and for advice. We also thank Jason Brickner for the protocol for the isolation of proteins from yeast cells, Christopher Patil for the secondary structure prediction of *HAC1* mRNA, Tania Gonzalez for Northern probes and Ira Herskowitz, Christine Guthrie and members of the Walter lab for comments on the manuscript. This work was supported by long-term fellowships from the European Molecular Biology Organization and the Human Frontier Science Program Organization to U.R., by a Chancellor's Fellowship in Genetics to J.L., and by grants from the National Institutes of Health to P.W. P.W. is an investigator of the Howard Hughes Medical Institute.

REFERENCES

Bertolotti, A., Zhang, Y., Hendershot, L.M., Harding, H.P., and Ron, D. (2000). Dynamic interaction of BiP and ER stress transducers in the unfolded-protein response. Nat. Cell Biol. *2*, 326-332.

Chapman, R.E., and Walter, P. (1997). Translational attenuation mediated by an mRNA intron. Curr. Biol. *7*, 850-859.

Clark, I.E., Wyckoff, D., and Gavis, E.R. (2000). Synthesis of the posterior determinant Nanos is spatially restricted by a novel cotranslational regulatory mechanism. Curr. Biol. *10*, 1311-1314.

Clark, M.W., and Abelson, J. (1987). The subnuclear localization of tRNA ligase in yeast. J. Cell Biol. *105*, 1515-1526.

Cox, J.S., Shamu, C.E., and Walter, P. (1993). Transcriptional induction of genes encoding endoplasmic reticulum resident proteins requires a transmembrane protein kinase. Cell *73*, 1197-1206.

Cox, J.S., and Walter, P. (1996). A novel mechanism for regulating activity of a transcription factor that controls the unfolded protein response. Cell *87*, 391-404.

Gonzalez, T.N., Sidrauski, C., Dörfler, S., and Walter, P. (1999). Mechanism of non-spliceosomal mRNA splicing in the unfolded protein response pathway. EMBO J. *18*, 3119-3132.

Gray, N.K., and Wickens, M. (1998). Control of translation initiation in animals. Annu. Rev. Cell Dev. Biol. *14*, 399-458.

Johansson, H.E., Belsham, G.J., Sproat, B.S., and Hentze, M.W. (1994). Target-specific arrest of mRNA translation by antisense 2'-O-alkyloligoribonucleotides. Nucleic Acids Res. *22*, 4591-4598.

Kaufman, R.J. (1999). Stress signaling from the lumen of the endoplasmic reticulum: coordination of gene transcriptional and translational controls. Genes Dev. *13*, 1211-1233.

Kawahara, T., Yanagi, H., Yura, T., and Mori, K. (1997). Endoplasmic reticulum stress-induced mRNA splicing permits synthesis of transcription factor Hac1p/Ern4p that activates the unfolded protein response. Mol. Biol. Cell *8*, 1845-1862.

Köhrer, K., and Domdey, H. (1991). Preparation of high molecular weight RNA. Methods Enzymol. *194*, 398-405.

Kozak, M. (1989). Circumstances and mechanisms of inhibition of translation by secondary structure in eucaryotic mRNAs. Mol. Cell. Biol. *9*, 5134-5142.

Lee, R.C., Feinbaum, R.L., and Ambros, V. (1993). The *C. elegans* heterochronic gene *lin-4* encodes small RNAs with antisense complementarity to *lin-14*. Cell *75*, 843-854.

Mehlin, H., Daneholt, B., and Skoglund, U. (1992). Translocation of a specific premessenger ribonucleoprotein particle through the nuclear pore studied with electron microscope tomography. Cell *69*, 605-613.

Mori, K. (2000). Tripartite management of unfolded proteins in the endoplasmic reticulum. Cell *101*, 451-454.

Mori, K., Ma, W., Gething, M.-J., and Sambrook, J. (1993). A transmembrane protein with a cdc2+/CDC28-related kinase activity is required for signaling from the ER to the nucleus. Cell *74*, 743-756.

Nonet, M., Scafe, C., Sexton, J., and Young, R. (1987). Eucaryotic RNA polymerase conditional mutant that rapidly ceases mRNA synthesis. Mol. Cell. Biol. *7*, 1602-1611.

Novick, P., Field, C., and Schekman, R. (1980). Identification of 23 complementation groups required for post-translational events in the yeast scretory pathway. Cell *21*, 205-215.

Oka, T., Nishikawa, S., and Nakano, A. (1991). Inhibition of GTP hydrolysis by Sar1p causes accumulation of vesicles that are a functional intermediate of the ER-to-Golgi transport in yeast. J. Cell Biol., *114*, 671-679.

Olsen, P.H., and Ambros, V. (1999). The *lin-4* regulatory RNA controls developmental timing in *Caenorhabditis elegans* by blocking LIN-14 protein synthesis after the initiation of translation. Dev. Biol. *216*, 671-680.

Patil, C., and Walter, P. (2001). Intracellular signaling from the endoplasmic reticulum to the nucleus: the unfolded protein response in yeast and mammals. Curr. Opin. Cell Biol. *13*, 349-355.

Shamu, C.E., and Walter, P. (1996). Oligomerization and phosphorylation of the Ire1p kinase during intracellular signaling from the endoplasmic reticulum to the nucleus. EMBO J. *15*, 3028-3039.

Sidrauski, C., Cox, J.S., and Walter, P. (1996). tRNA ligase is required for regulated mRNA splicing in the unfolded protein response. Cell *87*, 405-413.

Sidrauski, C., and Walter, P. (1997). The transmembrane kinase Ire1p is a site-specific endonuclease that initiates mRNA splicing in the unfolded protein response. Cell *90*, 1031 – 1039.

Spena, A., Krause, E., and Dobberstein, B. (1985). Translation efficiency of zein mRNA is reduced by hybrid formation between the 5'- and 3'-untranslated region. EMBO J. *4*, 2153–2158.

Tarun Jr., S.Z., and Sachs, A.B. (1995). A common function for mRNA 5' and 3' ends in translation initiation in yeast. Genes Dev. *9*, 2997-3007.

Travers, K.J., Patil, C.K., Wodicka, L., Lockhart, D.J., Weissman, J.S., and Walter, P. (2000). Functional and genomic analyses reveal an essential coordination between the unfolded protein response and ER-associated degradation. Cell *101*, 249-258.

Urano, F., Bertolotti, A., and Ron, D. (2000). IRE1 and efferent signaling from the endoplasmic reticulum. J. Cell Sci. *113*, 3697-3702.

van den Heuvel, J.J., Planta, R.J., and Raue, H.A. (1990). Effect of leader primary structure on the translational efficiency of phosphoglycerate kinase mRNA in yeast. Yeast *6*, 473-482.

Vega Laso, M.R., Zhu, D., Sagliocco, F., Brown, A.J., Tuite, M.F., and McCarthy, J.E. (1993). Inhibition of translational initiation in the yeast *Saccharomyces cerevisiae* as a function of the stability and position of hairpin structures in the mRNA leader. J. Biol. Chem. *268*, 6453-6462.

Welihinda, A.A., and Kaufman, R.J. (1996). The unfolded protein response pathway in *Saccharomyces cerevisiae*. Oligomerization and trans-phosphorylation of Ire1p (Ern1p) are required for kinase activation. J. Biol. Chem. *271*, 18181-18187.

Wightman, B., Ha, I., and Ruvkun, G. (1993). Posttranscriptional regulation of the heterochronic gene *lin-14* by *lin-4* mediates temporal pattern formation in *C. elegans*. Cell *75*, 855-862.

Figure 2-1: Translation attenuation requires both the *HAC1* 5' UTR and intron

The yeast strain W303 transformed with the low-copy plasmid pRS315 carrying no insert (control), hac·GFP·int, hac·GFP·act, glo·GFP·int or glo·GFP·act was plated on selective medium and the fluorescence of each strain determined by scanning the plate with a fluorescent scanner. Brightly fluorescent colonies appear white, non-fluorescent colonies black.

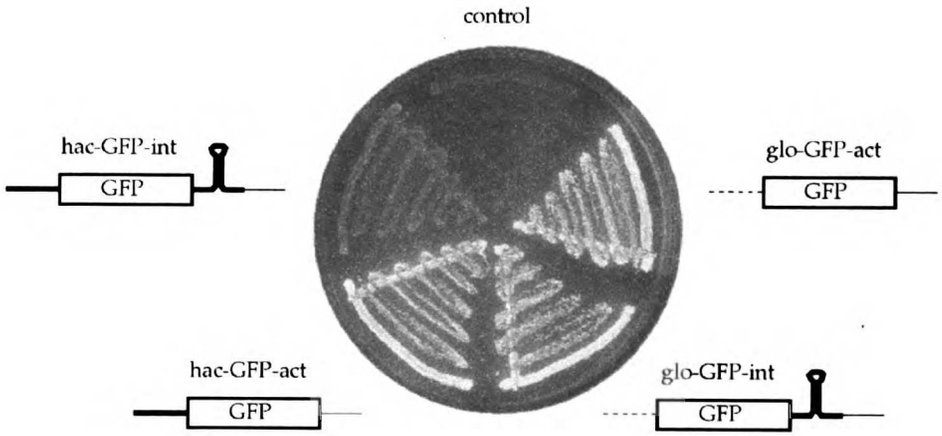
control
hac-GFP-int
GFP
glo-GFP-act
GFP
hac-GFP-act
GFP
glo-GFP-int
GFP

Table 1. Analysis of the strains shown in Figure 1 by flow cytometry

GFP construct [x]	mean fluorescence $[F_x/F_{hac\text{-}GFP\text{-}act}]$	GFP mRNA/SCR1 $[RNA_x/RNA_{hac\text{-}GFP\text{-}act}]$	normalized fluorescence $[(F_x/F_{hac\text{-}GFP\text{-}act})/(RNA_x/RNA_{hac\text{-}GFP\text{-}act})]$
hac-GFP-int	0.11 ± 0.01	0.91 ± 0.32	0.12 ± 0.04
hac-GFP-act	1.00 ± 0.06	1.00 ± 0.22	1.00 ± 0.23
glo-GFP-int	0.94 ± 0.08	0.68 ± 0.15	1.38 ± 0.33
glo-GFP-act	1.52 ± 0.08	0.88 ± 0.31	1.74 ± 0.62

The strains from Figure 1 were grown in selective liquid medium and their mean fluorescence F_x (x stands for hac-GFP-int, hac-GFP-act, glo-GFP-int or glo-GFP-act) was determined by flow cytometry. The amounts of mRNA encoding GFP relative to the amounts of *SCR1* RNA [RNA_x] were determined for the same cultures by Northern blot analysis and used to normalize the fluorescence of each strain. The results shown are the averages of at least three independent experiments.

Figure 2-2: *In vitro* reconstitution of translation attenuation by the *HAC1* 5' UTR and intron

(A) The transcripts indicated at the top were incubated in yeast extract in the presence of [^{35}S]methionine for 50 min and the products analyzed by SDS-PAGE followed by autoradiography. The molecular masses of the size standards are indicated in kDa on the left. The asterisk on the right marks the primary translation product while the bracket indicates all forms of HA-Hac1p^{u}. The amount of HA-Hac1p^{u} synthesized from each template relative to the amount synthesized from hac·HAC·act is shown below each lane. **(B)** The *HAC1* 5' UTR and intron contain complementary sequences. Exonic sequences are shown as solid lines, intronic sequences as dashed lines. The secondary structure shown is based on predictions but the splice sites have been shown experimentally to be located in the loops of stem-loop structures (Gonzalez et al., 1999). The model is not drawn to scale. ss: splice site. **(C)** An oligonucleotide directed against the intron stimulates translation of *HAC1^{u} in vitro*. The transcripts hac·HAC·hac (lanes 2-8) and hac·HAC·act (lanes 9-15) annealed to the oligonucleotides indicated at the top were incubated in yeast extract in the presence of [^{35}S]methionine for 50 min and the products analyzed by SDS-PAGE followed by autoradiography. The molecular masses of the size standards are indicated in kDa on the left. The asterisk on the right marks the primary translation product while the bracket indicates all forms of HA-Hac1p^{u}. The amount of HA-Hac 1p^{u} synthesized under each condition relative to the amount synthesized from hac·HAC·act in the absence of any oligonucleotide is shown at the bottom. Lane 1: no mRNA; lanes 2 and 9: no oligonucleotide; lanes 3, 5, 7, 10, 12 and 14: 2 pmol of the

oligonucleotide indicated at the top; lanes 4, 6, 8, 11, 13 and 15: 20 pmol of the oligonucleotide indicated at the top.

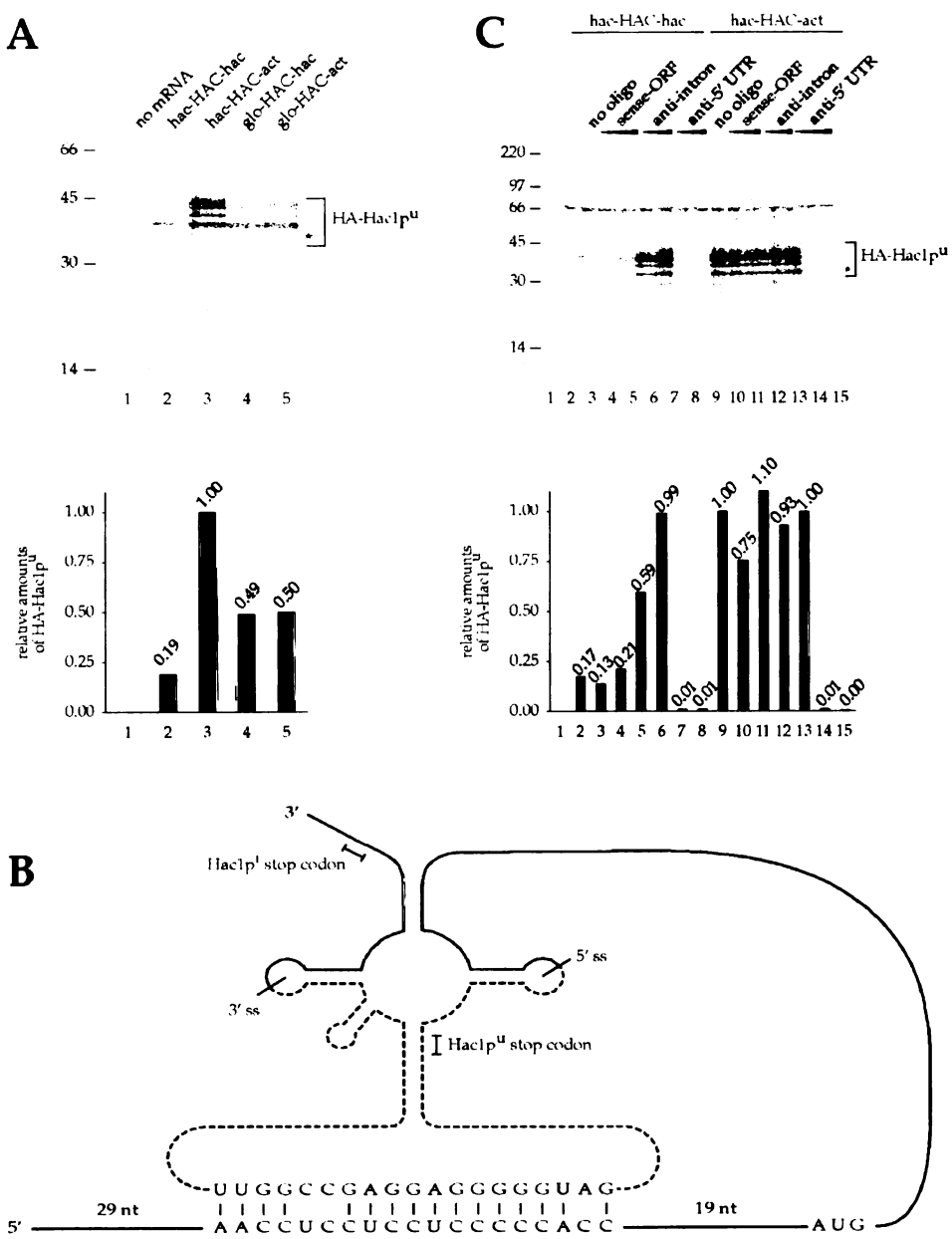
A
no mRNA
hac-HAC-hac
hac-HAC-act
glo-HAC-hac
glo-HAC-act
66 –
45 –
30 –
14 –
HA-Hac1p^u
1 2 3 4 5
relative amounts of HA-Hac1p^u
1.00
0.75
0.50
0.25
0.00
0.19
1.00
0.49
0.50
C
hac-HAC-hac
hac-HAC-act
no oligo
sense-ORF
anti-intron
anti-5′ UTR
220 –
97 –
66 –
45 –
30 –
14 –
HA-Hac1p^u
1 2 3 4 5 6 7 8 9 10 11 12 13 14 15
0.17
0.13
0.21
0.59
0.99
0.01
0.01
1.00
0.75
1.10
0.93
1.00
0.01
0.00
B
3′
Hac1p^i stop codon
5′ ss
3′ ss
Hac1p^u stop codon
U U G G C C G A G G A G G G G G U A G
5′
29 nt
A A C C U C C U C C U C C C C C A C C
19 nt
A U G

Figure 2-3: Disruption of the interaction between the *HAC1* 5' UTR and intron leads to the accumulation of Hac1p^u and inhibits splicing

A *Δhac1* yeast strain was transformed with plasmids pJC316, pJL179, pJL178, pJL177 or pJC834 [a previously described plasmid from which HA-Hac1p^u is expressed constitutively (Chapman and Walter, 1997)] and grown in selective liquid medium. The UPR was induced by adding 8 mM DTT for 50 min. **(A)** Overview of the relevant sequences in plasmids pJC316, pJL179, pJL178 and pJL177. Wild-type sequences are shown in bold. **(B)** Northern blot analysis. 15 μg total RNA were separated on a 1.5% w/v agarose gel and transferred to a membrane, which was incubated with probes directed against the *HAC1* 5' exon and *SCR1*. The amount of *HAC1* splicing after UPR induction is indicated at the bottom for each plasmid. The positions of HA-*HAC1*^{u}, HA-*HAC1*^{i} and *SCR1* are indicated on the right. The asterisks on the right indicate potential splicing intermediates (one asterisk: 5' exon-intron; two asterisks: 5' exon). wt: wild type; mt: mutant; bp rest.: base pairing restored. **(C)** Western blot analysis. 25 μg protein were separated on a 12.5% w/v SDS-polyacrylamide gel and transferred to a nitrocellulose membrane. HA-Hac1p was detected with an antibody directed against the HA tag and the ECL system. The middle panel is a longer exposure of the blot shown in the top panel. The brackets on the right of the top two panels indicate the different forms of HA-Hac1p. The open arrowhead on the left indicates a band unrelated to HA-Hac1p visible upon longer exposure, which is also detectable in extracts of the *Δhac1* strain transformed with an empty plasmid (data not shown). Lanes 2 (long exposure), 5, 6 and 7 (short exposure) are shown twofold enlarged at the bottom and the positions of the multiple forms of HA-Hac1p^u and HA-Hac1p^i are indicated for each lane by brackets and

diamonds, respectively. **(D)** Titration of selected samples from panel C. 25 μg (lane 1), 3 μg (lane 2) and 6 μg (lane 3) protein were separated in parallel on 12.5% w/v SDS-polyacrylamide gels and transferred to nitrocellulose membranes. HA-Hac1p was detected with an antibody directed against the HA tag and the ECL Plus system. The amount of total protein loaded relative to the amount loaded in lane 2 is indicated above each lane.

A

plasmid	description and sequences of relevant parts of 5'UTR and intron	
pJC316	intron wild-type:	3' U U G G C C G A G G A G G G G U 5'
	5'UTR wild-type:	5' A A C C U C C U C C U C C C C A 3'
pJL179	intron mutated:	3' A A C C U C C U C C U C C C C A 5'
	5'UTR wild-type:	5' A A C C U C C U C C U C C C C A 3'
pJL178	intron wild-type:	3' U U G G C C G A G G A G G G G U 5'
	5'UTR mutated:	5' U U G G C C G A G G A G G G G U 3'
pJL177	intron mutated:	3' A A C C U C C U C C U C C C C A 5'
	5'UTR mutated:	5' U U G G C C G A G G A G G G G U 3'

B

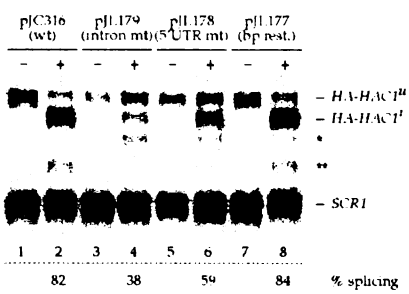

C

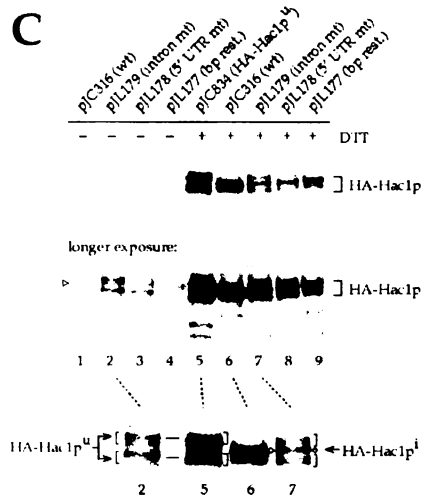

D

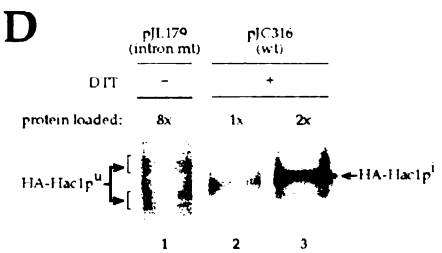

Figure 2-4: The interaction of the *HAC1* 5' UTR and intron diminishes the loading of ribosomes onto *HAC1*" mRNA

(A) Extracts from *Δhac1* strains carrying either pJC316 or pJL179 were fractionated over 10-50% w/v sucrose gradients and 750 μl fractions were collected across the gradients. The direction of sedimentation is from left to right. UV absorbance profile at 254 nm (top), Northern blot analysis (middle) and quantitation of the Northern blots (bottom). *Northern blots*: 50% of the fractions indicated at the bottom and 5% of the loads (L) were separated on 1.5% w/v agarose gels and the RNA transferred to membranes, which were incubated with a probe directed against the *HAC1* 5' exon and intron. Note that the HA-*HAC1* mRNA levels are substantially lower in the strain carrying pJL179 than in the one carrying pJC316 but the images of the two Northern blots were processed to give similar signal intensities. The strain analyzed is indicated at the left and the number of ribosomes (rb) per mRNA between the profile and the Northern blots. wt: wild type; mt: mutant. *Quantitation*: the amount of HA-*HAC1* mRNA in each fraction is expressed as percentage of the total amount of HA-*HAC1* mRNA recovered over the gradient (% total). **(B)** Extracts from *Δhac1* strains carrying either pJC316, pJL179, pJL178 or pJL177 were fractionated over 10-50% w/v sucrose gradients, fractions collected and analyzed by Northern blot as described in **A** and the number of ribosomes per mRNA was determined for each fraction based on the UV absorbance profile. The amounts of HA-*HAC1* mRNA associated with 0, 1-2 and more than 2 ribosomes are shown as percentage of the total amount of HA-*HAC1* mRNA recovered over the gradient (% total). The analysis across the gradient is shown in detail in **A** for pJC316 and pJL179. **(C)** Extract from the *Δhac1* strain carrying pJC316 was fractionated over a 10-50% w/v

sucrose gradient and twenty 180 μl fractions were collected from the middle of the gradient. The direction of sedimentation is from left to right. The UV absorbance profile at 254 nm is shown with a stippled line and the quantitation of HA-*HAC1*^{u} mRNA by Northern blot with a solid line. Northern blot analysis was carried out as described in A. arb. u.: arbitrary unit of quantitation by phosphor screen autoradiography.

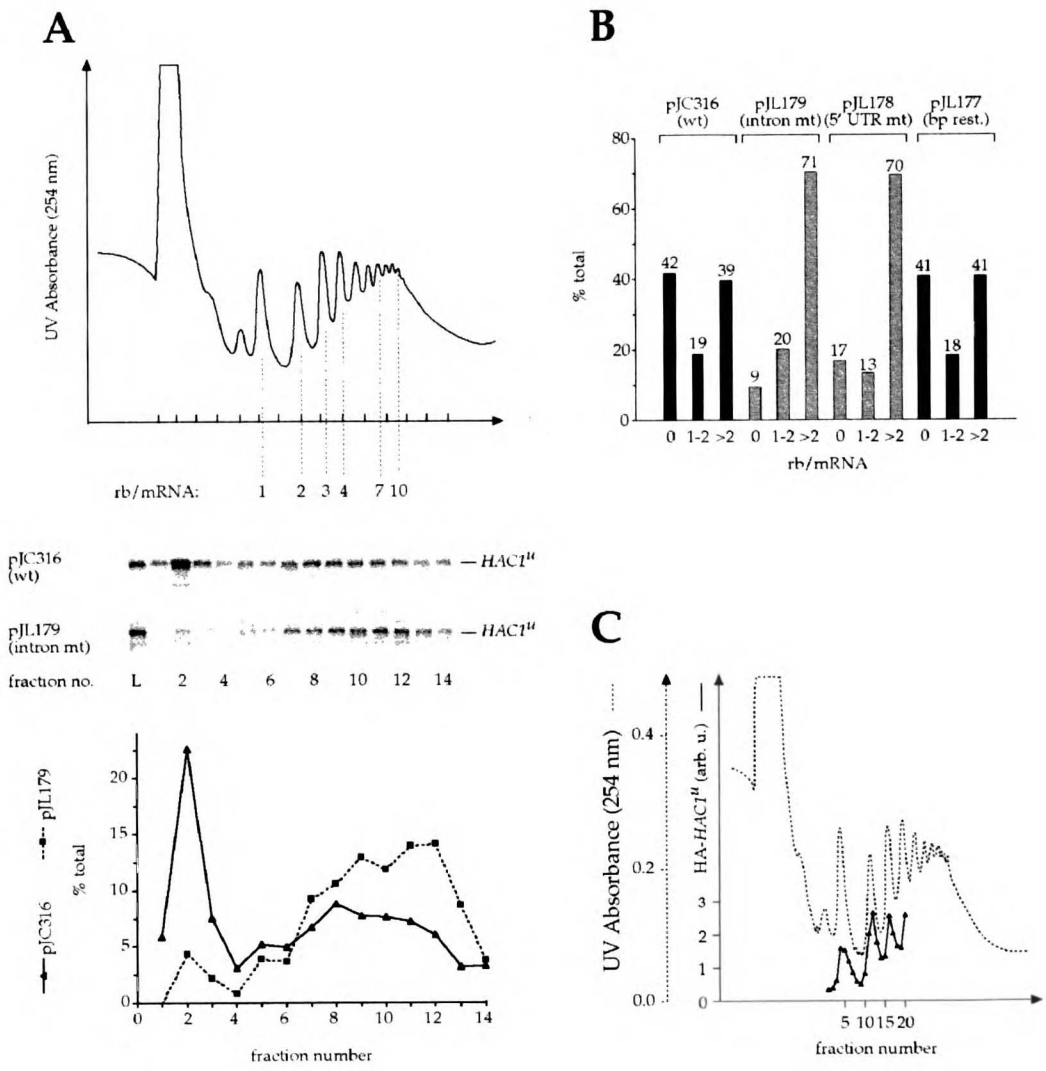
A
UV Absorbance (254 nm)
rb/mRNA: 1 2 3 4 7 10
pJC316 (wt)
pJL179 (intron mt)
— HAC1u
fraction no. L 2 4 6 8 10 12 14
pJC316
pJL179
% total
fraction number
B
pJC316 (wt)
pJL179 (intron mt)
pJL178 (5' UTR mt)
pJL177 (bp rest.)
% total
42 19 39 9 20 71 17 13 70 41 18 41
0 1-2 >2 0 1-2 >2 0 1-2 >2 0 1-2 >2
rb/mRNA
C
UV Absorbance (254 nm)
HA-HAC1u (arb. u.)
fraction number

Figure 2-5: The cytoplasmic pool of *HAC1*^{u} mRNA is a substrate for splicing

(A) Yeast cells expressing a temperature-sensitive allele of the largest subunit of RNA polymerase II were shifted to the non-permissive temperature for 10, 20, and 40 min. At these time points DTT was added to a final concentration of 8 mM. Total RNA was isolated from aliquots taken immediately before and 5, 10, 20, and 40 min after the addition of DTT. The amount of *HAC1* mRNA splicing was determined for each time point by Northern blot analysis with a probe directed against the 5' exon. **(B)** Yeast cells expressing a temperature-sensitive allele of *SEC12*, required for vesicle transport from the ER to Golgi, were shifted to the non-permissive temperature for 2 min, and then cycloheximide was added to a final concentration of 60 μg/ml. DTT was added after 1 min to a final concentration of 8 mM, and extracts were prepared from aliquots taken immediately before and 2, 5, and 10 min after the addition of DTT. Extracts were fractionated over a 10-50% sucrose gradient and analyzed by Northern blots, as in Figure 4C.

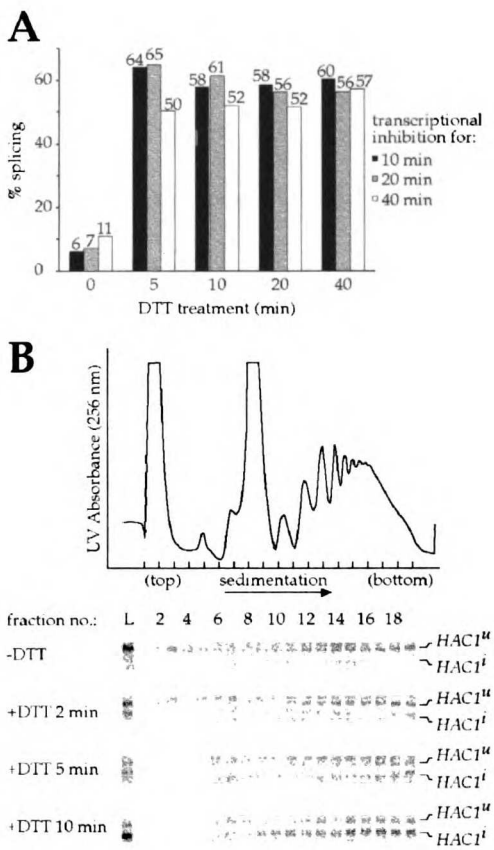
A
% splicing
0
20
40
60
6 7 11
64 65 50
58 61 52
58 56 52
60 56 57
0
5
10
20
40
DTT treatment (min)
transcriptional inhibition for:
10 min
20 min
40 min
B
UV Absorbance (256 nm)
(top)
sedimentation
(bottom)
fraction no.: L 2 4 6 8 10 12 14 16 18
-DTT
+DTT 2 min
+DTT 5 min
+DTT 10 min
HAC1u
HAC1i

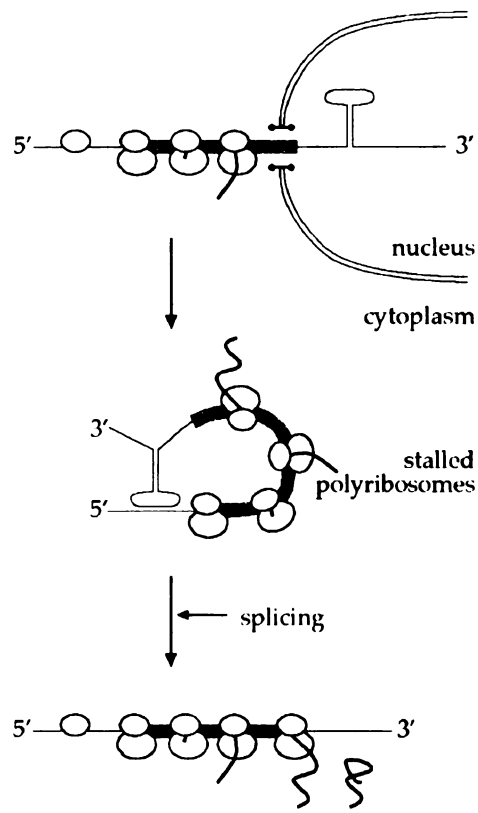

Figure 2-6: A model for translation attenuation and its relief by cytoplasmic splicing

Chapter 3

IRE1-independent Gain Control of the Unfolded Protein Response

IRE1-independent Gain Control of the Unfolded Protein Response

Jess H. Leber, Sebastián Bernales, and Peter Walter*

Howard Hughes Medical Institute, and
Department of Biochemistry and Biophysics
University of California at San Francisco
San Francisco, CA 94143-2200
USA

* Corresponding author

phone: (415) 476-5017
fax: (415) 476-5233
email: walter@cgl.ucsf.edu

SUMMARY

Non-conventional splicing of the gene encoding the Hac1p transcription activator regulates the unfolded protein response (UPR) in *S. cerevisiae*. This simple on/off switch contrasts with a more complex circuitry in higher eukaryotes. Here we show that a heretofore unrecognized ER surveillance pathway operates in yeast to regulate the transcription of *HAC1*. The resulting increase in Hac1p production, together with the production or activation of a putative UPR Modulatory Factor, is necessary for the cells to survive the conditions that trigger this response. This parallel ER-to-nucleus signaling pathway serves as "gain control" by modifying the UPR-driven transcriptional program. The results suggest a surprising conservation among all eukaryotes of the ways by which the elements of the UPR signaling circuit are connected. By adding an additional signaling element to the basic UPR circuit, a simple switch is converted into a complex response.

Running title: Transcriptional control of Hac1p expression

INTRODUCTION

In eukaryotes, the endoplasmic reticulum (ER) serves as the first station of the secretory pathway, through which all secreted and membrane proteins must pass. Within the ER, proteins are folded into their native structure and multi-subunit protein complexes are assembled. The ER is a dynamic organelle, capable of sensing and adjusting its folding capacity in response to increased demand: when misfolded proteins accumulate in the ER, a signaling pathway, termed the unfolded protein response (UPR), is activated (reviewed in (Patil and Walter, 2001)(Kaufman, 2002; Ma and Hendershot, 2001; Ron, 2002)). The UPR activates the expression of genes that enable the cells to adapt to and survive the stress, including those encoding ER-resident chaperones (Lee, 1987)(Kozutsumi et al., 1988), key enzymes in lipid biosynthesis (Cox et al., 1997), members of the ER-associated degradation (ERAD) machinery, and other components of the secretory system (Travers et al., 2000)(Ng et al., 2000; Urano et al., 2000).

In yeast, the UPR is controlled by a binary switch imposed by a non-conventional splicing reaction that governs the production of the Hac1p transcription factor (NP_116622) responsible for the activation of UPR target genes (Mori et al., 1992)(Kohno et al., 1993)(Cox and Walter, 1996)(Mori et al., 1996). In uninduced cells, direct base pairing between the 5' untranslated region (UTR) and an intron at the 3' end of the mRNA prevents *HAC1* mRNA translation (Chapman and Walter, 1997)(Rüegsegger et al., 2001). Accumulation of unfolded proteins activates the ER-resident transmembrane kinase/endoribonuclease Ire1p (NP_011946), which then cleaves the *HAC1* mRNA at two precise splice junctions, excising the intron (Cox et al., 1993)

(Mori et al., 1993)(Sidrauski and Walter, 1997). The two *HAC1* exons are then joined by tRNA ligase (NP_012448), allowing translation of Hac1p (Sidrauski et al., 1996).

To date, Ire1-dependent *HAC1* mRNA splicing is the only identified way by which signals from the ER affect transcription in yeast. By contrast, in metazoan cells three mechanistically distinct pathways are known that operate in parallel, although their relative importance in different tissues remains to be determined (reviewed in (Ma and Hendershot, 2001)). Hints that further complexity also exists in yeast comes from data presented in the accompanying paper, which demonstrates that Hac1p activity is modulated by interaction with Gcn4p, a transcription factor central to regulation of amino acid biosynthesis (Patil et al., 2004). The UPR, therefore, may integrate signals from more than one source to compute a transcriptional output appropriate for the physiological conditions of the cell.

In this paper, we describe a novel "gain control" regulating the UPR in yeast. We show that *HAC1* mRNA transcription is regulated, resulting in control of Hac1p abundance. Thus the on/off switch provided by *IRE1*-dependent splicing is not the only regulatory step of the UPR. This regulation responds to a bipartite signal that emanates from the ER and is communicated by an Ire1p-independent pathway. As a consequence, an alternate transcriptional program is triggered, with specific alterations to the normal UPR allowing the cell to survive. By imposing gain control on a binary switch in the UPR circuitry, the cell transforms a discrete transcriptional response into a more complex signaling function.

RESULTS

Secretory stress boosts *HAC1* mRNA abundance

To define the basic circuitry of signal transduction in the UPR, we reevaluated the *HAC1* mRNA processing step in a quantitative manner. To this end, we induced the UPR with either DTT or tunicamycin (both agents that cause protein misfolding selectively in the ER), and monitored *HAC1* mRNA by Northern blot analysis (Figure 1A). In agreement with previous results, we observed rapid and efficient splicing of *HAC1* mRNA, as apparent from the conversion of unspliced $HAC1^u$ mRNA ("*u*" for UPR-*u*ninduced) to spliced $HAC1^i$ mRNA ("*i*" for UPR-*i*nduced). Quantitation of the results shows that the relative abundance of *HAC1* mRNA (the sum of $HAC1^u$ and $HAC1^i$ mRNAs) remained unchanged over the time course of at least 12 hours (Fig. 1A and data not shown). These data demonstrate that acute induction of unfolded proteins triggers a simple on/off switch that controls *HAC1* mRNA splicing.

In light of these observations, we were surprised to find that blocking the secretory pathway distal to the ER resulted in a pronounced increase in *HAC1* mRNA abundance. As shown in Figure 1B, *HAC1* mRNA levels increased 3- to 4-fold in mutant strains compromised at various steps in the secretory pathway when shifted to the non-permissive temperature (*sec12-1*: ER → Golgi, lanes 5-8; *sec14-1*: intra-Golgi, lanes 9-12; and *sec1-1*: Golgi → plasma membrane, lanes 13-16) (Novick et al., 1980). Splicing was also induced, albeit to a lesser degree than was observed with DTT or tunicamycin treatment. The observed splicing suggests that blockages in ER-distal compartments of the secretory pathway lead to activation of Ire1p in the ER. Temperature shift alone only

transiently induced *HAC1* mRNA splicing and had no effect on *HAC1* mRNA abundance (lanes 1-4). To determine if any disruption of the secretory pathway had similar consequences, we blocked earlier stages of protein traffic. Mutations that block protein entry into the ER had no effect (Figure 1C: *sec62-101*, lanes 13-16; *sec63-201*, lanes 17-20) or only a mild effect (*sec61-101*, lanes 9-12) on *HAC1* mRNA abundance.

Thus, a surveillance pathway operates to adjust *HAC1* mRNA levels in response to altered conditions in the secretory pathway. In the experiments described above, we observed *HAC1* mRNA induction only in *sec* mutants that block transport distal to the ER, but not in those that block protein entry into the ER. One common consequence of blocking the secretory pathway at later stages is that proteins in transit will eventually back-up into the ER (Rose et al., 1989)(Chang et al., 2002). This condition results in protein folding defects, thereby activating Ire1p, as indicated by the observed *HAC1* mRNA splicing. From the data discussed above (Fig. 1A), however, we know that an accumulation of unfolded proteins alone is insufficient to trigger an upregulation of *HAC1* mRNA, suggesting that an additional inducing signal is required.

HAC1 mRNA induction requires a bipartite signal

To determine the nature of this second signal, we sought conditions that induce *HAC1* mRNA when combined with ER protein misfolding drugs. Canvassing different conditions, we found two scenarios under which wildtype cells can be induced to upregulate *HAC1* mRNA in wildtype cells: i) ER protein misfolding combined with a temperature shift from 23°C to 37°C (Figure 2A) and ii) ER protein misfolding combined with inositol starvation (Figure 2B). Intriguingly, while ER protein misfolding and

inositol starvation each activated the UPR individually (as shown by the activation of *HAC1* mRNA splicing, Fig. 2A lanes 5-8, and Fig. 2B lanes 1-4, 5-8), neither stress alone was sufficient to cause *HAC1* mRNA upregulation. Similarly, the temperature shift reproducibly caused a transient UPR induction (Fig. 1B, lanes 1-4; Fig. 2A, lanes 1-4), but by itself did not affect *HAC1* mRNA levels. Only the combination of ER stress with either temperature shift (Fig. 2A, lanes 9-12) or inositol starvation (Fig. 2B, lanes 9-12) led to an increase in *HAC1* mRNA abundance. Subjecting cells to both temperature shift and inositol deprivation had no additive effect, nor did treating cells with both DTT and tunicamycin (data not shown). Thus, *HAC1* mRNA induction requires a bipartite signal, consisting of one input provided by unfolded proteins in the ER (the "UP" signal), and the other input provided by inositol starvation or temperature shift (the "I/T" signal).

The heat shock response is transiently induced by shifting cells from 23°C to 37°C. To determine if the heat shock response is an important component of the I/T signal, we tested whether continued growth at 37°C or expression of a constitutively active allele of the heat shock factor Hsf1p (Sorger, 1991)(Bulman et al., 2001) would substitute for the temperature shift described above. Constitutive expression of active Hsf1p (Figure 2C, lanes 5-8) led to upregulation of *SSA1*, a known target of the heat shock response (Slater and Craig, 1989), but did not substitute for the I/T signal for *HAC1* upregulation. In contrast, continued growth at 37°C (Fig. 2C, lanes 9-12) allowed for modest induction of *HAC1* mRNA. Thus, elevated temperature elicits effects other than heat shock, which are important for *HAC1* mRNA upregulation.

HAC1 induction is _IRE1_-independent

The UP branch is experimentally induced by DTT or tunicamycin treatment of the cells. As Ire1p is a sensor of folding conditions within the ER lumen, we tested next whether Ire1p was required to transmit this signal. Surprisingly, it was not. *HAC1* mRNA abundance was induced 2.6-fold in Δ*ire1* cells (Figure 2D, lanes 9-12), similar to the 3-fold induction observed with wildtype cells (Fig. 2A, lanes 9-12). These results show that a previously unrecognized Ire1p-independent surveillance mechanism must exist that monitors protein folding in the ER.

HAC1 mRNA abundance is regulated transcriptionally

Increase of *HAC1* mRNA abundance could result from increased transcription, reduced degradation, or both. To distinguish between these possibilities, we constructed a reporter gene consisting of the *HAC1* promoter driving transcription of the open reading frame encoding the green fluorescent protein flanked by *ACT1* untranslated regions (*HAC1pro-GFP*). The resulting heterologous *GFP* mRNA therefore contains no *HAC1* mRNA sequences. Under conditions providing both the UP and I/T signals, the change in abundance of the *GFP* mRNA (Figure 3A, lanes 5-8) mirrored that of the endogenous *HAC1* mRNA (lanes 1-4), both in the kinetics and magnitude of the response. These data demonstrate that the observed increase in *HAC1* mRNA abundance was caused by increased transcriptional activity of the *HAC1* promoter.

To further test this notion, we compared the rate of decay of *HAC1* mRNA under both *HAC1* mRNA inducing and non-inducing conditions. To this end, we employed a strain bearing a temperature-sensitive allele of RNA polymerase II, which was subjected

to either elevated temperature alone, or to both elevated temperature and DTT treatment. In both cases, polymerase II transcription ceased upon temperature shift and mRNA decay was measured. As shown in Figure 3B, the rate of decay of *HAC1* mRNA was indistinguishable under both conditions. Therefore, the increase in *HAC1* mRNA abundance in response to the combination of UP and I/T signals is due solely to activation of the *HAC1* promoter.

HAC1 promoter regulation is required to survive certain stress conditions

The results presented so far define a novel regulatory mechanism whereby cells adjust the amount of *HAC1* mRNA. This mRNA is the substrate for the Ire1p-mediated splicing reaction, which in turn produces *HAC1*^{i} mRNA that is translated to produce Hac1p transcription factor. We therefore asked whether elevated levels of *HAC1* mRNA led to a proportional increase in the level of Hac1p. Quantitative Western blot analysis shows that this is indeed the case: when cells were treated with DTT and concomitantly shifted to 37°C, the levels of Hac1p increased 3-fold (Figure 4A, lanes 5-8), relative to the Hac1p levels observed in cells subjected to DTT treatment alone (lanes 1-4). Therefore, the transcriptional induction of *HAC1* mRNA combined with Ire1-mediated splicing results in elevated Hac1p levels, characterizing a new physiological state. Henceforth, we refer to this state as the "Super-UPR" (S-UPR).

To assess the physiological role of the S-UPR, we sought conditions that would allow us to directly monitor the consequences of changes in *HAC1* mRNA levels under otherwise identical growth conditions. To this end, we engineered a yeast strain unable to transcriptionally upregulate *HAC1*. In these cells, *HAC1* mRNA expression was removed

from the control of the *HAC1* promoter and was instead driven by the heterologous *ADH1* promoter (*ADH1pro-HAC1*), at levels closely approximating the uninduced *HAC1* state (Figure 4B; compare *ADH1pro-HAC1*, lanes 5-8 to *HAC1pro-HAC1*, lanes 1-4). Expression from the *ADH1* promoter was constitutive, and the levels of *HAC1* mRNA did not change significantly under the various inducing conditions described above. As expected, induction of the UPR in these strains led to efficient *HAC1* mRNA splicing and Hac1p production. This strain therefore allowed us to fix the cellular Hac1p concentration closely approximating the basal *HAC1* expression state observed during the UPR.

We next assessed whether we could identify physiological conditions under which elevated *HAC1* mRNA levels were required for cell growth. Therefore, we subjected wildtype cells and the engineered strain described above to the combinations of stresses described in Figure 2. Cells expressing *HAC1* from the endogenous or from the *ADH1* promoter grew equally well on plates lacking inositol (Figure 4C, left, first and third rows). This condition induces the UPR and requires the expression of at least a minimal amount of *HAC1* mRNA, as Δ*hac1* cells fail to grow (left, second row). In contrast, only wildtype cells, which are able to upregulate *HAC1* mRNA production, grew on plates lacking inositol and also containing tunicamycin. Cells expressing *HAC1* mRNA only at the basal levels from the *ADH1* promoter were non-viable on these plates (right, third row). As shown previously in Figure 2B, this combination of stresses induces the S-UPR. The data therefore reveal that regulation provided by the *HAC1* promoter is necessary to survive certain stress conditions that otherwise is lethal.

Differential UPR target gene induction by elevated Hac1p levels

To begin to characterize the cause for increased viability, we next sought to determine differences in UPR target gene expression resulting from either UPR or S-UPR induction. To this end, we used DNA microarray chip analysis to determine the complete mRNA profile of cells grown under UPR and S-UPR conditions. The results of this analysis are shown in Figure 5A. Each spot represents the fold induction of a UPR target under UPR conditions (X-axis) or S-UPR conditions (Y-axis) (see Experimental Procedures for definition of the UPR target set used in this analysis). UPR target genes for which the S-UPR has no additional effect should undergo equal induction under both conditions, and are expected to scatter around the diagonal, indicated by the dashed line. This was the case for many UPR targets. However, induction of a substantial number of genes was skewed to the top of the graph, indicating stronger induction under S-UPR conditions than under UPR conditions. These same data are displayed in Figure 5B to highlight and categorize these differences. In the histogram, the X-axis represents the ratio of the induction of a target gene during S-UPR and UPR conditions, and the Y-axis shows that the number of genes with a given ratio. We have operationally divided UPR target genes into three classes, based on their fold-induction during the S-UPR compared to their fold induction during the UPR:

- Class 1 targets (*red bars*, 123 out of 174, or 71%) exhibit little if any difference in induction during the UPR and S-UPR (S-UPR induction / UPR induction < 2). Thus the cellular Hac1p during the S-UPR does not lead to enhanced transcription, indicating that for these genes the response is already saturated at UPR Hac1p levels. Class 1 targets include many of the known ER lumenal

chaperones (including *KAR2*, *SCJ1*, *LHS1*, and *JEM1*) and redox proteins (including *PDI1*, *EUG1*, and *ERO1*).

- Class 2 targets (*blue bars*, 44 out of 174, or 25%) are induced to a 2- to 4-fold greater extent during S-UPR than during the UPR. Transcription of these genes is therefore roughly proportional to the Hac1p levels in the cell. Class 2 targets include *YIP3*, involved in ER to Golgi transport, *OPI3*, a phospholipid methyltransferase, and the hexose transporters *HXT12, HXT15, HXT16,* and *HXT17.*
- Class 3 targets (*green bars*, 7 out of 174, or 6%) are induced by the S-UPR greater than 4-fold more than by the UPR. Class 3 contains the UPR targets *DER1*, involved in ER-associated degradation (ERAD) (Knop et al., 1996) (Travers et al., 2000)(Ng et al., 2000), and *INO1*, critical for membrane biogenesis (Hirsch and Henry, 1986).

Role for a putative UPR Modulatory Factor

The increased transcriptional output under S-UPR conditions could occur for two reasons. It could be due to increased Hac1p concentrations in the cell, or it could result because an additional S-UPR specific transcription factor is produced or activated (perhaps the same that regulates *HAC1* transcription), or it could be due to a combination of these two scenarios. To distinguish between these possibilities, we determined the target gene induction profile in cells in which the *HAC1* mRNA concentration was artificially elevated to a similar level as found after S-UPR induction. We took advantage of a specific 15 base-pair deletion in the *HAC1* promoter (*HAC1pro*^{HI}), which

increases basal expression by about 3-fold, as compared to the endogenous promoter (Figure 5C). In cells bearing a *HAC1pro*^{HI}-*HAC1* gene ("*HAC1pro*^{HI} cells"), splicing of *HAC1* mRNA was somewhat reduced upon UPR induction (47%, compared to 67% for wildtype); though, even with this reduction, *HAC1pro*^{HI} cells produced approximately 2.5-fold more spliced *HAC1*^{i} mRNA than wildtype cells (compare Fig. 5C lanes 3-4 to lanes 1-2). The increased levels of *HAC1*^{i} mRNA led to a corresponding increase in Hac1p (Figure 5D, compare lanes 3-4 to lanes 1-2). The amount of Hac1p produced by DTT induction of *HAC1pro*^{HI} cells is approximately the same as the amount of Hac1p produced during the S-UPR (compare Fig. 5D, lanes 2 and 4 with Fig. 4A, lanes 4 and 8).

The ability to set *HAC1* mRNA levels to S-UPR levels allowed us to directly compare UPR target gene induction with the cellular Hac1p concentration being the only variable. We induced the UPR in both wildtype and *HAC1pro*^{HI} cells with DTT and determined the mRNA expression profiles. For each class of UPR target defined above, the expression analysis of UPR-induced wildtype and *HAC1pro*^{HI} cells is shown in Figure 5E. In the histograms, the X-axis shows the ratio of target gene induction during the UPR driven by a high level of Hac1p from *HAC1pro*^{HI} cells compared to induction during the UPR in wildtype cells. The Y-axis shows the number of genes at any given ratio. As expected, Class 1 targets (top panel of Fig. 5E) do not further respond to the higher levels of Hac1p produced in *HAC1pro*^{HI} cells. The majority of Class 2 and Class 3 targets (middle and bottom panels of Fig. 5E) also did not respond to higher levels of Hac1p (ratio < 2), indicating that only raising the Hac1p concentration in cells in not sufficient to account for their full increased induction during the S-UPR. By contrast, ten of the 32 Class 2 and Class 3 targets were significantly induced (ratio > 2) in cells expression high

levels of Hac1p. For the Class 3 target *DER1*, high levels of Hac1p was sufficient to elevate expression to S-UPR levels: *DER1* was induced 8-fold in DTT-treated *HAC1pro*^{III} cells, compared to roughly 9-fold in wildtype cells during the S-UPR. Otherwise, however, high levels of Hac1p did not fully reconstitute the induction seen during the S-UPR. For example, while the Class 3 gene *INO1* was induced 7.5-fold more in the S-UPR than in the UPR (77-fold induced by the S-UPR versus 11-fold induced by the UPR), it is only 3-fold more induced by high levels of Hac1p than normal levels (33-fold versus 11-fold, respectively). We conclude that elevated Hac1p levels are sufficient to selectively increase the induction of a few UPR targets, but that the full transcriptional program of the S-UPR predicts the production or activation of an additional transcriptional activator, which we term "UPR Modulatory Factor", or "UMF".

To further dissect the UMF contribution during the S-UPR, we sought conditions under which UMF activity was the only variable. To this end, we induced the S-UPR in *ADH1pro-HAC1* cells, which are prevented from achieving high level Hac1p expression, and compared the mRNA expression profile against the UPR in wildtype cells. In this analysis, Hac1p levels were approximately equivalent in the two conditions, so variations from the normal UPR transcriptional program reflect the activity of UMF. The results are shown in Figure 5F, with the data displayed similarly to Figure 5E: the X-axis shows the ratio of target gene induction during the S-UPR in *ADH1pro-HAC1* cells, compared to induction during the UPR in wildtype cells, and the Y-axis shows the number of genes at any given ratio. Not surprisingly, the induction of Class 1 targets (top panel, Figure 5F) was unaffected: these are targets that are fully induced by even low levels of Hac1p and are no more induced during the S-UPR. Two Class 3 targets, *YOR289W* and

YHR087W (both of unknown function) reach near wildtype S-UPR induction levels, without elevated levels of Hac1p (*YOR289W*: 30-fold and 40-fold, *YHR087W*: 13-fold and 12-fold, in *ADH1pro-HAC1* and wildtype strains, respectively); for these targets, UMF likely plays a leading role in their induction, with Hac1p having less influence. Most Class 2 and Class 3 targets (middle and bottom panels of Figure 5F), however, do not reach full S-UPR induction levels in the absence of elevated Hac1p levels. For example, the Class 3 target *INO1* is induced roughly 25-fold in *ADH1pro-HAC1* cells during S-UPR conditions; while this is roughly twice the induction observed during the UPR, this falls far short of the 75-fold S-UPR induction in wildtype cells.

These results reinforce the *in vivo* requirement for high levels of Hac1p to survive S-UPR stress, demonstrated in Figure 4C. Taken together with the data shown in Figure 5E, we conclude that the full S-UPR transcriptional program results from a collaboration between elevated Hac1p levels and UMF, with the relative contribution from each varying among different target genes.

DISCUSSION

The circuitry of the UPR

In this paper, we describe a novel ER surveillance pathway in yeast that modulates the unfolded protein response, resulting in a new physiological state that we term the S-UPR. In response to a bipartite signal transmitted from the ER by an *IRE1*-independent pathway, the *HAC1* promoter is activated, resulting in increased *HAC1* mRNA levels that, upon splicing, yield more Hac1p. The increased Hac1p concentration, in conjunction with an additional postulated factor(s) produced or activated by the S-UPR ('UMF'), allows the cell to mount a modified transcriptional response to cope with the inducing stress conditions.

Figure 6 shows the UPR as a circuit diagram utilizing multiple logical operations to integrate various signals. In the "classical UPR" (in *red*), basal transcription of *HAC1* produces $HAC1^u$ mRNA, which is translationally inactive due to the presence of the inhibitory intron. In response to unfolded proteins ('UP'), Ire1p performs an ON/OFF operation, excising the intron from $HAC1^u$ mRNA to generate spliced $HAC1^i$ mRNA, which is translated to produce the Hac1p transcription activator. The S-UPR provides another layer of regulation superimposed on the UPR (in *blue*). If ER folding stress ('UP') is combined with either a shift to elevated temperature or with inositol starvation ('I/T'), an AND gate integrates this bipartite signal and boosts *HAC1* mRNA levels. In turn, this regulation causes increased Hac1p production. Together with UMF, Hac1p induces UPR target genes, with particular genes responding differentially to differences in Hac1p and UMF concentration. Thus the S-UPR can be seen as an adaptation of the

classical (or basal) UPR, fine-tuning the activation of select targets to produce a response suited to the challenge faced by the cell.

In the accompanying paper, Patil *et al.* describe a third signaling element, which additionally modifies the transcriptional program of the yeast UPR (Patil et al., 2004). They show that the transcriptional activator Gcn4p collaborates with Hac1p at the promoters of UPR targets, providing an additional opportunity for integration of information about the physiological state of the cell. Gcn4p is a highly regulated transcription regulator that responds to metabolic conditions, such as amino acid availability. Gcn4p is not UMF, as S-UPR induction of *HAC1* proceeds normally in $\Delta gcn4$ cells (data not shown).

Bipartite signal requirement for S-UPR activation

Presently, the molecular details of the pathway by which the S-UPR signal exerts transcriptional control are not known. In particular, it will be of interest to determine where in the cell the two branches of the S-UPR signal are integrated, i.e. how the AND gate is constructed and where it resides. One possibility is that this signal integration event occurs close to the source at the ER membrane. Both temperature shift and inositol starvation can equally induce the I/T branch of the pathway, and it is conceivable that both conditions effect ER membrane properties similarly. Inositol is an essential precursor for phosphatidylinositol, a major structural phospholipid in yeast that is required for proper functioning of the secretory system (White et al., 1991)(Zinser and Daum, 1995)(Greenberg and Lopes, 1996). Previous work has demonstrated an intimate

link between inositol regulation and the UPR, presumably to coordinate the concentration of ER lumenal and membrane components (Cox et al., 1997). A similar sensing mechanism operates in cholesterol homeostasis, with sterol composition in ER membranes affecting the activity of SCAP, a membrane-bound regulator of SREBP intramembrane proteolysis (Espenshade et al., 2002). It is likely that elevated temperatures also affect ER membrane properties, such as fluidity (Laroche et al., 2001). If such a property were sensed, it would explain how the temperature effect contributing to the I/T signal is separate from the heat shock response. ER membranes distressed by either inositol deprivation or elevated temperature (the I/T signal) might then control the activity of a membrane-bound component of a signal transduction machine that also senses protein folding conditions (the UP signal) in the ER lumen.

Alternatively, the AND gate might be well removed from the ER membrane, with I/T and UP signals traveling separately through the cell and meeting possibly as late as at the promoters of the affected target genes. Components that map onto either signaling pathway need to be identified and placed into the circuit to distinguish between these possibilities.

The transcriptional output of the S-UPR

The transcriptional response elicited by the S-UPR reveals different classes of UPR targets. During the S-UPR, the further activation of UPR targets is not simply proportional to the increase in Hac1p concentration; rather, we observe a multitude of complex responses. Some targets are already maximally transcribed during UPR conditions and are not induced further during the S-UPR, while other targets become

significantly more induced. For some targets (a minority), elevated Hac1p concentrations are sufficient to increase transcriptional induction, while for others S-UPR-derived UMF is also required. We find evidence for both kinds of regulation. The promoters of target genes, therefore, display differential responsiveness to Hac1p concentration and UMF activity.

The production of different levels of Hac1p allowed us to isolate and directly assess the responsiveness of target genes to Hac1p concentration under otherwise-identical conditions. Those target genes that undergo equivalent activation under both conditions likely have promoters that are saturated by the lower amount of Hac1p, and thus reach full activation more readily. For UPR targets at the other end of the spectrum, induction continues to increase as Hac1p levels increase; lower concentrations of Hac1p are inadequate for full stimulation of these genes, which may have lower affinity for Hac1p. Because genes respond differentially to Hac1p levels, regulation of *HAC1* mRNA abundance can be used as a gene-specific gain control for target activation. This control is similar to that observed in regulation of phosphate metabolism, whereby the differential affinity of certain Pho4p phosphoforms for target promoters allows for the selective activation of a subset of phosphate-responsive genes (Springer et al., 2003).

For most target genes, however, the S-UPR further enhances the transcriptional activity even in the presence of high concentrations of Hac1p. For example, *INO1* is induced over 75-fold by the S-UPR in wildtype cells, compared to 33-fold during the UPR in *HAC1pro*^{HI} cells, while the amount of Hac1p produced in both cases is approximately the same. This added induction during the S-UPR is dependent on Hac1p, as *ADH1pro-HAC1* cells treated with DTT and shifted to elevated temperature show

significantly reduced induction of *INO1*. The simplest interpretation of these findings is that S-UPR induced UMF, which may or may not be identical to the transcription factor regulating *HAC1* mRNA, collaborates with Hac1p to further boost transcription of these genes.

Links with the metazoan UPR

Higher eukaryotes possess three separate pathways to sense ER stress and direct overlapping but distinct transcriptional outputs (reviewed in (Ma and Hendershot, 2001)). In the first branch, Ire1p senses unfolded proteins in the ER lumen and directs the cleavage of an intron from the mRNA encoding the XBP-1 transcription factor, analogous to the splicing of *HAC1* in yeast (Calfon et al., 2002)(Yoshida et al., 2001). In a second branch, the transmembrane kinase PERK phosphorylates and inactivates the eIF2-α translation initiation factor (Harding et al., 1999). This attenuates global protein synthesis, but selectively increases the translation of a small number of proteins including the ATF-4 transcriptional activator. Interestingly, ATF-4 is the metazoan ortholog of Gcn4p, the yeast transcription factor demonstrated by Patil *et al.* (Patil et al., 2004) to collaborate with Hac1p. Finally, in a third branch, activation of the UPR in metazoans allows for the ER-to-Golgi transit of the membrane-tethered ATF-6 protein. In the Golgi apparatus, ATF-6 undergoes proteolytic cleavage within its membrane-spanning domain, and the soluble fragment subsequently travels to the nucleus as an active transcription factor (Haze et al., 1999)(Ye et al., 2000). XBP-1, ATF-4, and ATF-6 all activate separate but overlapping transcriptional programs that enable the cell to respond to changing conditions in the ER. Notably, the *XBP-1* promoter is a target of ATF-6

activation (Yoshida et al., 2001), reminiscent of the circuitry described here for yeast. Conceptually, therefore, *HAC1* mRNA upregulation by the S-UPR pathway takes the place of *XBP-1* upregulation by the ATF-6 fragment. Moreover, ATF-6 and XBP-1 can heterodimerize (Lee et al., 2002), reminiscent of the proposed collaboration of UMF and Hac1p. Thus, intriguing parallels in the wiring that connects the elements of the UPR signaling circuit between yeast and metazoans are beginning to come to light.

These findings suggest a surprisingly common strategy of all eukaryotic cells to respond to challenges to the secretory system. Maintaining separate ER-surveillance pathways creates the potential for cells to integrate multiple signals that, in principle, could convey precise information regarding the nature of the imbalance to afford finely tailored corrective measures. In this view, the UPR operates as a homeostatic control circuit, in which such regulation ascertains that components of the secretory apparatus are produced according to need. The challenge now at hand is to decipher the logic between the UPR inducing conditions and the transcriptional output to add physiological explanations to complex regulation of the response that we observe experimentally.

EXPERIMENTAL PROCEDURES

Yeast Strains

The wildtype strain W303-1A, the Δ*ire1* strain CS165, and the Δ*hac1* strain JC408 are as described previously (Cox et al., 1993) (Cox and Walter, 1996). All *sec* strains used in this study were provided by Robert Fuller (University of Michigan, Ann Arbor), and are otherwise genotypically identical to W303. The *HSF1*^{c} strain was a kind gift of Hillary Nelson (University of Pennsylvania, Philadelphia) and contains the R222A allele of *HSF1* (Bulman et al., 2001) replacing the chromosomal locus in a W303 background. Strains used in the experiments described in Figure 3A were Δ*hac1* transformed with pPW598 ("*HAC1pro-HAC1*", HA-tagged *HAC1* (Cox and Walter, 1996) under its own promoter and with native *HAC1* flanking sequences, in a pRS304 background) or with pPW599 ("*HAC1pro-GFP*", the *GFP* ORF, driven by the *HAC1* promoter (defined as the region starting at the mapped start site of *HAC1* transcription (Rüegsegger et al., 2001) and extending 500 bp upstream) and flanked by 5'UTR and 3'UTR sequences from *ACT1*). Strains used in experiments described in Figure 4 were *HAC1pro-HAC1* and Δ*hac1* (described above) and Δ*hac1* transformed with pPW600 ("*ADH1pro-HAC1*", HA-tagged *HAC1* with 5' and 3'UTR *HAC1* sequence subcloned into the p414 ADH expression vector (Mumberg et al., 1995) and transferred to a pRS304 backbone). In Figure 5, *HAC1pro*^{III} (pPW601) was made by subjecting *HAC1pro-HAC1* to QuikChange mutagenesis (Stratagene) following the manufacturer's protocol, using oligonucleotides to remove the 15 base-pairs at coordinates –338 to –323 (+1 representing the start site of transcription).

Cell culture and plates

Cell culture

Yeast cultures were grown in YPD media (unless otherwise specified) at the indicated temperatures to mid-log phase ($OD_{600} \approx 0.5$). For temperature shift experiments, cultures were transferred to a preheated 37°C water bath shaking incubator. DTT (Roche) was added to a final concentration of 6 mM, and tunicamycin (Boehringer Mannheim) was added to a final concentration of 1 μg/ml. For experiments involving inositol deprivation in liquid media, yeast cells were grown in liquid complete synthetic media described by (Sherman, 1991), supplemented with myo-inositol (Sigma) to a final concentration of 100 μg/ml. Cells were then harvested by filtration, washed three times in pre-warmed complete synthetic media lacking inositol, and then filter transferred to a flask containing pre-warmed complete synthetic media lacking inositol.

Plates

For the experiment described in Figure 4C, yeast strains were grown in YPD to mid-log phase ($OD_{600} \approx 0.5$), transferred to a 96-well microtiter plate, and serially 5-fold diluted in fresh YPD. Using a liquid transfer prong ("frogging") tool (Aladin Enterprises), approximately 3 μl of all serial dilutions of all strains were simultaneously transferred to complete synthetic plates lacking inositol (described above), either in the absence or presence of 0.2 μg/ml tunicamycin. After approximately 2 days of incubation at 30°C,

plates were photographed using the Epi Chemi II Darkroom GelDoc system (UVP Laboratory Products).

RNA Analysis

Isolation of Total RNA and Northern Blot Analysis

Isolation of total RNA from yeast cells was carried out with the modified hot-phenol extraction method described in Rüegsegger *et al.* (2001). For Northern blot analysis, 10 μg of total RNA was separated on a 1.5% w/v agarose gel and transferred to a Duralon-UV nylon membrane (Stratagene), which was incubated with a probe directed against the 5' exon of *HAC1*. The mRNA abundance was quantitated using a PhosporImager (Molecular Dynamics). The membranes were then stripped with two serial washes using 0.1% SDS at 65°C for 60 min each, incubated with a probe directed against the 3' exon of *ACT1*, and mRNA abundance again quantitated. To control for the variable strength of Northern blot probes across multiple experiments, the relative *HAC1*/*ACT1* mRNA abundance ratio is always normalized to the untreated (t = 0) sample. For the detection of other mRNAs, membranes were incubated with the additional relevant probes (*GFP*, *SSA1*) concurrent with the *HAC1* probe. All data shown are an average of at least two independent experiments.

Microarray Experiments and Analysis

PolyA+ mRNA was isolated from total RNA using the PolyATract system (Promega) according to the manufacturer's instructions. Microarray analysis, using yeast ORF

arrays printed at the UCSF Core Center for Genomics and Proteomics (http://derisilab.ucsf.edu/core/), was performed as in Carroll *et al.* (2001) (Carroll et al., 2001) using protocols and reagents described at http://microarrays.org/. All array data are the average of two independent experiments. For this study, we were obliged to evaluate UPR targets differently than in Travers *et al.* (2000) (Travers et al., 2000), as we consider *HAC1*-independent responses, and the former study specifically isolated genes induced by unfolded proteins for which Hac1p was solely responsible (Z test score ≥ 3.6 σ). Here, UPR targets were defined as those genes that met the following three criteria in a parallel set of microarray experiments using wildtype (W303) and Δ*hac1* (JC408) strains. First, induction ($\log_2$ of the fold change in gene expression) in wildtype cells treated with DTT must be at least 1 standard deviation greater than the mean $[((\text{induction}^{WT,DTT} - \mu^{WT,DTT})/\sigma^{WT,DTT}) \geq 1]$. Second, induction in wildtype cells treated with tunicamycin must be at least 1 standard deviation greater than the mean $[((\text{induction}^{WT,TM} - \mu^{WT,TM})/\sigma^{WT,TM}) \geq 1]$. Third, induction in Δ*hac1* cells treated with DTT be at least 1 standard deviation less than the induction in wildtype cells treated with DTT [or, more awkwardly, $(((((\text{induction}^{WT,DTT} - \mu^{WT,DTT})/\sigma^{WT,DTT}) - ((\text{induction}^{\Delta hac1,DTT} - \mu^{\Delta hac1,DTT})/\sigma^{\Delta hac1,DTT}))-\mu^{WT,DTT - \Delta hac1,DTT})/\sigma^{WT,DTT - \Delta hac1,DTT}) \geq 1]$.

Isolation and Detection of Protein from Yeast Cells

Cells were collected by filtration, frozen in liquid nitrogen, and disrupted in 150 μl 8 M urea/1% SDS by vortexing for 5 min at 4°C in the presence of 150 μl silica beads. The samples were then boiled for 5 min and the lysates cleared by centrifugation at 16,200 x g for 5 min at room temperature. SDS-PAGE was performed on 20 μg of protein separated

on NuPAGE 10% w/v SDS-polyacrylamide gels (Invitrogen), and Western blots were visualized using SuperSignal West Dura Extended Duration ECL Substrate (Pierce) according to the instructions of the manufacturer. Hac1p was detected using a polyclonal antibody raised against the carboxy terminus (Figure 4) or a monoclonal antibody raised against the HA epitope and directly coupled to horseradish peroxidase (Figure 5) (Molecular Probes), and Pgk1p was detected using a commercially available polyclonal antibody (Molecular Probes). Protein abundance was quantified using the Epi Chemi II Darkroom GelDoc system (UVP Laboratory Products). Parallel experiments using serial protein dilutions were performed to confirm that the detected protein levels were within the linear range of the system.

Transcription Shut-off

The yeast strain JC218 ((Sidrauski et al., 1996); *rbp1-1*) was grown in YPD at 23°C to $OD_{600} \approx 0.5$ and then shifted to a 37°C water bath, shaking at 250 RPM. To induce the UPR, DTT was added to a final concentration of 6 mM. Cells were harvested and total RNA isolated, at 20 min intervals, as described above.

SUPPORTING INFORMATION

Accession Numbers

The GenBank accession numbers of the sequences discussed in this paper are NP_116622 (Hac1p), NP_011946 (Ire1p), and NP_012448 (tRNA ligase).

Microarray data can be accessed at the Gene Expression Omnibus (GEO) at the National Center for Biotechnology Information (NCBI) database as platform number GPL999 and sample numbers GSM16978-984.

ACKNOWLEDGMENTS

We thank Jason Brickner and other members of the Walter lab for helpful discussions and comments on the manuscript, Adam Carroll and Manuel Llinas for assistance with microarrays, Chris Patil and Hao Li for help with bioinformatic analyses, and Robert Fuller and Hillary Nelson for yeast strains. Also, we acknowledge Vladimir Denic for initial observations regarding *HAC1* mRNA transcriptional control. This work was supported by a UCSF Chancellor's Fellowship to J.L., by support from the UCSF Herbert H. Boyer Fund to S.B., and by grants from the National Institutes of Health to P.W. P.W. is an Investigator of the Howard Hughes Medical Institute.

Conflicts of Interest. The authors have declared that no conflicts of interest exist.

Author Contributions. J.L. and P.W. conceived and designed the experiments. J.L. and S.B. performed the experiments. J.L. and P.W. analyzed the data. J.L. and P.W. wrote the paper.

REFERENCES

Bulman, A. L., Hubl, S. T., and Nelson, H. C. (2001). The DNA-binding domain of yeast heat shock transcription factor independently regulates both the N- and C-terminal activation domains. J Biol Chem *276*, 40254-40262.

Calfon, M., Zeng, H., Urano, F., Till, J. H., Hubbard, S. R., Harding, H. P., Clark, S. G., and Ron, D. (2002). IRE1 couples endoplasmic reticulum load to secretory capacity by processing the XBP-1 mRNA. Nature *415*, 92-96.

Carroll, A. S., Bishop, A. C., DeRisi, J. L., Shokat, K. M., and O'Shea, E. K. (2001). Chemical inhibition of the Pho85 cyclin-dependent kinase reveals a role in the environmental stress response. Proc Natl Acad Sci U S A *98*, 12578-12583.

Chang, H. J., Jones, E. W., and Henry, S. A. (2002). Role of the unfolded protein response pathway in regulation of INO1 and in the sec14 bypass mechanism in Saccharomyces cerevisiae. Genetics *162*, 29-43.

Chapman, R. E., and Walter, P. (1997). Translational attenuation mediated by an mRNA intron. Current Biology *7*, 850-859.

Cox, J. S., Chapman, R. E., and Walter, P. (1997). The unfolded protein response coordinates the production of endoplasmic reticulum protein and endoplasmic reticulum membrane. Mol Biol Cell *8*, 1805-1814.

Cox, J. S., Shamu, C. E., and Walter, P. (1993). Transcriptional induction of genes encoding endoplasmic reticulum resident proteins requires a transmembrane protein kinase. Cell *73*, 1197-1206.

Cox, J. S., and Walter, P. (1996). A novel mechanism for regulating activity of a transcription factor that controls the unfolded protein response. Cell *87*, 391-404.

Espenshade, P. J., Li, W. P., and Yabe, D. (2002). Sterols block binding of COPII proteins to SCAP, thereby controlling SCAP sorting in ER. Proc Natl Acad Sci U S A *99*, 11694-11699.

Greenberg, M. L., and Lopes, J. M. (1996). Genetic Regulation of Phospholipid Biosynthesis in *Saccharomyces cerevisiae*. Microbiological Reviews *60*, 1-20.

Harding, H. P., Zhang, Y., and Ron, D. (1999). Protein translation and folding are coupled by an endoplasmic-reticulum-resident kinase. Nature *397*, 271-274.

Haze, K., Yoshida, H., Yanagi, H., Yura, T., and Mori, K. (1999). Mammalian transcription factor ATF6 is synthesized as a transmembrane protein and activated by proteolysis in response to endoplasmic reticulum stress. Molecular Biology of the Cell *10*, 3787-3799.

Hirsch, J. P., and Henry, S. A. (1986). Expression of the Saccharomyces cerevisiae Inositol-1-Phosphate Synthase (INO1) Gene Is Regulated by Factors That Affect Phospholipid Synthesis. Mol Cell Biol *6*, 3320-3328.

Kaufman, R. J. (2002). Orchestrating the unfolded protein response in health and disease. J Clin Invest *110*, 1389-1398.

Knop, M., Finger, A., Braun, T., Hellmuth, K., and Wolf, D. H. (1996). Der1, a novel protein specifically required for endoplasmic reticulum degradation in yeast. Embo J *15*, 753-763.

Kohno, K., Normington, K., Sambrook, J., Gething, M. J., and Mori, K. (1993). The promoter region of the yeast KAR2 (BiP) gene contains a regulatory domain that responds to the presence of unfolded proteins in the endoplasmic reticulum. Molecular and Cellular Biology *13*, 877-890.

Kozutsumi, Y., Segal, M., Normington, K., Gething, M. J., and Sambrook, J. (1988). The presence of malfolded proteins in the endoplasmic reticulum signals the induction of glucose-regulated proteins. Nature *332*, 462-464.

Laroche, C., Beney, L., Marechal, P. A., and Gervais, P. (2001). The effect of osmotic pressure on the membrane fluidity of Saccharomyces cerevisiae at different physiological temperatures. Appl Microbiol Biotechnol *56*, 249-254.

Lee, A. S. (1987). Coordinated regulation of a set of genes by glucose and calcium ionophores in mammalian cells. Trends Biochem Sci *12*, 20-23.

Lee, K., Tirasophon, W., Shen, X., Michalak, M., Prywes, R., Okada, T., Yoshida, H., Mori, K., and Kaufman, R. J. (2002). IRE1-mediated unconventional mRNA splicing and

S2P-mediated ATF6 cleavage merge to regulate XBP1 in signaling the unfolded protein response. Genes Dev *16*, 452-466.

Ma, Y., and Hendershot, L. M. (2001). The unfolding tale of the unfolded protein response. Cell *107*, 827-830.

Mori, K., Kawahara, T., Yoshida, H., Yanagi, H., and Yura, T. (1996). Signalling from endoplasmic reticulum to nucleus: transcription factor with a basic-leucine zipper motif is required for the unfolded protein-response pathway. Genes to Cells *1*, 803-817.

Mori, K., Ma, W., Gething, M.-J., and Sambrook, J. (1993). A Transmembrane Protein with a cdc2+/CDC28-Related Kinase Activity Is Required for Signaling from the ER to the Nucleus. Cell *74*, 743-756.

Mori, K., Sant, A., Kohno, K., Normington, K., Gething, M. J., and Sambrook, J. F. (1992). A 22 bp cis-acting element is necessary and sufficient for the induction of the yeast KAR2 (BiP) gene by unfolded proteins. Embo Journal *11*, 2583-2593.

Mumberg, D., Muller, R., and Funk, M. (1995). Yeast vectors for the controlled expression of heterologous proteins in different genetic backgrounds. Gene *156*, 119-122.

Ng, D. T., Spear, E. D., and Walter, P. (2000). The unfolded protein response regulates multiple aspects of secretory and membrane protein biogenesis and endoplasmic reticulum quality control. Journal of Cell Biology *150*, 77-88.

Novick, P., Field, C., and Schekman, R. (1980). Identification of 23 complementation groups required for post-translational events in the yeast secretory pathway. Cell *21*, 205-215.

Patil, C., Li, H., and Walter, P. (2004). A Role for Gcn4 and Novel Upstream Activating Sequences in the Unfolded Protein Response. PLoS Biology, *submitted.*

Patil, C., and Walter, P. (2001). Intracellular signaling from the endoplasmic reticulum to the nucleus: the unfolded protein response in yeast and mammals. Curr Opin Cell Biol *13*, 349-355.

Ron, D. (2002). Translational control in the endoplasmic reticulum stress response. J Clin Invest *110*, 1383-1388.

Rose, M. D., Misra, L. M., and Vogel, J. P. (1989). *KAR2*, a Karyogamy Gene, Is the Yeast Homolog of the Mammalian BiP/GRP78 Gene. Cell *57*, 1211-1221.

Rüegsegger, U., Leber, J. H., and Walter, P. (2001). Block of HAC1 mRNA translation by long-range base pairing is released by cytoplasmic splicing upon induction of the unfolded protein response. Cell *107*, 103-114.

Sherman, F. (1991). Getting started with yeast. Methods in Enzymology *194*, 3-21.

Sidrauski, C., Cox, J. S., and Walter, P. (1996). tRNA ligase is required for regulated mRNA splicing in the unfolded protein response [see comments]. Cell *87*, 405-413.

Sidrauski, C., and Walter, P. (1997). The transmembrane kinase Ire1p is a site-specific endonuclease that initiates mRNA splicing in the unfolded protein response. Cell *90*, 1031-1039.

Slater, M. R., and Craig, E. A. (1989). The SSA1 and SSA2 genes of the yeast Saccharomyces cerevisiae. Nucleic Acids Res *17*, 805-806.

Sorger, P. K. (1991). Heat Shock Factor and the Heat Shock Response. Cell *65*, 363-366.

Springer, M., Wykoff, D. D., Miller, N., and O'Shea, E. K. (2003). Partially Phosphorylated Pho4 Activates Transcription of a Subset of Phosphate-Responsive Genes. PLoS Biol *1*, E28.

Travers, K. J., Patil, C. K., Wodicka, L., Lockhart, D. J., Weissman, J. S., and Walter, P. (2000). Functional and genomic analyses reveal an essential coordination between the unfolded protein response and ER-associated degradation. Cell *101*, 249-258.

Urano, F., Wang, X., Bertolotti, A., Zhang, Y., Chung, P., Harding, H. P., and Ron, D. (2000). Coupling of stress in the ER to activation of JNK protein kinases by transmembrane protein kinase IRE1. Science *287*, 664-666.

White, M. J., Lopes, J. M., and Henry, S. A. (1991). Inositol Metabolism in Yeast. Advances in Microbial Physiology *32*, 1-51.

Ye, J., Rawson, R. B., Komuro, R., Chen, X., Davé, U. P., Prywes, R., Brown, M. S., and Goldstein, J. L. (2000). ER stress induces cleavage of membrane-bound ATF6 by the same proteases that process SREBPs. Molecular Cell *6*.

Yoshida, H., Matsui, T., Yamamoto, A., Okada, T., and Mori, K. (2001). XBP1 mRNA is induced by ATF6 and spliced by IRE1 in response to ER stress to produce a highly active transcription factor. Cell *107*, 881-891.

Zinser, E., and Daum, G. (1995). Isolation and biochemical characterization of organelles from the yeast, Saccharomyces cerevisiae. Yeast *11*, 493-536.

Figure 3-1: ER-distal secretory stress boosts *HAC1* mRNA abundance

(**A**) Determination of *HAC1* mRNA abundance during the UPR. The UPR was induced in wildtype (WT) cells by addition of either 6 mM DTT (lanes 1-4) or 1 μg/ml tunicamycin (lanes 5-8) for the times indicated. Total RNA was harvested at the indicated intervals, and the relative abundance of *HAC1* and *ACT1* mRNAs was analyzed by Northern blot analysis (see Experimental Procedures). Splicing is calculated at the ratio of spliced (*HAC1*^{i}) to total (*HAC1*^{i} + *HAC1*^{u}) mRNA. (**B**) Determination of *HAC1* mRNA abundance during ER-distal secretory stress. WT, *sec12-1*, *sec14-3*, and *sec1-1* strains were grown at 23°C and shifted to 37°C. (**C**) Determination of *HAC1* mRNA abundance during ER-proximal secretory stress. WT, *sec14-3*, *sec61-101*, *sec62-101*, and *sec63-201* strains were grown at 23°C and shifted to 37°C.

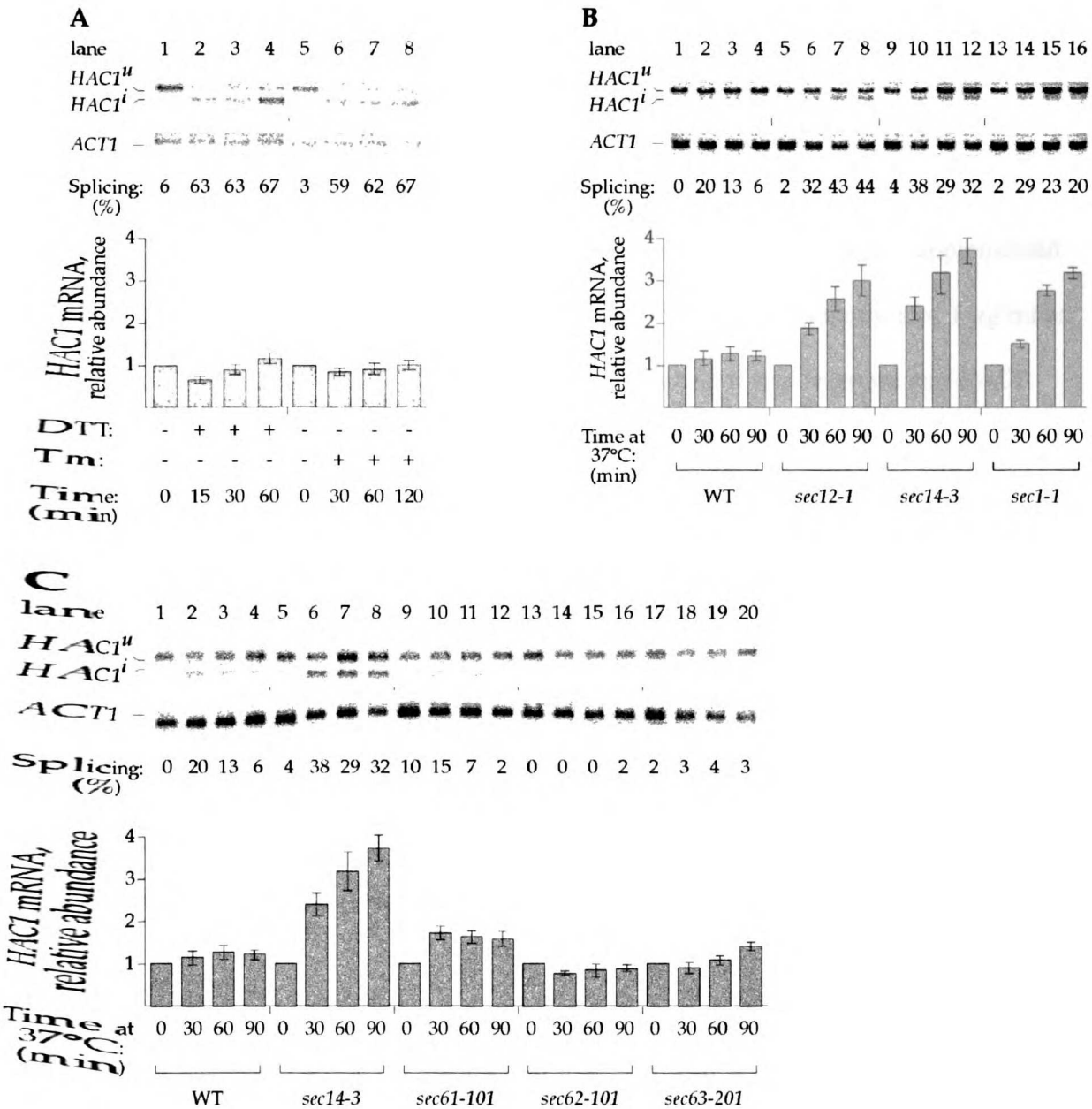
A
lane 1 2 3 4 5 6 7 8
HAC1u
HAC1i
ACT1
Splicing: (%) 6 63 63 67 3 59 62 67
HAC1 mRNA, relative abundance
DTT: - + + + - - - -
Tm: - - - - - + + +
Time: (min) 0 15 30 60 0 30 60 120
B
lane 1 2 3 4 5 6 7 8 9 10 11 12 13 14 15 16
HAC1u
HAC1i
ACT1
Splicing: (%) 0 20 13 6 2 32 43 44 4 38 29 32 2 29 23 20
HAC1 mRNA, relative abundance
Time at 37°C: (min) 0 30 60 90 0 30 60 90 0 30 60 90 0 30 60 90
WT sec12-1 sec14-3 sec1-1
C
lane 1 2 3 4 5 6 7 8 9 10 11 12 13 14 15 16 17 18 19 20
HAC1u
HAC1i
ACT1
Splicing: (%) 0 20 13 6 4 38 29 32 10 15 7 2 0 0 0 2 2 3 4 3
HAC1 mRNA, relative abundance
Time at 37°C: (min) 0 30 60 90 0 30 60 90 0 30 60 90 0 30 60 90 0 30 60 90
WT sec14-3 sec61-101 sec62-101 sec63-201

Figure 3-2: *HAC1* mRNA induction requires a bipartite signal, and is *IRE1*-independent

(**A**) Determination of *HAC1* mRNA abundance during ER stress and temperature shift. WT cells were grown at 23°C and shifted to 37°C (lanes 1-4, 9-12) or kept constant at 30°C (lanes 5-8). DTT was added as indicated (lanes 5-8, 9-12). (**B**) Determination of *HAC1* mRNA abundance during ER stress and inositol deprivation. WT cells were grown at 30°C in synthetic media supplemented with inositol and shifted to synthetic media lacking inositol (lanes 1-4, 9-12), or continuously grown in media supplemented with inositol (lanes 5-8). Tunicamycin was added to a final concentration of 1 μg/ml as indicated (lanes 5-8, 9-12). (**C**) Distinction between heat shock response and *HAC1* mRNA-inducing conditions. WT (lanes 1-4, 9-12) and *HSF1*^{c} (lanes 5-8) strains were grown at 23°C and shifted to 37°C (lanes 1-4, 5-8) or continuously grown at 37°C (lanes 9– 12), and DTT added as indicated. (**D**) Analysis of *IRE1* pathway for a role in *HAC1* mRNA induction. Δ*ire1* cells were grown at 23°C shifted to 37°C (lanes 1-4, 9-12) or continuously grown at 30°C (lanes 5-8), and DTT was added as indicated (lanes 5-8, 9-12). Note that in Δ*ire1* cells, *HAC1* mRNA is modestly induced in response to DTT alone (Fig. 2D, lanes 5-8). This observation is indicative of feedback regulation, whereby a block in the UPR induces the I/T signal.

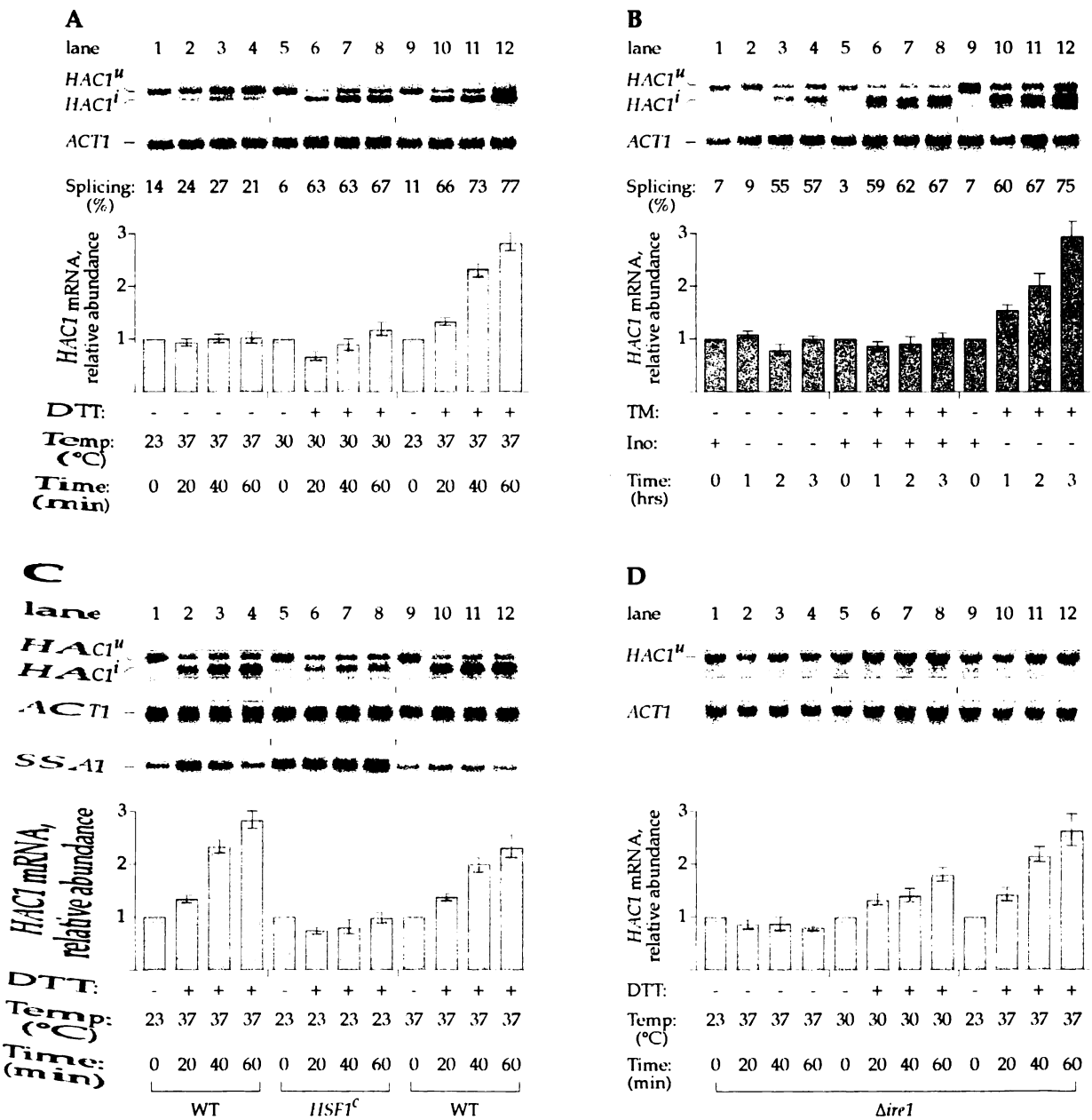
A
lane 1 2 3 4 5 6 7 8 9 10 11 12
HAC1u
HAC1i
ACT1
Splicing (%): 14 24 27 21 6 63 63 67 11 66 73 77
HAC1 mRNA, relative abundance
DTT: - - - - - + + + - + + +
Temp (°C): 23 37 37 37 30 30 30 30 23 37 37 37
Time (min): 0 20 40 60 0 20 40 60 0 20 40 60
B
lane 1 2 3 4 5 6 7 8 9 10 11 12
HAC1u
HAC1i
ACT1
Splicing (%): 7 9 55 57 3 59 62 67 7 60 67 75
HAC1 mRNA, relative abundance
TM: - - - - - + + + - + + +
Ino: + - - - + + + + + - - -
Time (hrs): 0 1 2 3 0 1 2 3 0 1 2 3
C
lane 1 2 3 4 5 6 7 8 9 10 11 12
HAC1u
HAC1i
ACT1
SSA1
HAC1 mRNA, relative abundance
DTT: - + + + - + + + - + + +
Temp (°C): 23 37 37 37 23 23 23 23 37 37 37 37
Time (min): 0 20 40 60 0 20 40 60 0 20 40 60
WT
HSF1c
WT
D
lane 1 2 3 4 5 6 7 8 9 10 11 12
HAC1u
ACT1
HAC1 mRNA, relative abundance
DTT: - - - - - + + + - + + +
Temp (°C): 23 37 37 37 30 30 30 30 23 37 37 37
Time (min): 0 20 40 60 0 20 40 60 0 20 40 60
Δire1

Figure 3-3: Activation of the *HAC1* promoter controls increase in *HAC1* mRNA abundance

(**A**) Analysis of *HAC1* promoter activity during bipartite stress conditions. Δ*hac1* cells containing either a construct restoring *HAC1* expression (lanes 1-4) or a construct expressing *GFP* driven from the *HAC1* promoter (lanes 5-8), were grown at 23°C and shifted to 37°C concurrent with addition of DTT as indicated. (**B**) Determination of mRNA half-life during *HAC1* mRNA inducing conditions. *polII*^{ts} cells were grown at 23°C and were shifted to 37°C either in the absence (open symbols) or presence (filled symbols) of DTT. *HAC1* (circles) and *ACT1* (squares) mRNA abundance is normalized to the abundance of the PolIII transcript *SCR1*.

Figure 3-3

Leber et al. (2004)

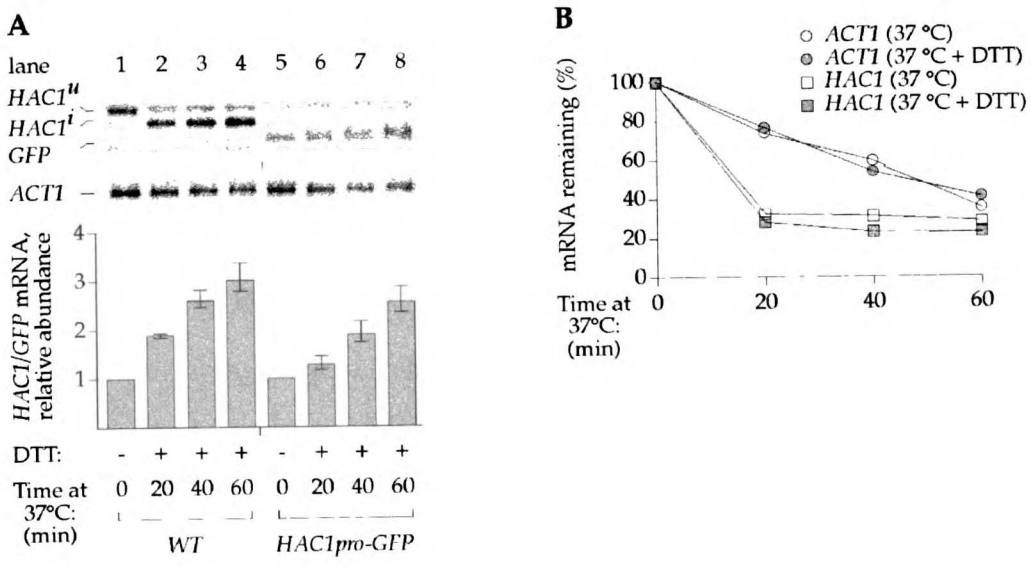

Figure 3-4: *HAC1* promoter regulation is required to survive stress

(**A**) Determination of Hac1p levels during either ER stress alone or during both ER stress and temperature shift. WT cells were either grown at 30°C and treated with DTT (lanes 1-4) or grown at 23°C and simultaneously shifted to 37°C and treated with DTT (lanes 5-8). Protein lysates were prepared, and protein levels were analyzed by Western blot analysis. The relative Hac1p/Pgk1p ratio is normalized to the DTT treated sample (lane 4). (**B**) Characterization of *HAC1* expression in strain used to approximate basal *HAC1* expression. Cells expressing *HAC1* from the endogenous promoter (lanes 1-4), or the *ADH1* promoter (lanes 5-8) were grown at 30°C in synthetic media supplemented with inositol and shifted to synthetic media lacking inositol simultaneous with addition of tunicamycin. (**C**) Reduced viability of strains unable to express *HAC1* at elevated levels. The strains described in Figure 4B were plated in serial dilutions (left to right) on synthetic media lacking inositol ("-ino") and synthetic media lacking inositol and containing tunicamycin ("-ino +TM").

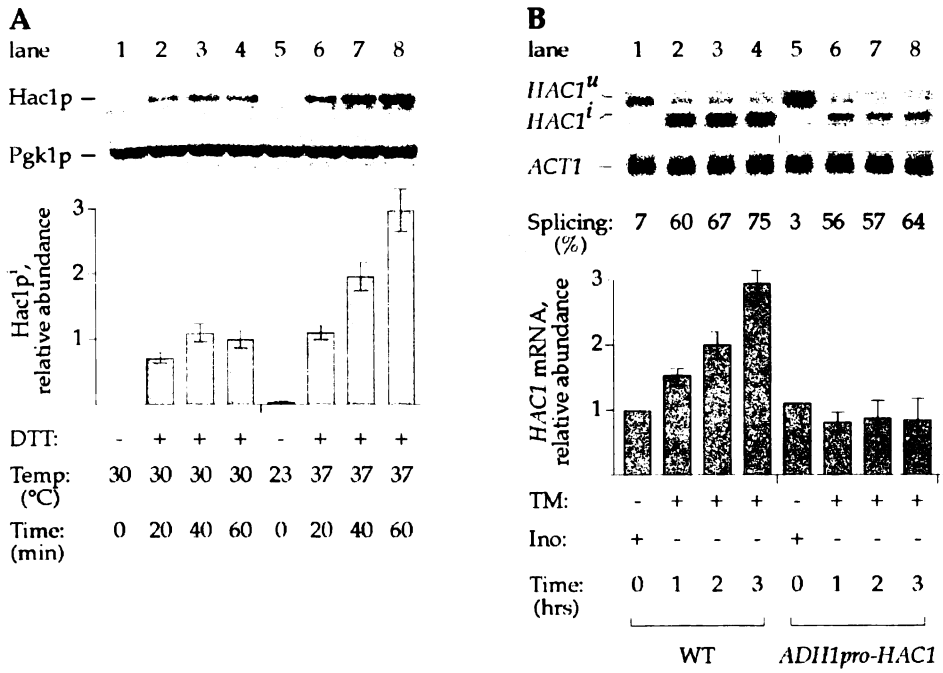
A
lane 1 2 3 4 5 6 7 8
Hac1p –
Pgk1p –
Hac1p', relative abundance
3
2
1
DTT: - + + + - + + +
Temp: (°C) 30 30 30 30 23 37 37 37
Time: (min) 0 20 40 60 0 20 40 60
B
lane 1 2 3 4 5 6 7 8
HAC1u –
HAC1i –
ACT1 –
Splicing: (%) 7 60 67 75 3 56 57 64
HAC1 mRNA, relative abundance
3
2
1
TM: - + + + - + + +
Ino: + - - - + - - -
Time: (hrs) 0 1 2 3 0 1 2 3
WT
ADH1pro-HAC1
C
-ino
-ino +TM
WT
Δhac1
ADH1pro-HAC1

Figure 3-5: Differential UPR target gene induction by elevated Hac1p levels

(**A**) Comparison of UPR target gene induction during either UPR or S-UPR conditions. Whole-genome mRNA expression analysis was carried out on WT cells harvested after 60 min of treatment, either grown at 30°C and treated with 6 mM DTT (X-axis), or grown at 23°C and simultaneously shifted to 37°C and treated with 6 mM DTT (Y-axis). Fold changes in gene expression are in reference to the untreated (t=0) samples. Only shown are those genes designated as targets of the UPR (see Experimental Procedures). The dashed diagonal line represents equal induction under both conditions. (**B**) Comparison of UPR target gene induction during either UPR or S-UPR conditions (alternate display). The data from Figure 5A were analyzed to generate a ratio (X-axis) for each gene, dividing the induction during S-UPR inducing conditions by the induction during UPR inducing conditions, with target genes of similar ratio grouped together (Y-axis). (**C**) Characterization of *HAC1* expression in strain constitutively expressing *HAC1* at high levels. Cells expressing *HAC1* from the endogenous promoter (WT, lanes 1-2), or a modified promoter constitutively expressing *HAC1* at high levels (*HAC1pro*^{HI}, lanes 3-4) were treated with 6 mM DTT for 60 min. Although the basal transcription of *HAC1pro*^{HI} is elevated, the promoter is still capable of further induction during the S-UPR (data not shown). (**D**) Determination of Hac1p level in strain constitutively expressing *HAC1* at high levels. Protein lysates were prepared from the strains described in Figure 5C, and protein levels were analyzed by Western blot analysis. The relative Hac1p/Pgk1p ratio is normalized to the WT DTT treated (t = 60) sample from Figure 4A. For Figures 5E and 5F: *a* = *DER1*, *b* = *INO1*, *c* = *YOR289W*, *d* = *YHR087W*. (**E**) Transcriptional response of different classes of UPR targets to high levels of Hac1p.

Whole-genome mRNA expression analysis was carried on *HAC1pro*^{III} and WT cells treated with 6 mM DTT and harvested after 60 min. For the genes in each of the three classes of UPR targets defined in Figure 5B, a ratio (X-axis) is calculated by dividing the fold induction in DTT-treated *HAC1pro*^{III} cells by the fold induction in DTT-treated WT cells. This ratio is plotted against the number of genes with a similar ratio (Y-axis). The Class 2 target *YFR026C* (*) that is DTT-induced approximately 10-fold more in *HAC1pro*^{III} than in WT cells is of unknown function. (**F**) Transcriptional response of different classes of UPR targets to UMF. Whole-genome mRNA expression analysis was carried on *ADH1pro-HAC1* cells grown at 23°C and simultaneously shifted to 37°C and treated with 6 mM DTT, and WT cells treated with 6 mM DTT, both harvested after 60 min. For the genes in each of the three classes of UPR targets defined in Figure 5B, a ratio (X-axis) is calculated by dividing the fold induction in *ADH1pro-HAC1* cells during S-UPR-inducing conditions by the fold induction in WT cells during UPR-inducing conditions. This ratio is plotted against the number of genes with a similar ratio (Y-axis).

Figure 3-5 *Leber et al. (2004)*

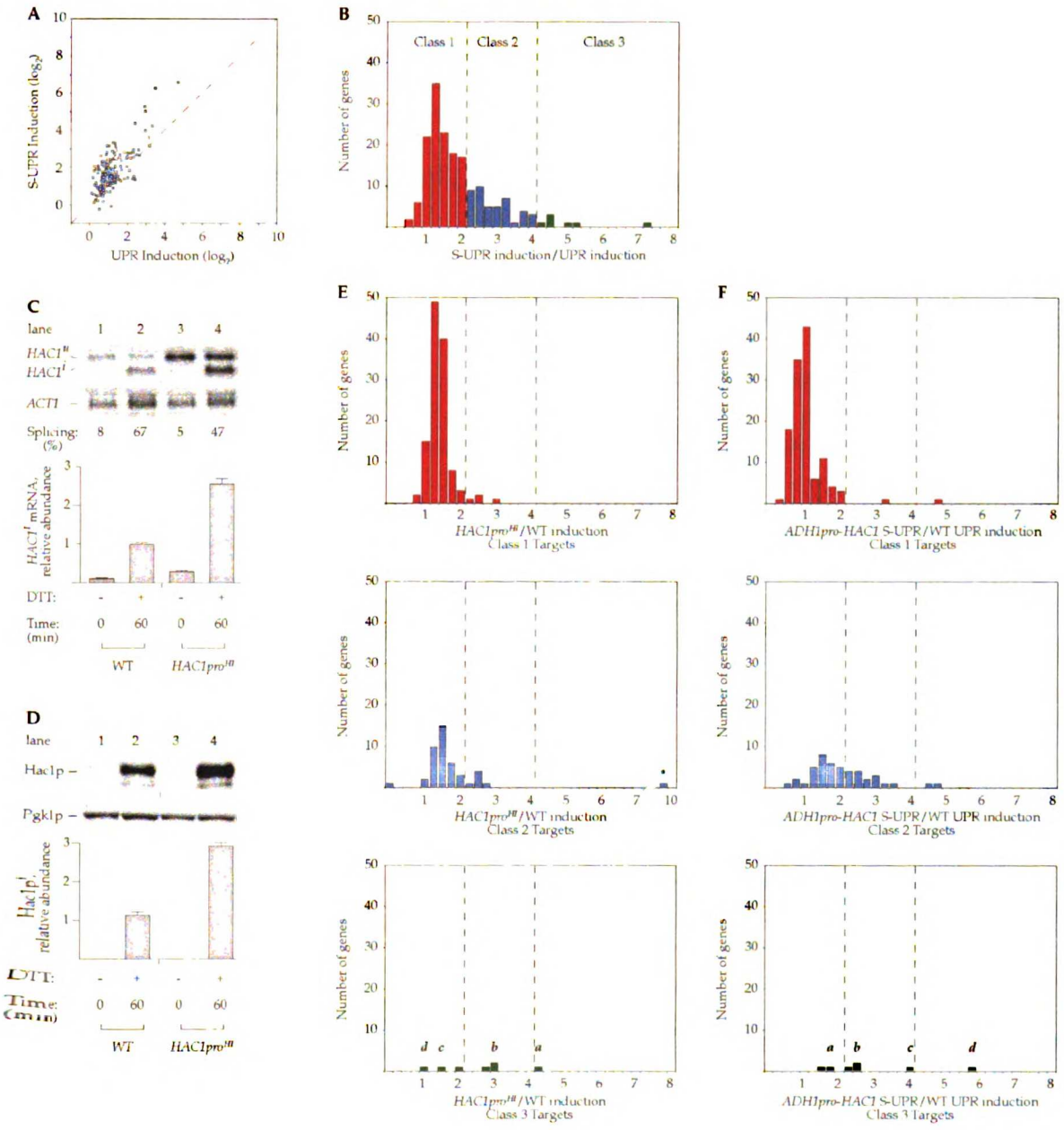

Figure 3-6: A schematic of the circuitry of the Unfolded Protein Response

The model depicts the circuitry of the UPR (in *red*) and the S-UPR (in *blue*). Transcriptional control of *HAC1* is indicated by an icon representing a rheostat affording gain control of the UPR; Ire1p-dependent *HAC1*^{u} mRNA splicing by an icon representing an ON/OFF switch. The I/T and UP signals in the S-UPR are integrated by an AND gate (half-circle, top right), *i.e.* both conditions must be met to propagate the S-UPR signal. The putative UPR Modulatory Factor UMF may both collaborate with Hac1p to control transcription of UPR target genes (shown) and also be involved in regulating *HAC1* transcription (not shown); alternatively, different factors may be involved. The collaboration of Hac1p and UMF is indicated by the diamond-shaped icon, which integrates the information coming from both Hac1p and UMF concentration and activity.

Figure 3-6 *Leber et al. (2004)*

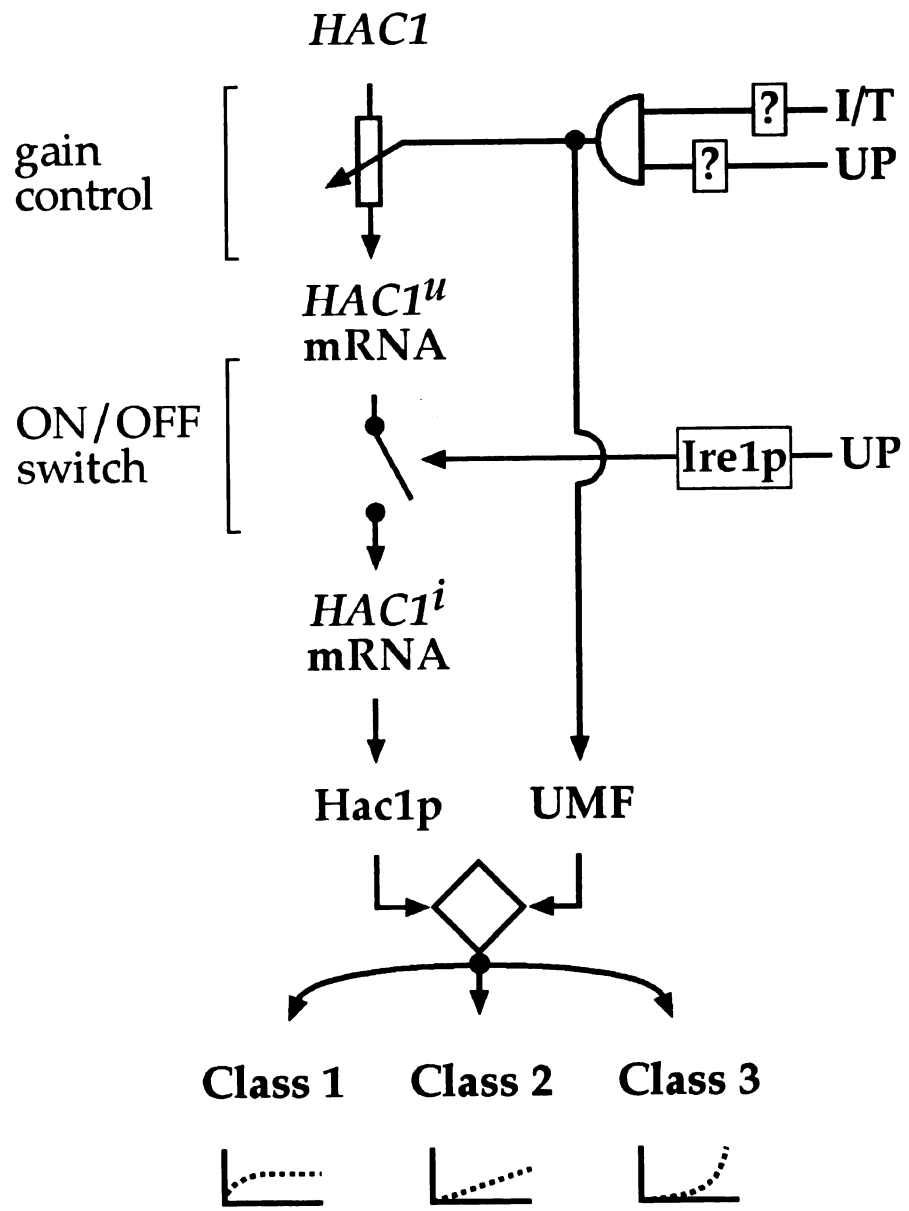

Chapter 4

Unfinished business, loose ends, and perspectives on *HAC1* and the UPR

INTRODUCTION

In this final chapter, I hope to provide the seeds for future fruitful projects in the Walter Lab. The two published papers I have presented as earlier chapters of this thesis represent only those projects that have come to tidy conclusions, which represent only a fraction of my efforts. Here I will present both potentially interesting offshoots of those projects, and also experiments that address aspects of the UPR other than transcriptional or translational regulation of Hac1p, including equal parts initial results and pure speculation. Overall, I hope that whoever reads this will keep in mind three things: 1) The more you examine a seemingly-simple aspect of the UPR, the more it will surprise you; 2) I would wager that *every* possible step leading to active Hac1p is regulated; and 3) If Peter mentions an idea of his to you three times or more, put aside any preconceived notions as to why it won't, and give it a try.

TRANSLATIONAL REGULATION OF *HAC1*

Mechanism of translational attenuation of metazoan Hac1p orthologs

The mechanism of translational attenuation of unspliced *HAC1*^{u} mRNA, presented in Chapter 2, represents an "intramolecular anti-sense" regulation that, to our knowledge, is unique (Figure 4-1A). While reminiscent of the anti-sense regulation observed in flies in worms (*e.g.* the small non-coding *lin-4* RNA repressed the translation of *lin-14* in *C. elegans* by binding to its 3'UTR (Lee et al., 1993; Wightman et al., 1993)) (Figure 4-1B), it is difficult to imagine that intramolecular anti-sense is an often used mechanism. In order for translational attenuation to be a "switch", the inhibitory pairing between

complementary bases must be disrupted; for an intramolecular inhibition to occur, the two contiguous elements must be physically separated by splicing. However, the splicing of most all mRNA occurs in the nucleus, whereas polyribosome loading occurs in the cytoplasm. Hence, only for those mRNAs that undergo non-canonical, cytoplasmic splicing is intramolecular anti-sense translational regulation a possibility.

At present, the only mRNAs known to be spliced in the cytoplasm are the substrates of Ire1p. Furthermore, in an elegant microarray-based approach, Maho Niwa found that *HAC1* mRNA is the only substrate for Ire1p-mediated splicing in yeast (M. Niwa and P. Walter, unpublished results). Therefore, the possible set of mRNAs subject to intramolecular anti-sense regulation is likely to be confined to the metazoan orthologs of *HAC1*. At present, this includes only *XBP-1*, identified in worms and mammalian cells as both subject to splicing by Ire1p and encoding a transcription factor that activates UPR targets (Calfon et al., 2002; Yoshida et al., 2001). However, it appears that even *XBP-1* is not likely to be regulated in a manner strictly analogous to that of *HAC1*; while the unspliced *XBP-1* mRNA appears to be translated less efficiently than the spliced form, the attenuation is not complete, and protein in made in un-induced cells (Calfon et al., 2002). Furthermore, the *XBP-1* intron that is removed by Ire1p splicing is only 22 bases, and examination of this sequence reveals no complementarity to the 5'UTR. Hence, any translational attenuation potentially mediated by an interaction between the *XBP-1* 5'UTR and intron would likely involve a protein intermediary, rather than direct base-pairing (Figure 4-1C).

This raises the question: Is the translation inhibition of *HAC1* in yeast accomplished strictly by the 5'UTR/intron base-pairing, or are accessory proteins

involved here, as well? While the *in vitro* experiments described in Rüegsegger *et al.* (Rüegsegger et al., 2001) suggest that direct base-pairing is primarily responsible for the translation attenuation of *HAC1*, the residual translation of the unspliced mRNA in these experiments allows for the possibility of participation of additional factors *in vivo* (see Figure 2-2C, lanes 2-4). Even after Ire1p splicing of *HAC1* upon UPR activation, the 5'UTR and intron remain paired (Gonzalez et al., 1999), suggesting that a helicase may be necessary to relieve the translation inhibition by separating the base-paired but no longer physically linked elements. Therefore, I consider it possible, if not probable, that: 1) intramolecular anti-sense translational regulation occurs only in *HAC1* and its orthologs; 2) inhibition of *XBP-1* is primarily protein-mediated rather than mediated strictly by base-paired mRNA; and 3) further studies will uncover proteins participating in the translational attenuation of unspliced *HAC1* in yeast.

A microarray- and polysome gradient-based screen for mRNAs subject to translation elongation control

While optimizing the polysome gradients used to demonstrate the *HAC1*^{u}-polyribosome interaction shown in Chapter 2 and Rüegsegger *et al.* (Rüegsegger et al., 2001), Ursula Rüegsegger noticed that this interaction is particularly magnesium requiring. In fact, it was because of the different magnesium chloride concentration she was using in her assays that she had a difficult time at first recreating the earlier results of Jeff Cox (Cox and Walter, 1996). I have followed up on her initial observations, and indeed find that the *HAC1*^{u}-polyribosome interaction appears biochemically distinct from that of other mRNAs: when the concentration of $MgCl_2$ used in the preparation of extracts for polysome gradients is lowered below approximately 25 mM, *HAC1*^{u} begins to

disassociate from polyribosomes, whereas *ACT1* does not (Figure 4-2, above dashed line). The exact protocol used in these preparations can be found on the Walter Lab web site (www.walterlab.ucsf.edu). Quantitation of these results (Figure 4-3) shows that at 50 mM $MgCl_2$ both *HAC1* (upper panel) and *ACT1* (lower panel) mRNAs are comparably and extensively ribosome-loaded, whereas at 5 mM $MgCl_2$ the bulk of ribosomes have fallen off the *HAC1* message but remain bound to *ACT1* mRNA.

There are at least two possible explanations for these results: 1) The interaction between mRNA and non-translating ribosomes requires higher concentrations of $MgCl_2$ *in vitro* than does the interaction between mRNA and translating; or 2) The interaction between highly structured mRNA and ribosomes requires higher concentrations of $MgCl_2$ *in vitro* than does the interaction between less structured mRNA and ribosomes. In the first hypothesis, one could imagine that the ribosomes bound to unspliced *HAC1* mRNA differ from those bound to *ACT1*, perhaps in the composition of accessory proteins, and therefore have altered *in vitro* behavior. This is similar to the scenario seen in ceruplasmin (Cp) expression in mammalian cells: in gamma interferon-induced cells, the L13a ribosomal accessory protein is phosphorylated and released; an element within the Cp mRNA 3'UTR binds L13a and silences translation of the upstream ORF (Mazumder et al., 2003). Alternately, in support of the second hypothesis, precedent exists for *in vitro* ion conditions affecting RNA structure (see (Villa et al., 2002) and references therein); perhaps the base-paired, unspliced *HAC1* mRNA changes conformations upon decrease in $MgCl_2$ concentration, and the interaction with ribosomes is disrupted. Both hypotheses predict that the magnesium requirement of the *HAC1*-ribosome interaction should be mitigated in extracts produced from UPR-induced cells: the ribosomes are

released from their stalled state and are actively translating, and the *HAC1* intron is excised and thus can no longer contribute to mRNA secondary structure. This is exactly what we observe, as shown in the bottom of Figure 4-2 (below dashed line). In a sucrose gradient using an extract prepared with 5 mM $MgCl_2$ from cells treated with DTT, *HAC1* remains bound to many more ribosomes than does *HAC1* in untreated cells.

While the reason for the special magnesium requirement of the unspliced *HAC1*-polyribosome complex is still unknown, we envision using this biochemical distinction as the basis for a screen for other mRNAs with *HAC1*-like characteristics. As schematized in Figure 4-4, extracts are prepared for polysome profiles with varying concentrations of $MgCl_2$. These different extracts are run over sucrose gradients, and fractions representing mRNAs unbound by ribosomes (top of gradient), bound to 1-3 ribosomes (middle of gradient), or bound to 4+ ribosomes (bottom of gradient) are harvested and pooled. PolyA+ is extracted from the sucrose gradient pools, reverse transcribed, labeled with fluorescent Cy-dyes, and hybridized to microarrays. Those mRNAs that are concentrated in the top fractions of the sucrose gradient in extracts prepared from low concentrations of $MgCl_2$, but not in extracts with high concentrations of $MgCl_2$, would be analyzed further. These mRNAs should be reciprocally depleted from the heavier, polyribosome-containing fractions in extracts prepared from low concentrations of $MgCl_2$, but not in extracts with high concentrations of $MgCl_2$. Candidate mRNAs thus isolated may have no role in the UPR, as their isolation in this screen requires only that they are either bound by stalled ribosomes, have an unusually structured mRNA, or share whatever feature results in an mRNA-ribosome complex that requires higher levels of $MgCl_2$.

Only after candidate mRNAs are identified will we really understand the biochemical characteristics that allowed for their isolation. For instance, Western analysis will determine if the expression of the candidate mRNA is repressed in wildtype cells in untreated conditions. If this is what we observe, then the magnesium requirement is more likely to have resulted from a feature of stalled ribosomes, and our screen will therefore have succeeded in isolating other mRNAs whose translation is regulated at the elongation step, which would be quite exciting as this mechanism is quite rare. Alternately, if expression of the candidate mRNAs is not repressed, then the magnesium requirement and subsequent isolation is more likely to have resulted from a feature of highly structured mRNAs. This would be confirmed both using structure prediction programs, such as mfold (Zuker, 2003), and also biochemical assays such as modification interference. In either case, subsequent experiments would be required to identify the mechanism of regulation for each individual candidate mRNA, such as the appropriate inducing condition that switches stalled ribosomes to the elongating state.

TRANSCRIPTIONAL REGULATION OF *HAC1*

In Chapter 3 I describe our recent work describing an *IRE1*-indepdendent ER surveillance pathway that upregulates *HAC1* mRNA, which we call the "Super-UPR" ("S-UPR"). When ER folding stress in combined with either temperature shift or inositol starvation, the *HAC1* promoter is activated, leading to the production of elevated levels of Hac1p. The transcriptional output of the UPR is modified, with the selective upregulation of certain targets, which allows the cells to survive the bipartite stress. However, this altered UPR program does not result simply from elevated levels of Hac1p; rather, our

microarray data suggest that an additional "UPR Modulatory Factor" ("UMF") must collaborate with Hac1p to activate UPR target genes. While we have learned a great deal about the S-UPR, the identity of UMF is still unknown. Here I present two approaches that I have devised to find UMF.

A genetic screen for UMF

In the course of studying the S-UPR, I found that certain plate conditions discriminate between cells that are able to upregulate *HAC1* and those that cannot. As shown in Figure 4-5A, both wildtype cells and cells in which *HAC1* has been placed under the control of the *ADH1* promoter (*ADH1pro-HAC1*) can grow on plates lacking inositol. The *ADH1* promoter is approximately the same strength as the uninduced *HAC1* promoter, and therefore fixes Hac1p levels during the S-UPR to UPR levels (please see Chapter 3, and Figure 3-3 specifically, for more discussion of this construct). Only wildtype cells, and not *ADH1pro-HAC1* cells, can grow on plates both lacking inositol and containing tunicamycin. Therefore, UPR-levels of Hac1p are necessary (*Δhac1* cells do not grow) and sufficient for growth on the first condition, while S-UPR levels of Hac1p are required for growth on the second. These discriminating conditions therefore allow for the isolation of both UMF and the sequence within the *HAC1* promoter to which UMF binds (Figure 4-5B). Mutated cells in which either UMF activity has been reduced (EMS mutagenesis) or the binding site for UMF within the *HAC1* promoter destroyed (PCR mutagenesis) should be unable to upregulate *HAC1*, and will therefore not grow on plates lacking inositol and containing tunicamycin. As discussed in Chapter 3, UMF may actually be comprised of two, separate transcriptional activities, each provided by the individual stimuli necessary to trigger the S-UPR. Also, the

transcriptional activator responsible for *HAC1* mRNA upregulation may be different from the activity that contributes to the induction of S-UPR target genes. In either of these scenarios, the described genetic screen should still uncover the relevant molecules. As shown in Chapter 3 and Figure 4-5A, elevated levels of Hac1p are required to survive S-UPR conditions; even if UMF is only responsible for *HAC1* activation, and not the activation of S-UPR targets, Δ*umf* cells will die on –ino +TM plates. If there is a separate transcription factor(s) that participates in the activation of S-UPR target genes, it would also be found by this screen; elevated levels of Hac1p are insufficient for the full induction of S-UPR targets (Figure 3-5), some of which are likely to be required for survival of S-UPR-triggering conditions.

This screen has already begun, in the capable hands of Sebastián Bernales. Sebastián has used the plate conditions that I have devised, and has succeeded in isolating mutants that fail to upregulate *HAC1* mRNA during the S-UPR, and has also identified elements within the *HAC1* promoter that are necessary and sufficient for *HAC1* upregulation during the S-UPR. You'll have to wait for his thesis to learn the identity of UMF.

A bioinformatic approach to identifying UMF

In the course of characterizing the altered transcriptional output of the S-UPR, we have accumulated much microarray data that can now be enlisted in the cause of identifying UMF. It should be possible to mine this data to find genes that are likely activated by UMF, find elements within their promoters that are necessary and sufficient to confer responsiveness to UMF, and then use these defined elements in either genetic or biochemical screens for UMF. An excellent example and description of the utility of this

approach is presented in Patil *et al.* (Patil et al., 2004), wherein the transcriptional activator Gcn4p is identified as a participant in the UPR by binding to and activating the promoters of some target genes. A back-of-the-envelope analysis of the S-UPR array data yields a short list of genes that may be targets of UMF (Figure 4-5C). These are genes upregulated at least 3-fold in the S-UPR, and show greater induction in S-UPR-induced *ADH1pro-HAC1* cells (which cannot attain high levels of Hac1p) than in UPR-induced *HAC1proHI-HAC1* cells ((S-UPR induction in *ADH1pro-HAC1*)/(UPR induction in *HAC1proHI-HAC1*) > 2; to stress UMF-induced activation as opposed to Hac1p-induced activation). This is by no means bioinformatically rigorous, and is included simply to illustrate the possibilities of such an approach. What are the bioinformatically-relevant characteristics that one could reasonably expect of a UMF target? Certainly, it should be induced during the S-UPR. Further, it should be induced during the S-UPR in a Δ*hac1* strain; while this will eliminate targets whose induction requires both UMF and Hac1p, it will not exclude targets induced by *either* UMF or Hac1p (as is the case for some targets of *ATF-6* and *XBP-1* in the metazoan UPR; reviewed in (Ma and Hendershot, 2001)) and is likely to make the subsequent analysis easier. I consider it likely that for some targets of the S-UPR, UMF will be predominantly if not solely responsible. For example, activation of the *HAC1* promoter during the S-UPR requires neither *IRE1* (Figure 3-2D) nor *HAC1* (data not shown), demonstrating that Hac1p does not participate in the activation of its own mRNA. This view is further supported by the results shown in Figures 3-5E and F, which identify *YHR087W* and *YOR289W* as targets of the S-UPR for which UMF, and not Hac1p, is likely the primary inducing factor.

HAC1P PHOSPHORYLATION AND INTERACTIONS BETWEEN THE UPR AND THE *PKC1* CELL INTEGRITY PATHWAY

Hac1p is phosphorylated (Chapman and Walter, 1997; Mori et al., 2000), but it is not clear what effect, if any, this has on Hac1p activity, or if this is a regulated process. Phosphorylation of transcription factors has been shown to control their nuclear localization (Komeili and O'Shea, 1999) and their target specificity (Springer et al., 2003), and be responsive to cellular and environmental conditions (Schneider et al., 1994). It was therefore of considerable interest when I first observed a species of Hac1p with altered gel mobility, in the course of investigating the link between the UPR and secretory stress (Figure 4-6A, compare 90 min to 120 min). At the time, I was focusing on the induction of the *HAC1* promoter in *sec* mutants. It had been reported that blocks in the secretory pathway downregulate ribosome biogenesis and decrease global translation (Nanduri and Tartakoff, 2001), and I was curious to what extent an increase in *HAC1* mRNA abundance translated to an increase in Hac1p levels. Upon seeing the altered gel mobility, I first suspected that the use of an initiating ATG further upstream in the *HAC1* mRNA than the normal start of translation might be responsible; at that time, there was still some confusion as to the transcription start site in the *HAC1* mRNA, and we were not sure if the mRNA contained an alternative, upstream ATG. As I found by Northern analysis (Figure 4-6B), the *HAC1* mRNA that gave rise to the two forms of Hac1p was indistinguishable, therefore the suspected cause of altered protein mobility shifted to post-transcriptional modification. This was indeed the case: when the protein samples shown in Figure 4-6A were treated with calf intestinal phosphatase (this enzyme

is so robust that it works even when added to 8M urea/SDS protein samples), all of the samples collapsed to an identical, faster migrating species (data not shown). Thus, we determined that Hac1p can exist in at least two distinct phosphorylation states, and that this phosphorylation is a regulated event.

We still did not know, however, what effect this phosphorylation had on Hac1p, nor what kinase(s) was responsible. Noah Dephoure, then a rotation student in the Walter Lab, sought to determine the answer to the later. We hypothesized that phosphorylation of Hac1p is likely to serve some necessary role for Hac1p function, and deleting the responsible kinase should therefore decrease the cell's ability to respond to ER stress. The strategy was to canvass the entire collection of viable kinase-deleted yeast strains for those that had decreased fitness on plates containing tunicamycin. Using this strategy, Noah identified *BCK1*, a kinase in the *PKC1* cell integrity pathway (reviewed in (Heinisch et al., 1999)) (Figure 4-7A). These cells had somewhat reduced viability even on plates with no added drug ("-TM"), but completely failed to grow at all on plates containing tunicamycin ("+TM"). This was especially exciting, as we had previously heard that Mary Jane Gething, another researcher working on the UPR, believed that the *PKC1* pathway somehow synergized with the UPR. The *PKC1* pathway is known to bifurcate at various points, and while Δ*bck1* cells exhibited a defect on tunicamycin-containing plates, cells lacking the kinase directly upstream of *BCK1* (Δ*pkc1*) did not display as severe a phenotype, nor did cells deleted for the transcription factor Rlm1p whose activity is regulated by the *PKC1* pathway. Therefore, we expected that Bck1p was the kinase that phosphorylates Hac1p, and that the observed plate phenotype in Δ*bck1* cells resulted from decreased activity of non-phosphorylated Hac1p.

Western analysis (Figure 4-7B) quickly disproved this notion. Not only was Hac1p produced in Δ*bck1* cells the same mobility as in wildtype cells, the abundance of Hac1p in DTT-treated Δ*bck1* cells was surprisingly massively increased; if anything, a *decrease* in Hac1p levels would have been more consistent with the failure of Δ*bck1* cell to grow on tunicamycin. Cells deleted for *SLT2*, the kinase directly downstream of Bck1p, also shown an increase in Hac1p abundance upon UPR activation. From parallel studies investigating whether the *PKC1* pathway is involved in the transcriptional induction of *HAC1* mRNA during the S-UPR, I knew that Δ*bck1* cells produced *HAC1* mRNA at the same level as wildtype (Figure 4-7C). Hence, the observed increase in Hac1p levels likely resulted from either increased translation of *HAC1* mRNA, or decreased degradation of the protein.

While we do not know what is defective in Δ*bck1* cells that triggers this response (but is not impaired in Δ*pkc1* or Δ*rlm1* cells), we have nonetheless discovered that the UPR integrate signals from compartments other than the ER lumen, and that a pathway exists to post-transcriptionally increase the abundance of Hac1p. This pathway is distinct from the Super-UPR; the S-UPR controls the transcriptional abundance of *HAC1* mRNA, and Δ*bck1* cells are not impaired in the S-UPR.

Why do Δ*bck1* cells fail to grow on plates containing tunicamycin? They have no defect in producing Hac1p of the wildtype form – in fact, they produce much more. The *PKC1* pathway has no reported involvement in the folding state of the ER lumen. One possibility is that these cells are defective for some process that feeds into the ER (*e.g.* secretion, or membrane biogenesis), and that some feedback mechanism increases the abundance of Hac1p in a futile effort at overcoming the stress.

An alternative, and more interesting, hypothesis is that Δ*bck1* cells are defective in a pathway that down-regulates Hac1p abundance, and they die because they produce *too much* Hac1p. Production of Hac1p is thought to remodel the secretory pathway (Travers et al., 2000), and perhaps excessive Hac1p leads to an aberrant secretory system. Cells that are required to constitutively express Hac1p, even in the absence of ER stress, grow much less well than wildtype cells (personal observation), implying that Hac1p expression can be deleterious if not controlled properly.

This is an intriguing possibility, as it would be consistent with the notion that the UPR tightly regulates Hac1p expression to produce a transcriptional response perfectly commensurate with cellular conditions. Cells die when faced with ER folding stress if they cannot produce sufficient Hac1p, but producing too much can be equally lethal. Different pathways could serve to sample various cellular processes, and feed this information into the many steps that regulate Hac1p abundance or activity. This idea is supported by the regulatory mechanisms presented earlier in this thesis, describing the translational and transcriptional regulation of Hac1p expression, and by the story presented in Patil *et al.* (Patil et al., 2004) that demonstrates the modulation of Hac1p activity by heterodimerization with Gcn4p. That cells regulate Hac1p expression and activity at a multitude of different control points, rather than at a single step, only adds to the mystery and excitement of the Unfolded Protein Response.

REFERENCES

Calfon, M., Zeng, H., Urano, F., Till, J. H., Hubbard, S. R., Harding, H. P., Clark, S. G., and Ron, D. (2002). IRE1 couples endoplasmic reticulum load to secretory capacity by processing the XBP-1 mRNA. Nature *415*, 92-96.

Chapman, R. E., and Walter, P. (1997). Translational attenuation mediated by an mRNA intron. Current Biology *7*, 850-859.

Cox, J. S., and Walter, P. (1996). A novel mechanism for regulating activity of a transcription factor that controls the unfolded protein response. Cell *87*, 391-404.

Gonzalez, T. N., Sidrauski, C., Dörfler, S., and Walter, P. (1999). Mechanism of non-spliceosomal mRNA splicing in the unfolded protein response pathway. EMBO Journal *18*, 3119-3132.

Heinisch, J. J., Lorberg, A., Schmitz, H. P., and Jacoby, J. J. (1999). The protein kinase C-mediated MAP kinase pathway involved in the maintenance of cellular integrity in Saccharomyces cerevisiae. Mol Microbiol *32*, 671-680.

Komeili, A., and O'Shea, E. K. (1999). Roles of phosphorylation sites in regulating activity of the transcription factor Pho4. Science *284*, 977-980.

Lee, R. C., Feinbaum, R. L., and Ambros, V. (1993). The C. elegans heterochronic gene lin-4 encodes small RNAs with antisense complementarity to lin-14. Cell *75*, 843-854.

Ma, Y., and Hendershot, L. M. (2001). The unfolding tale of the unfolded protein response. Cell *107*, 827-830.

Mazumder, B., Sampath, P., Seshadri, V., Maitra, R. K., DiCorleto, P. E., and Fox, P. L. (2003). Regulated release of L13a from the 60S ribosomal subunit as a mechanism of transcript-specific translational control. Cell *115*, 187-198.

Mori, K., Ogawa, N., Kawahara, T., Yanagi, H., and Yura, T. (2000). mRNA splicing-mediated C-terminal replacement of transcription factor Hac1p is required for efficient activation of the unfolded protein response. Proceedings of the National Academy of Sciences of the United States of America *97*, 4660-4665.

Nanduri, J., and Tartakoff, A. M. (2001). The arrest of secretion response in yeast: signaling from the secretory path to the nucleus via Wsc proteins and Pkc1p. Mol Cell *8*, 281-289.

Patil, C., Li, H., and Walter, P. (2004). A Role for Gcn4 and Novel Upstream Activating Sequences in the Unfolded Protein Response. PLoS Biol, *submitted.*

Rüegsegger, U., Leber, J. H., and Walter, P. (2001). Block of HAC1 mRNA translation by long-range base pairing is released by cytoplasmic splicing upon induction of the unfolded protein response. Cell *107*, 103-114.

Schneider, K. R., Smith, R. L., and O'Shea, E. K. (1994). Phosphate-regulated inactivation of the kinase PHO80-PHO85 by the CDK inhibitor PHO81. Science *266*, 122-126.

Springer, M., Wykoff, D. D., Miller, N., and O'Shea, E. K. (2003). Partially Phosphorylated Pho4 Activates Transcription of a Subset of Phosphate-Responsive Genes. PLoS Biol *1*, E28.

Travers, K. J., Patil, C. K., Wodicka, L., Lockhart, D. J., Weissman, J. S., and Walter, P. (2000). Functional and genomic analyses reveal an essential coordination between the unfolded protein response and ER-associated degradation. Cell *101*, 249-258.

Villa, T., Pleiss, J. A., and Guthrie, C. (2002). Spliceosomal snRNAs: Mg(2+)-dependent chemistry at the catalytic core? Cell *109*, 149-152.

Wightman, B., Ha, I., and Ruvkun, G. (1993). Posttranscriptional regulation of the heterochronic gene lin-14 by lin-4 mediates temporal pattern formation in C. elegans. Cell *75*, 855-862.

Yoshida, H., Matsui, T., Yamamoto, A., Okada, T., and Mori, K. (2001). XBP1 mRNA is induced by ATF6 and spliced by IRE1 in response to ER stress to produce a highly active transcription factor. Cell *107*, 881-891.

Zuker, M. (2003). Mfold web server for nucleic acid folding and hybridization prediction. Nucleic Acids Res *31*, 3406-3415.

Figure 4-1: Anti-sense regulation in eukaryotes

The 5'UTR/intron interaction regulating *HAC1* translation (**A**) is strikingly similar to the anti-sense regulation observed with *lin-4* and *lin-14* in *C. elegans* (**B**). In both cases, it appears that translation is regulated at the elongation step, allowing for the rapid resumption of translation once the base-pairing interaction is relieved. (**C**) *XBP-1*, the metazoan ortholog of *HAC1*, possesses no obvious complementarity between its 5'UTR and intron; any translation-inhibiting interaction between these two elements might therefore proceed through a protein intermediary.

Figure 4-1

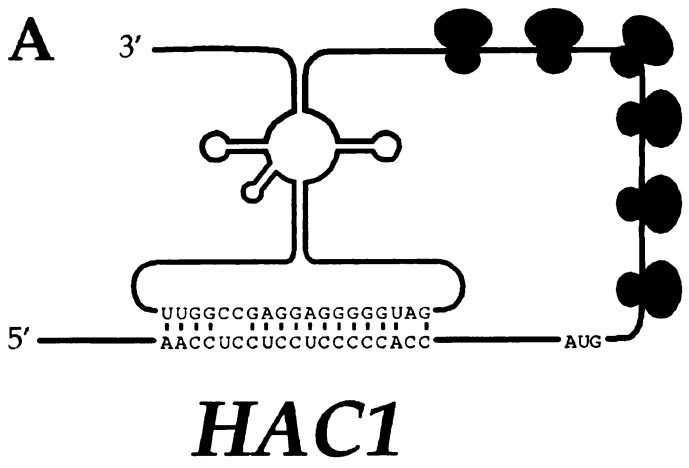
A
3′
UUGGCCGAGGAGGGGGUAG
5′
AACCUCCUCCUCCCCCACC
AUG
HAC1

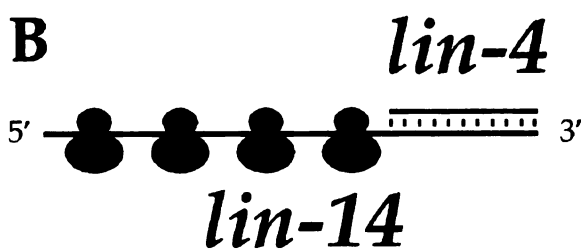
B
lin-4
5′
3′
lin-14

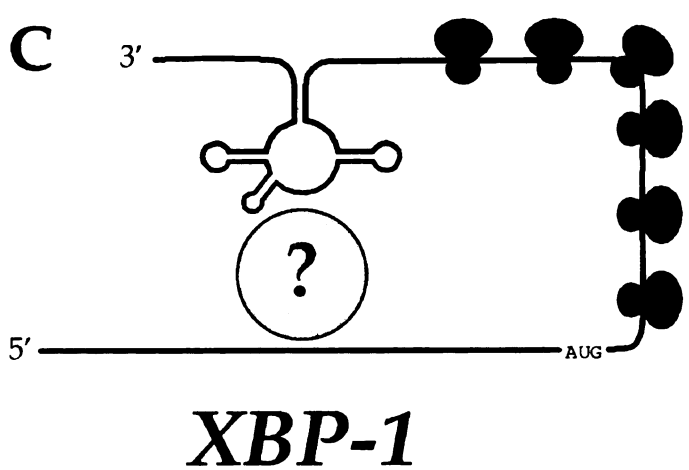
C
3′
?
5′
AUG
XBP-1

Figure 4-2: The *HAC1*^{u}-polyribosome interaction requires elevated magnesium concentrations *in vitro*

Extracts from wildtype cells were prepared identically, with the exception of the concentration of $MgCl_2$, which varied as indicated. Extracts were run on sucrose gradients with matching $MgCl_2$ concentrations, RNA was harvested from the fractions, and *HAC1* and *ACT1* mRNAs associated with each fraction were visualized by Northern analysis. An extract containing 5 mM $MgCl_2$, prepared from a parallel culture that had been treated with 6 mM DTT for 60 min prior to harvesting (below dashed line), shows reduced magnesium sensitivity of the *HAC1*^{u}-polyribosome complex.

Figure 4-2

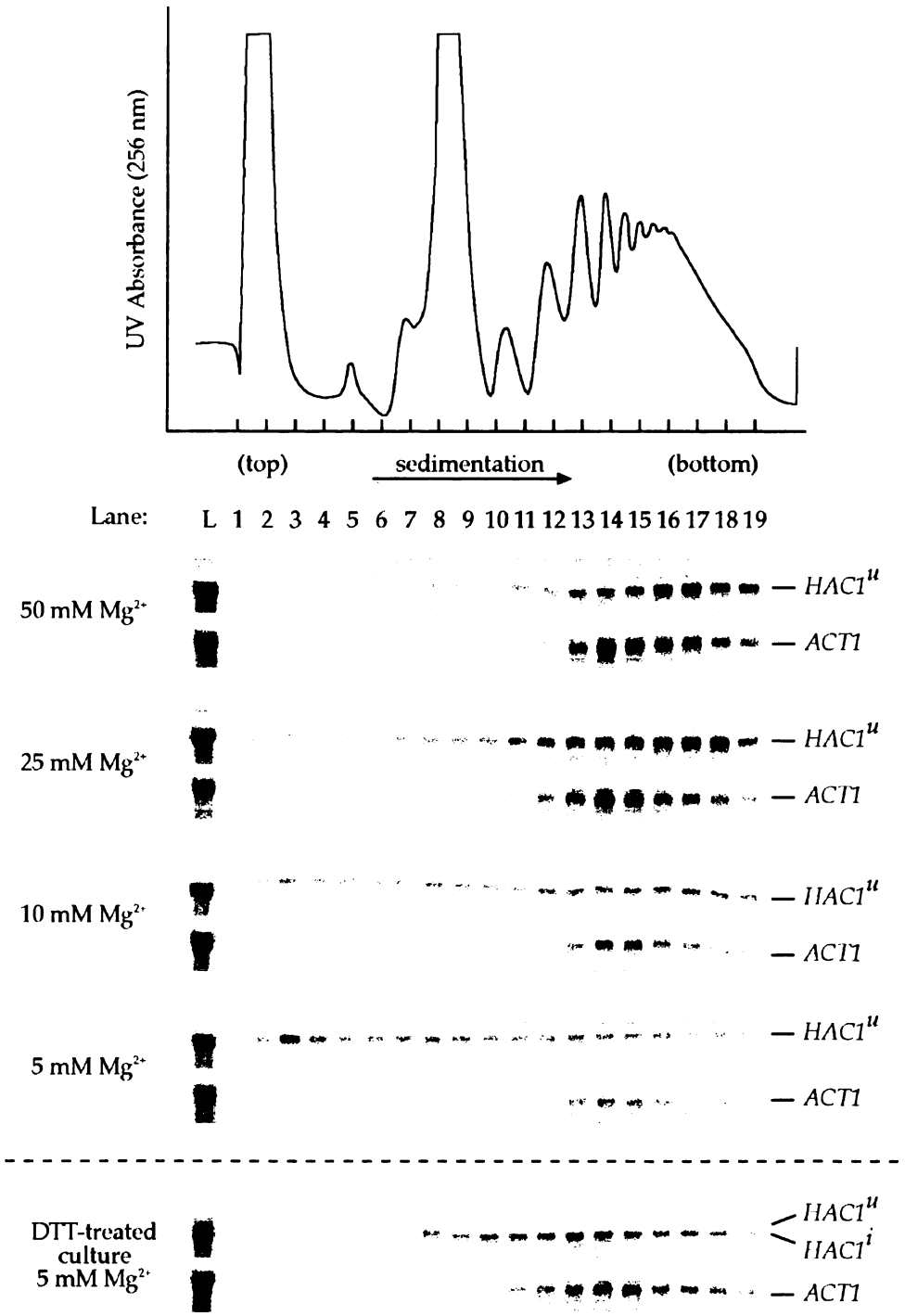
UV Absorbance (256 nm)
(top)
sedimentation
(bottom)
Lane:
L 1 2 3 4 5 6 7 8 9 10 11 12 13 14 15 16 17 18 19
50 mM Mg2+
25 mM Mg2+
10 mM Mg2+
5 mM Mg2+
HAC1u
ACT1
DTT-treated culture 5 mM Mg2+
HAC1i

Figure 4-3: Quantitation of *HAC1* and *ACT1* ribosome association as a function of magnesium concentration

The Northern blots shown in Figure 4-2 were quantified, and the fraction of total *HAC1* (upper panel) and *ACT1* (lower panel) mRNA are plotted as a function of position within the sucrose gradient, with higher fractions numbers representing heavier fractions containing more ribosomes.

Figure 4-3

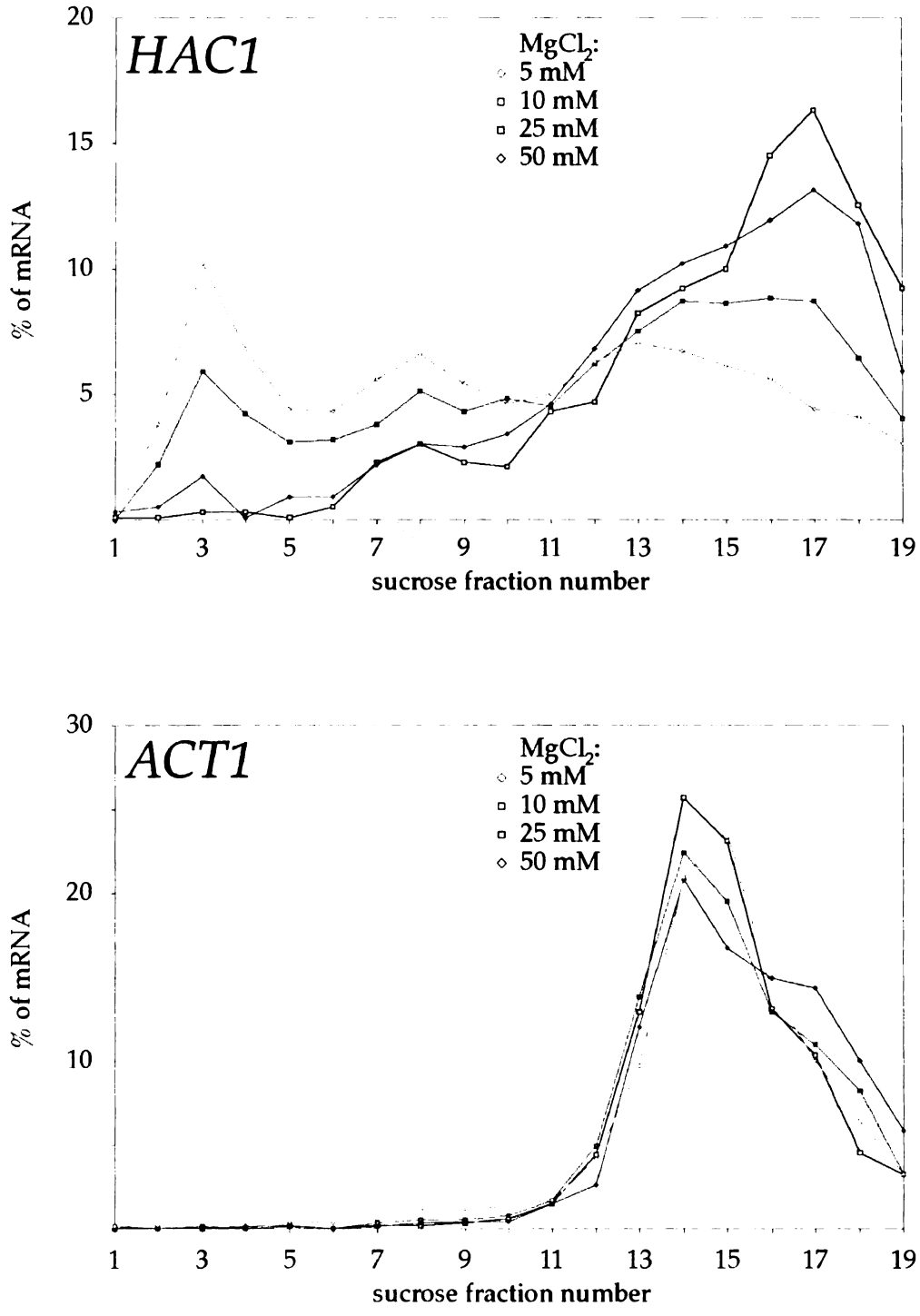
HAC1
MgCl2:
5 mM
10 mM
25 mM
50 mM
% of mRNA
20
15
10
5
1
3
5
7
9
11
13
15
17
19
sucrose fraction number
ACT1
MgCl2:
5 mM
10 mM
25 mM
50 mM
% of mRNA
30
20
10
1
3
5
7
9
11
13
15
17
19
sucrose fraction number

Figure 4-4: A microarray- and polysome profile-based screen for mRNAs whose interaction with ribosomes is distinctly magnesium-requiring

From a single initial culture, separate extracts are prepared for polysome profiles with varying concentrations of $MgCl_2$. These different extracts are run over sucrose gradients, and fractions representing mRNAs unbound by ribosomes (top of gradient), bound to 1-3 ribosomes (middle of gradient), or bound to 4+ ribosomes (bottom of gradient) are harvested and pooled. PolyA+ is extracted from the sucrose gradient pools, reverse transcribed, labeled with fluorescent Cy-dyes, and hybridized to microarrays. Those mRNAs that are concentrated in the top fractions of the sucrose gradient in extracts prepared from low concentrations of $MgCl_2$, but not in extracts with high concentrations of $MgCl_2$, would be analyzed further. These mRNAs should be reciprocally depleted from the heavier, polyribosome-containing fractions in extracts prepared from low concentrations of $MgCl_2$, but not in extracts with high concentrations of $MgCl_2$.

Figure 4-4

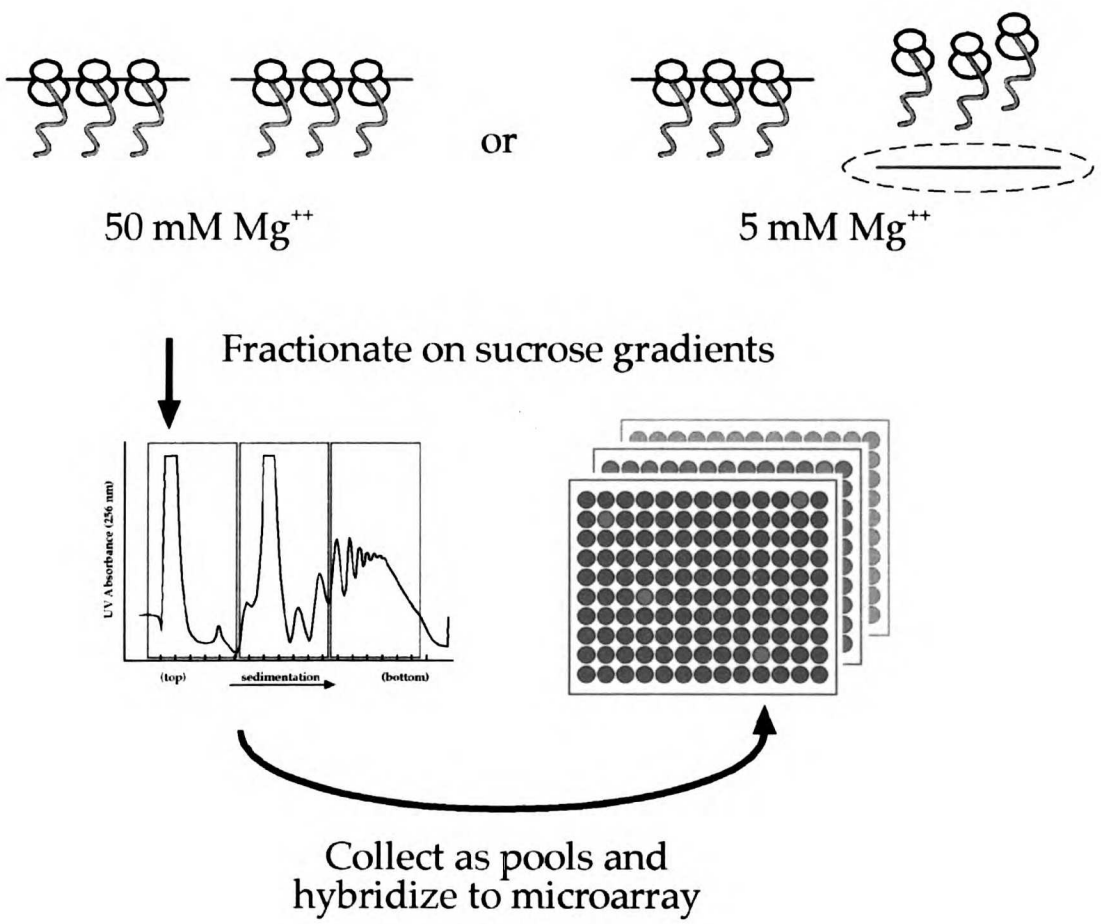
or
50 mM Mg++
5 mM Mg++
Fractionate on sucrose gradients
UV Absorbance (256 nm)
(top)
sedimentation
(bottom)
Collect as pools and
hybridize to microarray

Figure 4-5: Strategies for isolating UPR Modulatory Factor

(**A**) Reduced viability of strains unable to express *HAC1* at elevated levels. Wildtype (WT), Δ*hac1*, and *ADH1pro-HAC1* cells were plated in serial dilutions (left to right) on synthetic media lacking inositol ("-ino") and synthetic media lacking inositol and containing tunicamycin ("-ino +TM"). (**B**) A schematic for parallel genetic screens to isolate UMF. Mutated cells in which either UMF activity has been reduced (EMS mutagenesis) or the binding site for UMF within the *HAC1* promoter disrupted (PCR mutagenesis) should be unable to upregulate *HAC1*, and will therefore not grow on plates lacking inositol and containing tunicamycin, as described above. (**C**) UPR targets whose induction under S-UPR conditions is most likely due to UMF activity.

Figure 4-5

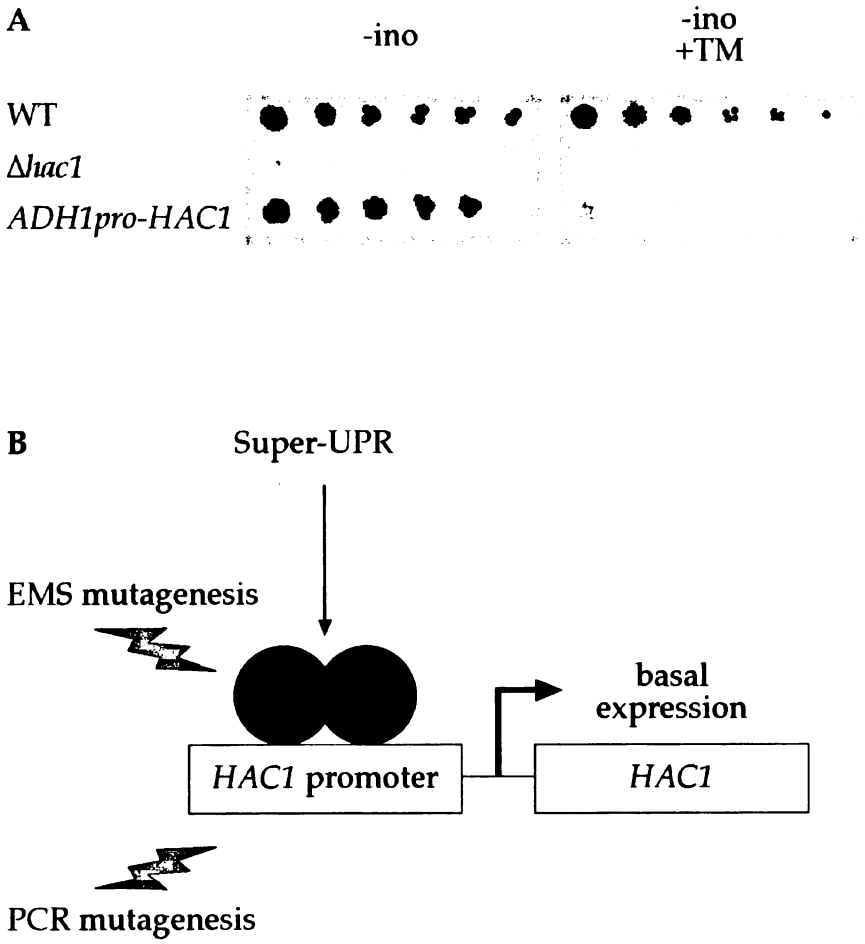

C S-UPR targets most likely influenced by UMF:

YHR087W	*GIF1*
YMR173W-A	*RMD12*
PBI2	*YDL023C*
GLK1	*GPD1*
YOR289W	*YSC84*
ALD2	*YOL107W*

Figure 4-6: Hac1p is modified during prolonged secretory stress

(**A**) Hac1p mobility is decreased in *sec14-3* cells. Western blot of *sec14-3* cells shifted to non-permissive temperature for the time indicated. Samples were run on denaturing SDS-polyacrylamide gels, so the decreased mobility of Hac1p starting at 120 min likely reflects a more massive species. (**B**) *HAC1* mRNA is not modified in *sec14* cells. The samples shown in **A** were analyzed by Northern blot. No change in *HAC1* mRNA mobility is observed that correlates with the altered protein mobility starting at 120 min.

Figure 4-6

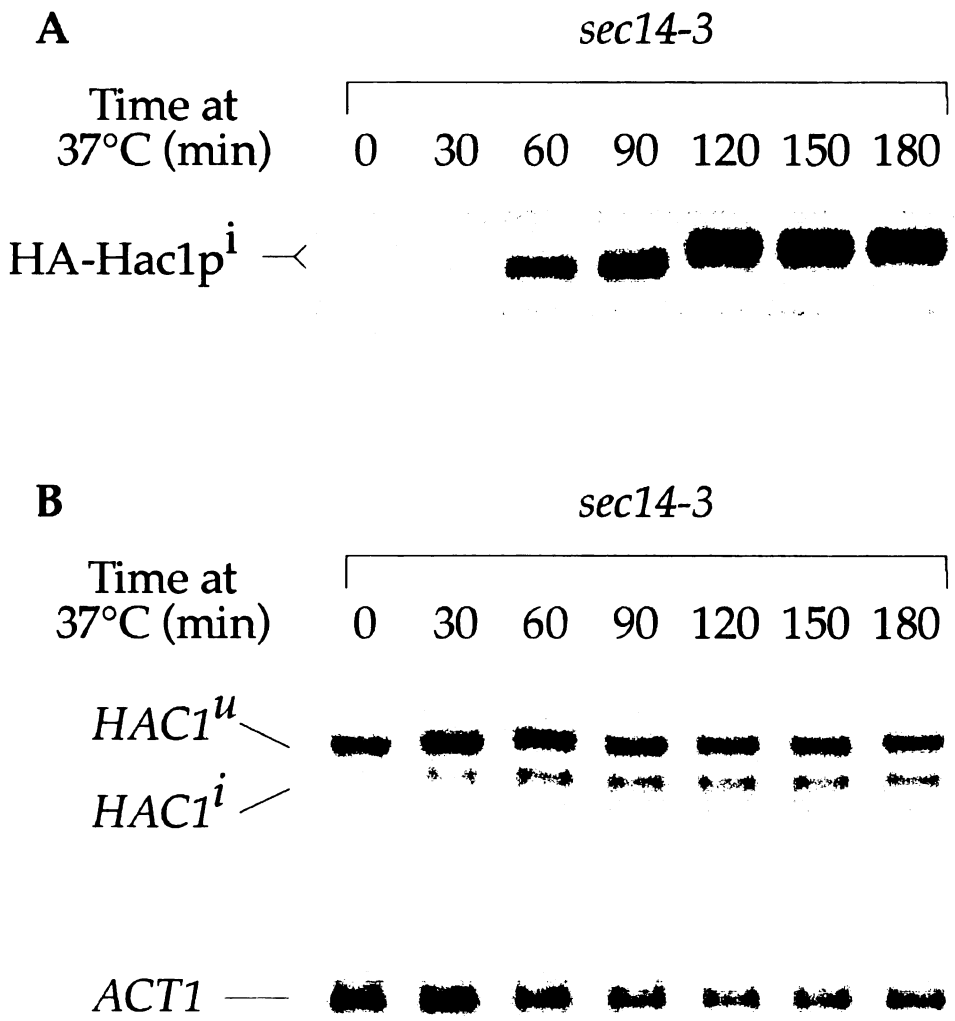
A
sec14-3
Time at 37°C (min)
0 30 60 90 120 150 180
HA-Hac1p^{i}
B
sec14-3
Time at 37°C (min)
0 30 60 90 120 150 180
HAC1^{u}
HAC1^{i}
ACT1

Figure 4-7: An interaction between components of the *PKC1* cell integrity pathway and the Unfolded Protein Response

(**A**) Reduced viability of Δ*bck1* cells, but not strains defective elsewhere in the *PKC1* pathway, under UPR-inducing conditions. Wildtype (WT), Δ*wsc1*, Δ*pkc1*, Δ*bck1*, and Δ*rlm1* cells were plated in serial dilutions (left to right) on complete media lacking ("-TM") and complete media containing tunicamycin ("+TM"). (**B**) Hac1p abundance is increased in Δ*bck1* and Δ*slt2* cells. Western analysis of WT, Δ*bck1*, and Δ*slt2* cells treated with DTT for 60 min. (**C**) *HAC1* mRNA abundance is unaffected in strains lacking *PKC1* pathway components. Northern analysis of WT, Δ*ire1*, Δ*wsc1*, Δ*pkc1*, Δ*bck1*, and Δ*rlm1* strains shifted from 23°C to 37°C concurrent with DTT treatment. Shown are the 0 (untreated) and 60 min timepoints.

Figure 4-7

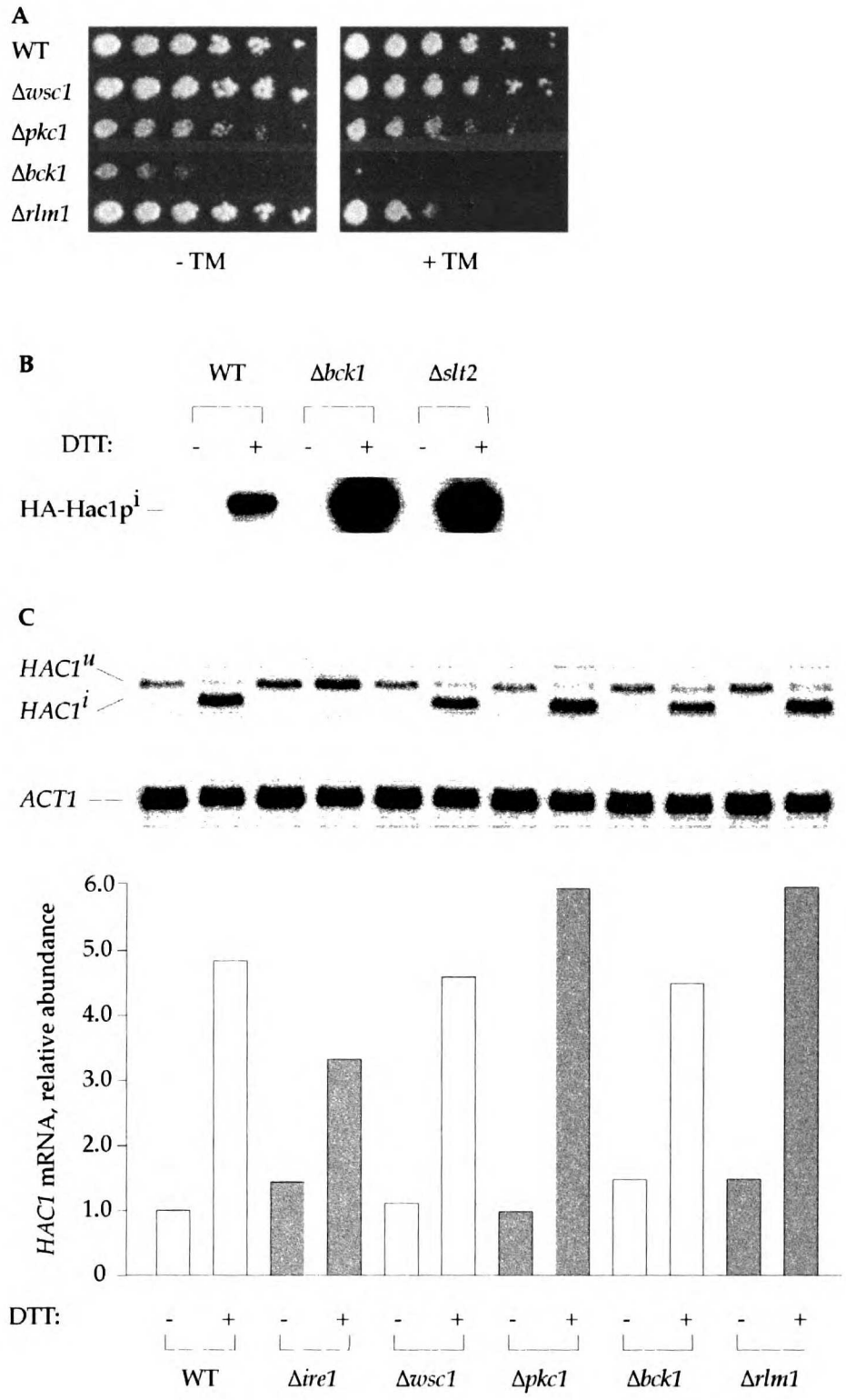
A
WT
Δwsc1
Δpkc1
Δbck1
Δrlm1
- TM
+ TM
B
WT
Δbck1
Δslt2
DTT:
- + - + - +
HA-Hac1p^i
C
HAC1^u
HAC1^i
ACT1
HAC1 mRNA, relative abundance
6.0
5.0
4.0
3.0
2.0
1.0
0
DTT:
- + - + - + - + - + - +
WT
Δire1
Δwsc1
Δpkc1
Δbck1
Δrlm1

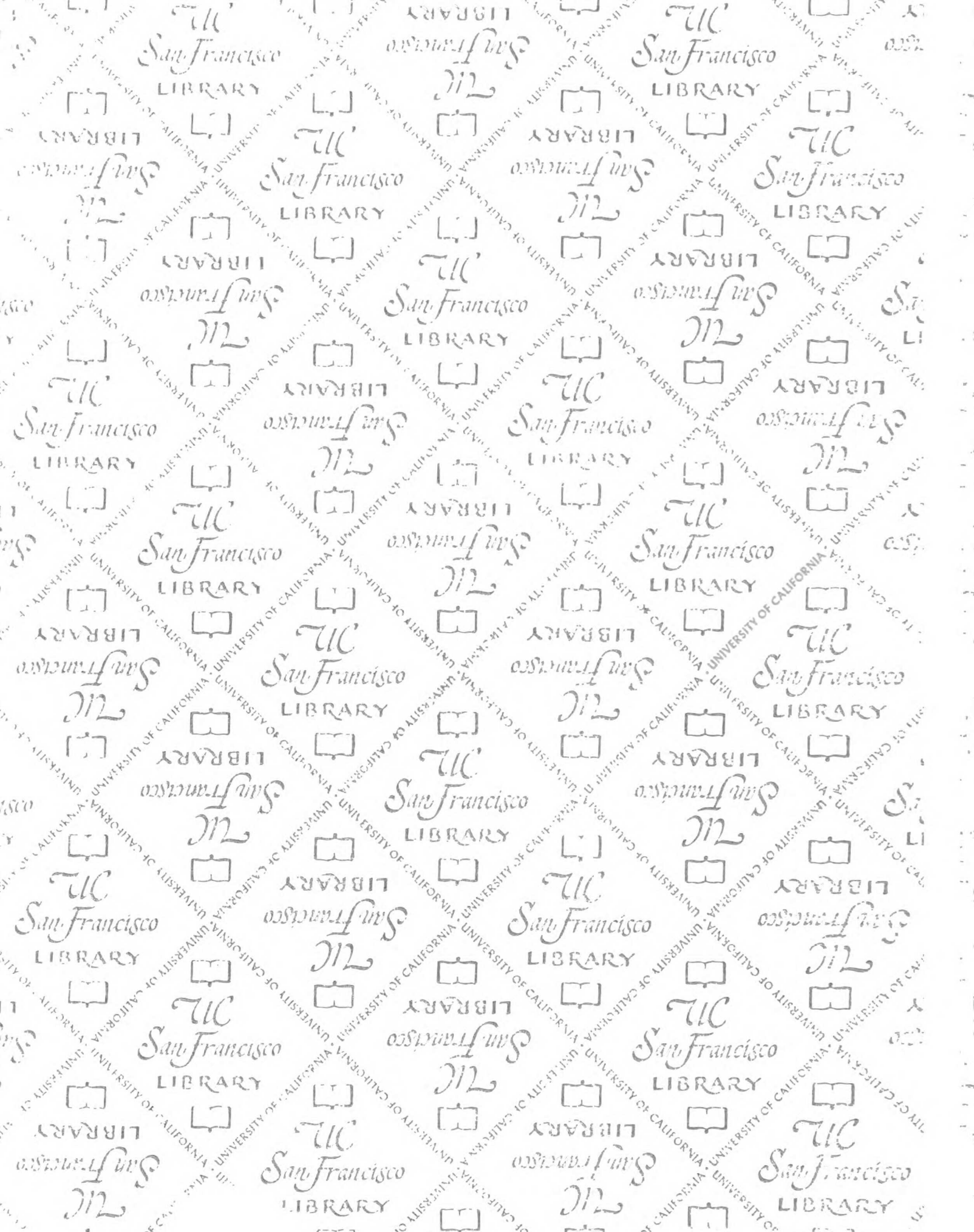
UC
San Francisco
LIBRARY
UNIVERSITY OF CALIFORNIA